Aufgabenstellung

Titel der Studienarbeit:

Messmethode zur Charakterisierung des Benetzungsverhaltens von Elektroden und Separatoren in Lithium-Ionen-Zellen

Inv.- Nr.: 22996
Verfasser: Sergi Rexach **Betreuer:** Thomas Knoche
Ausgabe: 15.10.2014 **Abgabe:** 15.04.2015

Ausgangssituation:
Die steigende Nachfrage nach individueller Mobilität sowie die Endlichkeit fossiler Energieträger fordern heute die Entwicklung umweltverträglicher, emissionsfreier Antriebstechnologien. Ein weit verbreiteter Ansatz ist die Elektrifizierung des Antriebsstranges. Dabei kommt der Energiespeicherung eine enorm wichtige Rolle zu, da sie maßgeblich die Reichweite und den Komfort der Fahrzeuge mitbestimmt. Lithium-Ionen-Batterien, die in großen Stückzahlen bereits in Notebooks und Mobiltelefonen verbaut sind, haben sich auch für die Anwendung in Elektrofahrzeugen als vielversprechende Energiespeicher erwiesen, da sie eine hohe Energie- und Leistungsdichte besitzen.

Zur Erforschung der Produktion von großformatigen Lithium-Ionen-Zellen wurde am *iwb* eine vollständige Produktionslinie aufgebaut. Ein Kernprozess ist hierbei die Befüllung der Zelle mit Elektrolytlösung. Dies wird maßgeblich von der Benetzbarkeit der Zelllagen, insbesondere des Separators, bestimmt. Dennoch existieren in der Literatur keine etabilierten Benetzungsmessverfahren. Am *iwb* wurde daher eine Methode vorgeschlagen, die die Benetzung von Zelllagen anwendungsnah messen soll. Konzeptionell wurde diese Messmethode bereits umgesetzt. Die detaillierte Umsetzung und die Durchführung statistisch belastbarer Versuche stehen jedoch noch aus.

Zielsetzung:
Ziel der Arbeit ist es, die konzeptionell vorhandene Messmethode am iwb soweit zu entwickeln, dass reproduzierbare Messungen durchgeführt und

ausgewertet werden können. Anschließend soll das Benetzungsverhalten von Zelllagen mit Fokus auf Separatoren anhand statistisch belastbarer Versuchsreihen charakterisiert werden.

Vorgehensweise und Arbeitsmethodik:
Die Vorgehensweise umfasst die folgenden Punkte:

- Erstellung eines Arbeitsplans
- Einarbeitung in die Prozesskette zur Herstellung von Lithium-Ionen-Zellen, speziell in die Befüllung von LIZ
- Einarbeitung in die Messmethode
- Weiterentwicklung der Messmethode und Modifikation des Versuchsstandes
- Durchführung statistisch belastbarer Versuche zur Charakterisierung des Benetzungsverhaltens von Zelllagen
- Schriftliche Dokumentation der Arbeit in englischer Sprache

Vereinbarung:
Mit der Betreuung von Sergi Rexach durch Herrn Dipl.-Ing. Thomas Knoche fließt geistiges Eigentum des *iwb* in diese Arbeit ein. Eine Veröffentlichung der Arbeit oder eine Weitergabe an Dritte bedarf der Genehmigung durch den Lehrstuhlinhaber. Der Archivierung der Arbeit in der *iwb*-eigenen und nur für *iwb*-Mitarbeiter zugänglichen Bibliothek als Bestand und in der digitalen Studienarbeitsdatenbank des *iwb* als PDF-Dokument stimme ich zu.

Garching, den 15.10.2014

Dipl.-Ing. T. Knoche S. Rexach Prof. Dr.-Ing. G. Reinhart

Abstract

The actual manufacturing process of lithium-ion batteries has a few potential areas to be improved. At *iwb* has been built a complete production line with the purpose of improving all the stages, including the filling and the following wetting of the cells. Because of the barely existence of a wetting measurement method in the literature, a method was already proposed in a former work. The system was composed of a vacuum chamber, a case to hold the cell's layers that were pressed with a Plexiglas block, a liquid circuit, and a camera to record the phenomena. This master thesis has contributed to improve the method, redesigning the setup, and creating a completely new video analysis. A statistical model with four main factors has been formulated. These describe a pressure profile using as variables a filling and a wetting pressure, a held time, and the number of cycles this is repeated. The chosen response is the percentage that the electrolyte has soaked at the end on the process. The study is performed to provide guidance on the trends of the response. The maximal process's performance with two cycles is one of the most relevant acquired results. Another worthy finding has been the great influence that the wetting pressure has on the soaked surface, in addition to the interaction that has this one with the filling pressure. The establishment of these patterns could serve as a guideline to develop improved battery production lines.

Keywords:

Wetting, Lithium-ion Batteries, Manufacturing, Electrolyte, DoE, Method, Spreading phenomena, Soaking, Electric Vehicle.

Acknowledgments

I would like to give my most sincere gratitude to my thesis supervisor Dipl.-Ing. Thomas Knoche. He has made an effort on helping me throughout all my work, especially on requesting new components, devoting his time and attention when desired, and being always kind to provide guidance when required. I truly appreciate his disposition to help and provide with me whatever was needed. Without the quick delivery of those materials and resources, the final objectives of this project would have not been achieved within the planned time.

I would like to my heartfelt gratitude to my family and the sacrifices they made for sending me abroad and giving me the chance to study in an internationally recognized institution as the Technische Universität München is. I would like to dedicate a part of this work to my grandfather, who left a void in our family during the process of this thesis. He has always been to me a role model of effort and devotion.

Finally, I would like to render thanks to all friends, which have been giving support to each other during the four years of diploma in Barcelona. Also, lots of thanks to those who made these two years in Munich special and unforgettable experience. They helped me to go ahead during though times, becoming truly a second family abroad.

List of Abbreviations

ANOVA: Analysis of variance

CI: Confidence interval

DoE: Design of experiments

BEV: Battery electric vehicle

EC: Ethylene carbonate

EMC: Ethyl methyl carbonate

iwb: Institut für Werkzeugmaschinen und Betriebswissenschaften (in English: Institute of machine tools and Industrial Management)

Li^+: Lithium ions

LIB: Lithium-ion battery

PE: Polyethylene

PPE: Polypropylene

SOC: State of charge

StDev: Standard deviation

Table of Contents

1 Introduction

The present energy economy claims urgently for a cheap and sustainable power supply. One of the most energy-consumptive activities is travelling. Especially in this case, newly contrived battery devices could be the solution. They own the characteristic to store energy derived from sustainable sources such as wind and solar power (ARMAND & TARASCON 2008). The need for a sustainable transport is incredibly high: climate change, shortage of fossil fuels, higher rates of individual mobility, and a settled energy transition; these are the requested factors for an emission-free driving technology, which bring us to the actual expanded trend of electro mobility (IWB 2014B).

Battery electric vehicles (BEVs) require high-performance and cost-effective energy storage systems to reach the specifications of actual internal combustion engines. The other barrier to gain faith in BEVs, is their short limited range (KAHN RIBEIRO ET AL. 2007). Lithium-ion batteries (LIBs) are ideally suited to accomplish those needs, due to a high energy and power density, a low self-discharge, and no memory-effect. However there are still many challenges to achieve, i.e., slashing the costs and improving the quality (IWB 2014B, IWB 2014A).

Nowadays, the battery pack is the most expensive individual component that determines the price of the final product in the electrical automotive industry. These high-voltage accumulators are not so costly because of expensive raw materials. These have a share of about 30 % in the total cost of a battery. The remaining 70 % is caused by production and logistics. Cells for automotive applications require economic production processes with much higher standards than those for consumer applications. Automated production techniques contribute in better qualities and lower prices. Hence, investigation and development of new technologies for the production of battery cells has an outstanding importance. (DINGER ET AL. 2010)

To investigate the production of LIBs, at the Institute of Machine Tools and Industrial Management (*iwb*) in Munich, a complete battery production line has been constructed (IWB 2014C). One of the phases under investigation is the filling of the cell with an electrolytic solution. Despite being the filling one of the most significant processes defining cells' quality, barely exists any

measurement method in the literature that clarifies the soaking of the electrolyte in cell layers (KNOCHE 2013).

According to WOLLERSHEIM & PFLEGING (2012), the pores have to be completely filled with the electrolyte for an optimal operation. The liquid electrolyte is the medium of transport, via the ions are diffused between anode and cathode in the battery. Without this, there would be no charge equalization inside the cell, and consequently, no electric current would flow. However, the materials used in conventional high-energy batteries for automotive industry show poor wetting effects on the electrode surface by the liquid electrolyte.

Therefore, a method to determine the wetting phenomena of the battery cells with the electrolyte was proposed and implemented in a previous work; but it requires further development. The strategy in this thesis differs from the existing method so far that this aims to upgrade different aspects of the construction and to conduct it in another way. The effects on the different variables will be calculated and the results analyzed in order to acquire a better understanding of the filling conditions that minimize the wetting time and ensure a completely soaked surface.

1.1 Thesis Outline

The thesis starts with the description of the basic principles of LIBs and a list of established methods and tests to measure the spreading phenomena of liquids in Chapter 2. This is followed by the description of statistic fundamentals for a design of experiments (DoE), statistical model creation and the measure of effects and interaction in a process response along Chapter 3. After this overview about the background of the work, in Chapter 4 is examined and reviewed the former work done in this field.

Chapter 5 gathers the upgrades done in relation to the former work and the creation of a new set of experiments. In addition, this explains the video analysis with MATLAB and the steps that the script takes. The subsequent procedures to gain necessary information in order to create a model and extract interpretations are shown in Chapters 6. This includes a review of the ultimately selected design points in a D-optimal design.

Chapter 7 includes the process to extract a numerical response from the graphical material, the followed process to select the most appropriate statistical model, and all the information extracted from this. The thesis ends with a discussion and a summary of the obtained results in Chapters 8, 9, and 10.

2 Background and State of the Art

This chapter overviews some basics about LIBs: how they function, their components, the different design forms, and their manufacturing's process. The major sources for the section of batteries come from LINDEN & REDDY (2002), NAZRI & PISTOIA (2009), and KORTHAUER (2013).

The second section is a resume about developed methods and techniques used to measure the spreading phenomena on different applications. YUAN & LEE (2013) is the principal source of information for this section. At the end it is included an evaluation of each method focused on the application of cells.

2.1 Lithium-Ion Battery

Lithium-ion batteries are secondary or rechargeable batteries. It means that their charge and discharge proceed nearly reversible and with minimal physical changes that could limit battery's life. LIBs consist in two different lithium insertion materials, the positive and negative electrode.

Their major relative advantages to other batteries' types are:

- High specific energy (~150 Wh/kg)
- High energy density (~400 Wh/L)
- Low self-discharge rate (2 to 8 % per month)
- Long cycle life (greater than 1000 cycles)
- Broad temperature range of operation (-40 ºC to 65 ºC)

Disadvantages of LIBs are that they degrade when are discharged below 2 V, they have to be vent when are overcharged, and they lose capacity at temperatures below 65 ºC. LIBs typically employ management circuits and mechanical disconnection devices to provide protection from over-discharge, over-charge and high temperature conditions. The combination of these qualities with a competitive cost enables to use this technology in unnumbered applications.

2.1.1 History

Earliest LIBs concepts came out around 1970 and provided an apparent solution to the energy density problem compared to the existent batteries and higher voltage (WAKIHARA & YAMAMOTO 1998, TIRADO 2003). Lithium metals were the firsts used materials on that new generation of batteries, because of their high specific capacity. Despite performing impressively, lithium metal shows instability in aqueous electrolytes, had poor safety properties, and exhibited a relative low cell's voltage of 2.5 V. In 1991 Sony succeeded in the development of a rechargeable lithium battery with low density carbon-based insertions in the anode (WAKIHARA & YAMAMOTO 1998). Although the replacement of metallic lithium by carbon caused an important sacrifice in energy density, this new material offered significant advantages in terms of safety and cycle life. The battery from Sony consisted of $LiCoO_2$ as cathode and petroleum coke as anode, whose maximal charge's voltage was 4.1 V. (OHZUKU & BRODD 2007)

Greater capacities and cell voltages were obtained replacing the petroleum coke for a graphitic carbon, achieving voltages of 4.2 V. Since then, LIBs market has grown to about 1 billion produced units in 1999. Although manufacturers are careful to ensure their safety in normal conditions, safety is still a watchword for LIBs. (YOSHIO ET AL. 2009)

2.1.2 Intercalation Processes

Cells of LIBs employ lithium-intercalated compounds as positive and negative materials, i.e., active materials. A microporous separator film isolates electrically both electrodes, but ensures ionic conduction between electrodes if wetted with liquid electrolyte. The cells are connected with the exterior through two current collectors, both situated on the positive and negative electrodes.

Active materials operate thanks to the called intercalation process of lithium ions (Li^+). The positive material is a metal oxide and the negative a graphitic carbon; both act incorporating Li^+ reversibly to form "sandwich"-like structures. This function is carried out when Li^+ are inserted into/extracted from a solid matrix without the destruction of core structures. The lithium insertion/extraction process occurs with the reduction/oxidation reaction of

both electrodes' materials, creating a flow of ions through the electrolyte, and therefore, a flow of electrons through the external circuit.

During discharge, Li^+ migrate from negative to positive electrode. In this process, Li^+ are de-intercalated from the negative material and intercalated into the positive material. Meanwhile, electrons move through an external circuit in the same direction as Li^+. When it charges, an external electrical power source applies an over-voltage that forces Li^+ to circulate in the reverse direction, being the positive material oxidized and the negative reduced. This action is illustrated in Figure 2-1 as a schematic view and as chemical reactions in formulas (2.1) for the positive electrode and (2.2) for the negative.

$$LiCoO_2 \underset{\text{Discharge}}{\overset{\text{Charge}}{\rightleftharpoons}} Li_{2-x}CoO_2 + xLi^+ + xe^- \qquad (2.1)$$

$$C + xLi^+ \; xe^- \underset{\text{Discharge}}{\overset{\text{Charge}}{\rightleftharpoons}} Li_xC \qquad (2.2)$$

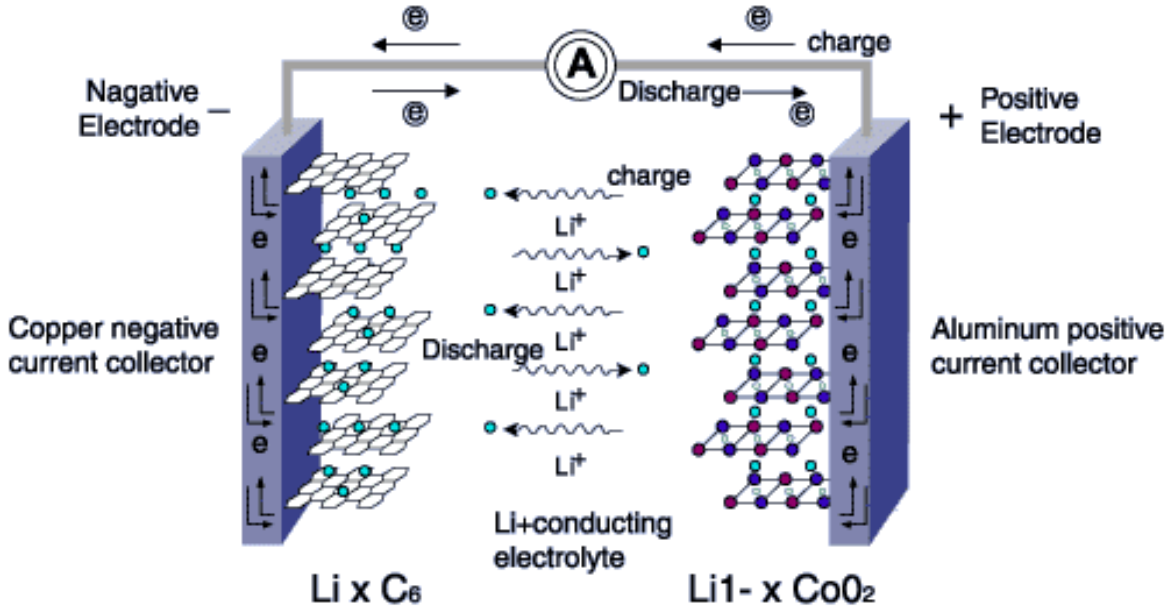

Figure 2-1: Schematic of an intercalation process in a Lithium-ion battery (MIRET 2011)

2.1.3 Active Materials

Electrodes are the materials that make possible the intercalation of lithium atoms, which are capable to admit high quantities of Li^+ reversibly. Moreover, materials suitable for positive electrodes should have a high chemical potential, while for negative a low one. They must remain under a potential's zone, in which the electrolyte could not go into undesirable reactions. Additionally, they should also satisfy additional conditions such as economically affordable, availability, low density, and environmentally harmless. (YOSHIO ET AL. 2009)

Positive Electrode

The positive electrode, also called cathode, is typically made of a ~15 µm aluminum current collector coated with a lithiated metal oxide. During the charging stage, Li^+ travel into the anode. Advantageous properties for positive electrodes are:

- High free reaction's energy with lithium, to achieve high cell voltages and high energy densities
- High energy's capacity
- Suffer no structural changes when it incorporates ions
- High electronic conductivity and ionic mobility
- Insoluble in the electrolyte

$LiCoO_2$ and $LiMn_2O_4$ are the most commercial interesting compounds. $LiCoO_2$ offers a higher capacity, a high voltage, and longer cycle life; whereas $LiMn_2O_4$, is particularly cheaper than $LiCoO_2$, it also offers an exceptional stability, a higher voltage, and a lack of toxicity. On the other hand, $LiMn_2O_4$ has a lower capacity and a higher capacity loss at elevated temperatures. (BESENHARD 1999)

Negative Electrode

The negative electrode, also named anode, is typically made of a ~10 µm copper foil coated with a mixture of high tapped density artificial graphite and non-fluorinated binder. A suitable carbon for the use as anode in LIBs should have the following characteristics:

- Low cost
- Easily tractable
- High capacity in a working electrochemical range of 0 – 0.5 V

Graphite has ideal properties to use as negative electrode, as it offers high capacity, light weight, and a relatively cheap price (RITCHIE & HOWARD 2006, BIRKE & SCHIEMANN 2013). The quality and quantity of holes that graphite is capable to accommodate reversibly Li^+ depend on the structure and micromorphology of the carbonaceous material.

Cooper is almost the unique material used, because it is stable in the electrode potential's range and does not react with lithium or electrolyte components (COUSSEAU ET AL. 2006, JOSSEN & WEYDANZ 2006).

2.1.4 Separator

LIBs use a microporous polymer's membrane of ~20 µm thickness (LOVE 2011) that permits the Li^+ to shuttle between the anode and the cathode. Simultaneously, this isolates electrically both electrodes preventing short-circuits. Due to its condition of "passive" component, separators have attracted little scientific interest; its significance lies on the challenge to build batteries even more compact and long-lasting (BESENHARD 1999). Nevertheless, they are required to accomplish several requirements such as:

- Mechanically robust and resistant (LOVE 2011)
- Effective pore size less than 1 µm
- Easily wetted by electrolyte
- Compatible and stable in contact with electrolyte and electrode materials (LIU 2012)

Porosity is an essential aspect of the separator that greatly influences its permeability. A high porosity guarantees great electrolyte storage. A non-uniform porosity leads to non-uniform current densities and therefore to an accelerated aging of the electrodes. Commercial separators offer a pore size between 0.03 and 0.1 µm and porosities from 30 to 50 %. While the temperature approaches the polymer's melting point, the porosity is lost and pores are closed, stopping the exchange of Li^+.

Two other physical properties of the separator are the absorption and retention of electrolyte. Any good separator should be able to absorb a significant amount of electrolyte and retain it over cell's operative life. A maximum amount of electrolyte in the separator is sought to decrease cell's internal resistance and to avoid the chances of dendrite's formation. Thereby the power is higher and the life expectancy longer. Alternative materials, such as surfactant-coated nonwovens, are designed to offer a better soaking acceptance to the electrolyte. (SANTHANAGOPALAN & ZHANG 2012)

Microporous polyolefin materials are made of polyethylene (PE), polypropylene (PPE), or laminates from both. The low melting point of PE is used as a thermal fuse, since its porosity is lost around 135 ºC, creating a high-resistance barrier (BESENHARD 1999). On the other hand, PPE is tough and resistant to fatigue, and with a higher melting temperature. Tri-layer separators (PPE/PE/PPE) are designed such as PPE maintain the film's integrity and PE shuts the flow down if over temperatures are reached.

2.1.5 Electrolyte

The electrolyte is an ionically conductive liquid that enables to boost ions between both electrodes. The basic requirements of a suitable electrolyte are:

- Low melting and high boiling temperatures
- Stable and non-toxic
- High ionic conductivity in a range of -40 ºC and +80 ºC
- Chemically and electrochemically compatible with electrodes and inactive materials
- Selective solvation properties (BESENHARD & EICHINGER 1976)
- High wetting

An electrolyte consists of a lithium-salt's solution, mixed with one or more organic solvents and additives. Liquid electrolytes are typically used in LIBs, because the electrodes and the separator can absorb.

Lithium hexafluoride ($LiPF_6$) is the most used salt, because it offers a high ionic conductivity and provides acceptable safety properties. However, this salt is costly and yields hydrofluoric acid (HF) upon reaction with water. The ionic conductivity is of considerable interest because it determines the internal resistance and the rate performance of the battery (WAKIHARA & YAMAMOTO

1998). Although many solvents show strong ionic conductivities when they are used with a suitable solute, only a few of them are stable. The industry is decided on solvents for their steadiness such as the carbonates.

Other positive characteristics of carbonate solvents are that they can solvate high concentration rates of lithiated salts, own good safety properties, and are compatible with the electrodes. Nowadays, LIBs employ from three to five solvents to achieve better cell's performance, higher conductivity, and a broader working-temperature range.

Undesired reactions in LIBs can appear in either the positive or the negative electrode. The use of additives enhances significantly the stability and expels HF or water. Additives correspond less than 10 % of electrolyte's formulations. Vinylene carbonate (VC) is widely used as additive in many commercial cells, lengthen the number cell's cycles and reducing the undesirable irreversible capacity loss. With the increasing demand on LIBs and the new application of electric mobility, the additives in electrolytes play a decisive role.

2.1.6 Batteries Forms

Three major cell types can be distinguished to meet the wide battery demand: cylindrical cell, prismatic cell, and pouch cell (see Figure 2-2) (YOSHIO ET AL. 2009). Their parameters of design depend mostly on cell's type, for example, the charge can go from 0.1 A h to 160 Ah, or the fact that the layers in small cells are mostly wounded while in large ones are flat plate constructions more common. Although the ideal geometric form for big cells, i.e., more than 1 Ah, remain in controversial discussion, some tendencies are being manifested according to the application. Otherwise, in little marked cells, the use of pouch cells predominates undoubtedly (BIRKE & SCHIEMANN 2013). The developed designs at the *iwb* are prismatic-flatted and pouch cells.

Cylindrical Cell

Cylindrical cells are the most common in the field of small applications, used for instance on consumer applications. Even though there are examples for BEVs using cylindrical cells, like Tesla Motors, due to their reliable and economic manufacturing process (SAUER 2010). The most used cells in the

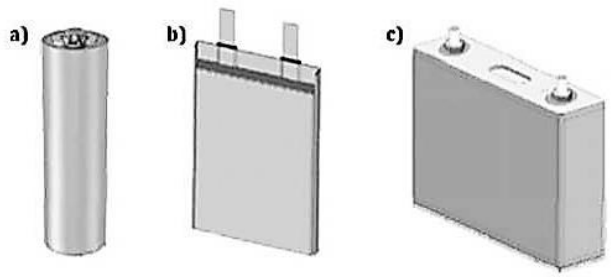

Figure 2-2: Lithium-ion cell types: (a) cylindrical cell, (b) pouch cell, and (c) prismatic cell (FINK 2010)

automobile field are the known 18650 (LIENKAMP 2014, JOSSEN & WEYDANZ 2006).

The layers are wounded inside an aluminum, or an injection molded plastic, or a stainless steel case. Most available cells employ nowadays a header that incorporates disconnecting devices, which are automatically activated by pressure or temperature, such as a safety vent or a PTC[1] switch (BRAIN 2006). The most remarkable features of cylindrical cells are:

- Cheap production
- High energy density
- Mechanical stability
- Demanding cooling

Prismatic Cell

Most automobile OEM[2]s opt for prismatic cells, as well as cylindrical too, because of the safety properties their hard cases provide.

In prismatic cells, the layers are assembled in flat layers, being mounted one next to each other and intercalated. Every electrode's plate has a tab, which is bundled together and welded to its respective terminals. The main difference with the disposition of layers is illustrated in Figure 2-3. The housing is a deep-drawn metal can that incorporates on the cover an electrolyte filling port, connection terminals, and a rupture disk that is broken with an unusual rise of pressure. (COUSSEAU ET AL. 2006, REDDY 2010, SAUER 2010)

[1] Positive Temperature Coefficient

[2] OEM: Original Equipment Manufacturer

The main features for prismatic cells are:

- Good cooling properties
- Easy integration to a battery pack
- Efficiently use of space
- Expensive production

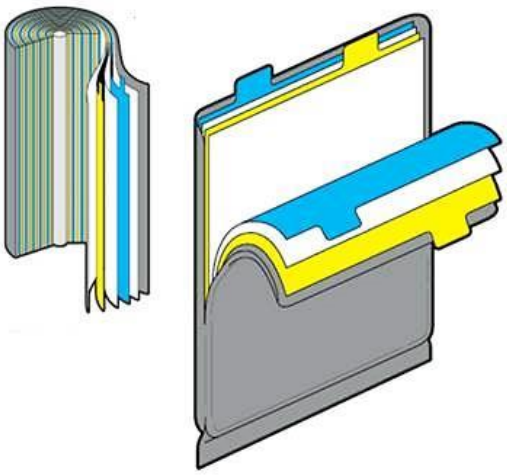

Figure 2-3:Comparison of layers disposition in cylindrical cells and prismatic cells (COLWELL 2011)

Pouch Cell

Cells marked as pouch cells, are a regular lithium-ion cell mounted in a flexible package. This case is a compound-foil made of a heat-sealable aluminized plastic, using heat or ultrasonic welding. The cells are assembled like prismatic cells. The major weakness of pouch cells is their lack of a safety vent. This type of cells are primarily addressed to applications requiring a thin rechargeable battery, like portable communications and computing devices. Nevertheless, this cell is also an interesting option for automotive applications due to its high energy density, especially resulting from the substitution of the hard case. (KURFER ET AL. 2012)

The most relevant characteristics of pouch cells are:

- High energy density
- Compact and light design
- Distortion of vibrations (BIRKE & SCHIEMANN 2013)
- Excellent cooling properties

- Cheap and simple production
- Impermeability problems (LIENKAMP 2014)

2.1.7 Cell Manufacturing

The manufacture of electrodes, cells and modules for large-format power batteries is still in its infancy. To assure a successfully future for LIBs, the operations need to become faster and less expensive. These costs and times savings cannot come from deteriorating cell's quality, since the security of them would be at stage. The solution lies on fully automated and integrated production lines (SIEMENS AG 2014).

Lithium-ion cells complete manufacturing process splits in four defined phases represented in Figure 2-4 the one for pouch cells.

First, basic materials are prepared, such as the anode and cathode active compounds and the electrolyte. These materials determine the electrical and chemical properties of the cells. In the second phase, wrought materials are manufactured. Anode and cathode coils are produced using coating processes. The active materials, mixed up in solvent, binding agents, and conductive additives, are coated on an aluminum (for the cathode) and a copper (for the anode) foil. The finished foil is expected to have a thickness between 150 and 300 µm, hence the foil is intensively revised during this phase. The goal of this process is the fabrication of continuous, homogeneous and smooth electrodes (SCHUH ET AL. 2012). After the coating, the active layer is heated in order to dry out the solvent and to fix the coating on the foils. After that, the sheets are compressed, reducing the surface's roughness, homogenizing the whole foil, and giving the desired porosity. (SIEMENS AG 2014, WAKIHARA 2001, KNOCHE 2012)

In the third phase, the cell is assembled. The central process is the building of the cell stack. There are a few strategies to intercalate the three layers. At *iwb* has been chosen the z-folding with single electrodes (see Figure 2-5). Once the stack is built up, the cell is assembled joining the current collectors with ultrasonic welding, housing the cell stack in compound sacks or in aluminum cases, filling the cell with electrolyte, and sealing it. In this stage, a water-free production is a very important issue. Thus, cell assembly takes place in

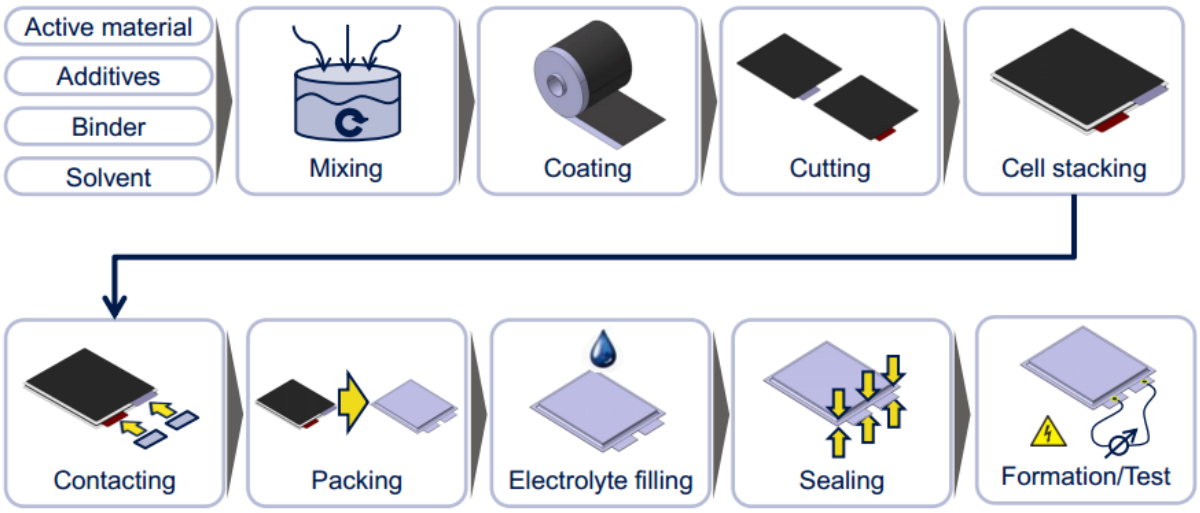

Figure 2-4: Process chain of a pouch-cell production at iwb (KNOCHE 2013A)

climate chambers with low humidity of about 0.1 %. (WOODBANK 2014, SCHUH ET AL. 2012, REINHART ET AL. 2013)

The fourth phase contains the start of operation of the cell. This means that the cell is charged for the first time, i.e., formation. During this process the "solid electrolyte interface" (SEI) is formed, which is highly responsible for the operation quality and the cycle stability of the ultimate cell. Afterwards, this is aged and tested in defined procedures (KURFER ET AL. 2012).

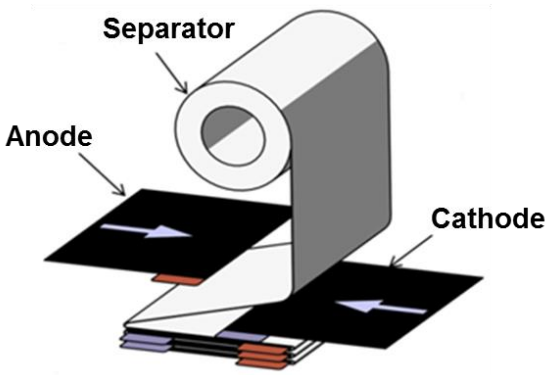

Figure 2-5: Z-folding with single sheet electrodes (REINHART ET AL. 2013)

Electrolyte Filling and Wetting

The process to fill and wet a cell with electrolyte is a technologically sophisticated and a crucial process for the functionality and quality of the cell. It is complicated all the pore volume of the layers must be homogeneously

soaked with electrolyte, to reach cell's designed capacity and planned service life. An incomplete wetting leads to dry spots that do not contribute to battery's capacity and represent sources of accelerated aging and degradation (see representation of Figure 2-6).

In order to enable the correct wetting of the pores, the air located in them must be removed. Then, a needle injects the electrolyte into the cell. This process can be done under both vacuum and atmospheric pressure conditions. A complete wetting is more probable to be achieved under vacuum conditions, since there is less air inside the pores. The actual process requires a period of 12-24 hours to achieve the appropriate wetting under vacuum. Some applied pressures go below 50 mBar to reduce the process's time to the minimum. (WOOD ET AL. 2015)

For this reason, the filling is a time-critical action, and thus one of the limiting steps of cell manufacture. The procedure mainly depends on the cell's type and the physical-chemical properties of layers and the separator and the electrolyte. Further challenges for the wetting process are the toxicity of this, the danger of explosion when it reacts with water, the possible inclusions of gas inside the cell, and the quantity of electrolyte to be introduced (KNOCHE 2013). All processes that manipulate electrolyte must be carried out in a dry room with humidity values near to zero. On the contrary, the electrolyte could react with water, causing the decomposition of $LiPF_6$ into hydrofluoric acid (HF) (WOODBANK 2014).

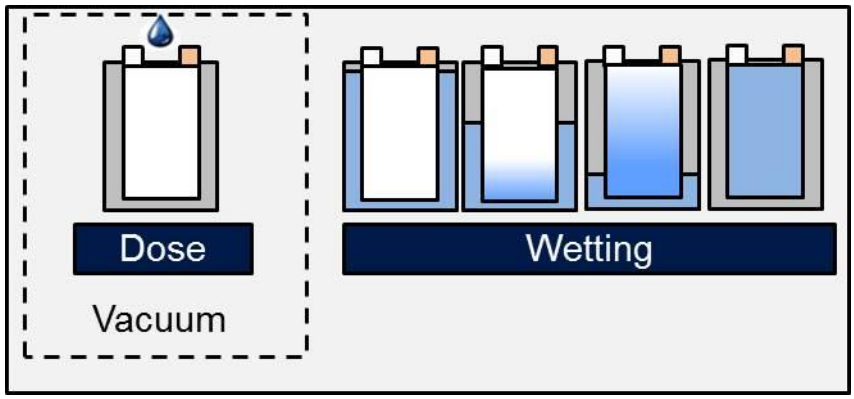

Figure 2-6: Filling process: first, the cell is dosed under vacuum conditions, and then it is proceeded to the wetting process (KNOCHE 2013)

2.2 Wetting Phenomena

The term wettability can be defined in different ways depending on the application's field and the reference describing it. Wettability is defined as "the tendency of one fluid to spread or adhere to a solid surface in the presence of other immiscible fluids" ANDERSON (1986). According to ISO norms, absorbency is described as "the ability of a paper or board to take up and retain a liquid with which it is in contact " (Norm ISO 4046). In ERBIL (2014), wetting refers to the study of macroscopic manifestations of intermolecular interactions between contacting liquids and solids.

There are few methods to measure how a liquid interacts with a solid; the problem is the difficulty of their appliance and the lack of accuracy in most of them (ABDALLAH ET AL. 2007). The knowledge of how a solid material surface wets is usually characterized with the contact angle between solid and liquid interfaces. Nonetheless, the measurement of contact angles is complicated and demanding for direct methods such as sessile techniques and the Wilhelmy balance method. The capillary rise technique, however, is extensively used to measure the contact angles of small particles and porous materials, whose is based Washburn's equation (LUO ET AL. 2014).

On the specific field of cells, there is no standard method to evaluate the wetting phase; there is a lack of information and literature about the topic.

Already existent physical methods and tests to measure how a liquid spreads are described at this section.

2.2.1 Contact Angle

Considering a liquid drop resting on a flat and horizontal solid, there are three different phases present with their surface tensions (see Figure 2-7): solid-liquid, liquid-gas, and solid-gas. Therefore, the contact angle is defined as the angle formed by the intersection of the liquid-solid and the liquid-vapor interfaces, geometrically acquired by applying a tangent line from the contact point along the liquid-vapor interface in the droplet profile. Young's equation (2.3) gives the thermodynamic equilibrium of the drop under the three interfacial tensions, where $\gamma_{SV}, \gamma_{SL}\ and\ \gamma_{LV}$ represent the interfacial tensions between phases, and θ the contact angle.

Figure 2-7 illustrates how a small contact angle looks when a liquid spreads on a surface. Contact angles greater than 90º mean that the fluid minimizes its contact with the surface, i.e., repulsiveness. Thereby, complete wetting occurs when the contact angle is zero. The interface where solid, liquid and vapor co-exist is called “three-phase contact line”.

$$\gamma_{SV} = \gamma_{SL} + \gamma_{LV}\cos\theta \qquad (2.3)$$

In general, contact angles’ values depend on the measuring method and on the physical and chemical properties of the surface (SCHMITT ET AL. 2014). For their measurements is frequently demanded either visual or mathematical extrapolations of the macroscopic interfaces (BONN ET AL. 2009).

Techniques and tests to measure contact angels are explained in the following.

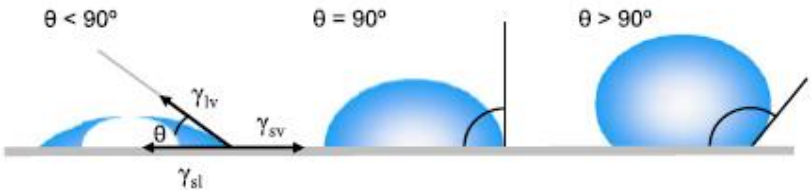

Figure 2-7: Illustration of contact angles formed by sessile liquid drops on a smooth homogeneous solid surface (YUAN & LEE 2013)

Goniometer- Camera

The simplest and most widely used technique to measure contact angles is a direct measurement of the tangent angle at the three-phase contact point on a sessile drop profile. The equipment consists of a horizontal stage to mount the sample, a micrometer pipette to form a liquid drop, an illumination source, and a telescope equipped with a protractor eyepiece. The angle is acquired aligning the tangent of the sessile drop profile at the contact point with the surface and reading the protractor through the eyepiece.

Nowadays, a high-resolution camera captures the picture and then is analyzed with a goniometer or an image-analysis software. Figure 2-8 shows an actual Goniometer.

Advantages for this method are the possibility to take samples in a wide range of temperatures, its high precession, and the possibility to observe θ variations during long periods. However, the method has experimental shortcomings,

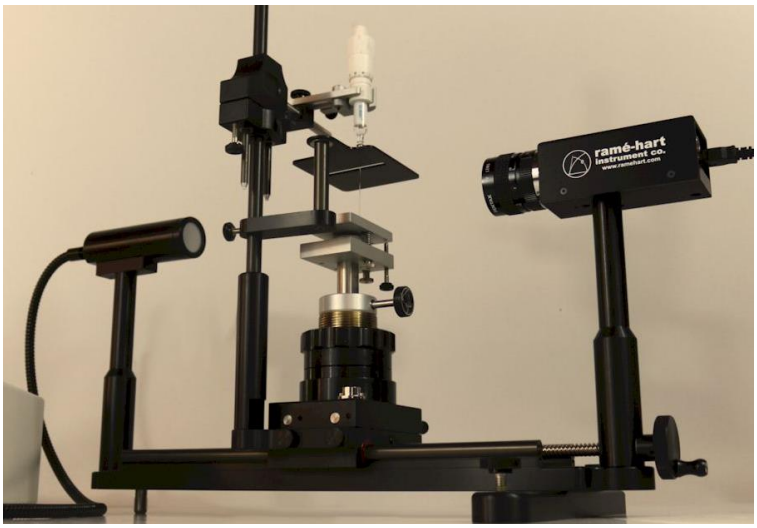

Figure 2-8: Advanced goniometer, with the camera, light source and drop plate (RAMÉ-HART INSTRUMENT CO.)

such as the required pricey system and the variation of the angle due to interactions with external agents, like evaporation, representing a great uncertainty on the outcomes. (RODRÍGUEZ GARCÍA-CEBADERA 2010, ROSANO ET AL. 1971)

An alternative way to obtain the contact angle is analyzing the drop shape. A balance between surface tension and external forces is reflected mathematically in Laplace's equation of capillarity. Surface tension tends to minimize the surface area making the drop spherical, while gravity deforms the drop in two ways: elongation a pendant drop or flattening a sessile drop. During the early years of contact angle measurement, this method was widely employed to analyze the profile of a sessile drop, which was assumed to be part of a sphere. Geometrically, the contact angle can be calculated by measuring the drop diameter *d* and the height of the peak *h*, (2.4), represented in Figure 2-9.

$$\frac{h}{d} = \tan\frac{\theta}{2} \qquad (2.4)$$

This method yields reasonable results when the liquid drop is extremely small. However, the spherical shape assumption cannot be applied if the drop shape is large enough to be affected by gravity.

If this technique would focus on cells field, a drop would be placed on a single layer. Tests are recommended to be done on different types of separators or electrodes with distinct porosity percentages and materials (Norm DIN 55660-1). The whole montage could be placed inside a pressure-controlled chamber and change However, this test would not appropriate for observe a spreading process through the pre-packed layers.

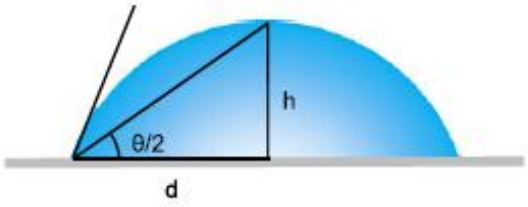

Figure 2-9: Demonstration of the θ/2 method according to geometrical relation (2.4) (YUAN & LEE 2013)

Tilting Plate Method

In this method, a solid plate with one end gripped above the liquid is rotated toward the liquid surface until the end of the plate is immersed in the liquid. This forms a meniscus on both sides of the plate as illustrated in Figure 2-10. This method is used to measure small contact angles. The main advantage of this technique is the simultaneous determination of the advancing and receding motions. Advancing motion refers to the advance move of the triple line to formerly non-wetted area, and by receding motion to the retraction of the triple line to formerly wetted area (SCHMITT ET AL. 2014).

This method has no direct application on the cell's spreading phenomena, since the layers are not rigid enough nor are the conditions appropriate for vacuum appliance. This test measures the dynamic contact angles when a solid is totally immersed into a liquid. The desired work's objective is to observe the interaction between liquid and layer during the absorption, represented with static contact angles.

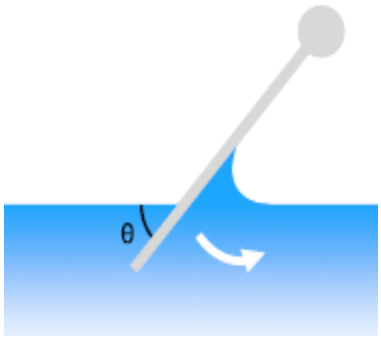

Figure 2-10: Tilting plate method, where θ is the contact angle (YUAN & LEE 2013)

Wilhelmy Balance Tensiometry

The Wilhelmy balance method is with the goniometry the standard and most popular techniques to measure contact angles. When a thin, smooth, vertical plate deeps into a probe-liquid pool, a balance detects the change in its weight (see Figure 2-11). The detected change of force is a combination of the buoyancy and the force of wetting. The wetting force f is defined in (2.5), where γ_{lv} is the liquid surface tension, p is the perimeter of contact line and θ is the contact angle. Consequently, the total detected force change F on the balance is formulated in (2.6), where W is the weight of the plate, V is the volume of the displaced liquid, $\Delta\rho$ is the difference in density between the liquid and air, and g is the acceleration of gravity. (AL-SHAREEF ET AL. 2013)

$$f = \gamma_{lv} p \cos\theta \tag{2.5}$$

$$F = w - \gamma_{lv} p \cos\theta - V \Delta\rho g \tag{2.6}$$

As the solid sample is pushed into or pulled out of the liquid, an advancing or receding contact angle can be established respectively. The entire process appears in Figure 2-12. The cycle divides in 4 steps: (1) the sample approaches the liquid, being the force zero. (2) The sample is in contact with the liquid surface, forming a contact angle below 90°; therefore, the liquid rises up, causing a positive wetting force. (3) The sample is further immersed, and the increase of buoyancy causes a decrease in the force; the force is measured for the advancing angle. (4) The sample is pulled out of the liquid

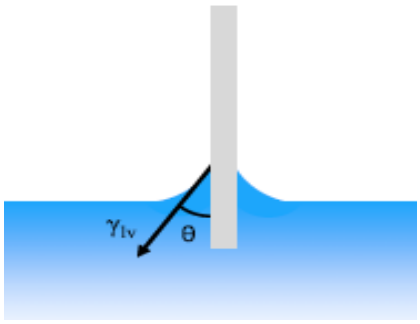

Figure 2-11: Wilhelmy balance method, where θ is the contact angle (YUAN & LEE 2013)

after having reached the desired depth; the force is measured for the receding angle.

This technique has several advantages over conventional optical methods. The task to be done during the tests is to measure the weight and length of the sample, which can be performed with high accuracy. Another is that the measured force at any given depth of immersion is already an averaged value. In addition, the graph produced by this technique (*Figure 2-12*) is useful to study dynamic contact angles and contact angle hysteresis at different wetting speeds. It is even possible to study absorption or surface reorientation by repeating the submersion circle. However, the method also suffers from several drawbacks: it is only appropriate when both sides of the sample have identical compositions and topographies. Rods, plates, and fibers with known perimeters are ideal samples, but it is sometimes difficult to measure the perimeter and the wetted length precisely.

This is not the appropriate way to measure the wetting behavior of the cell layers, for equal reasons as for the tilting plate.

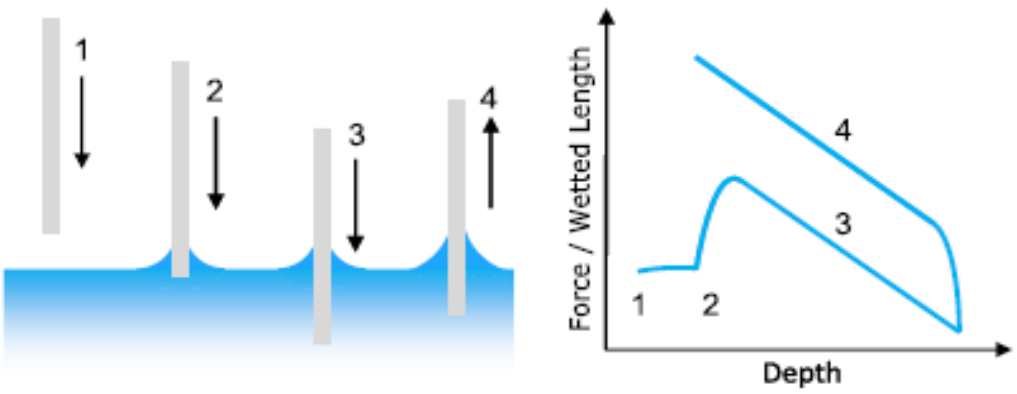

Figure 2-12: A submersion cycle for the Wilhelmy balance (YUAN & LEE 2013)

Capillary Tube

In circumstances when both the inside and outside surfaces of the capillary tube are made of the exact same material, the Wilhelmy balance method can be used for measuring the contact angle. This test gets the surface tension with the measure of the meniscus' angle formed on pipe's face. For a vertical tube with a sufficiently narrow circular cross section, the meniscus is considered spherical, and the surface tension, γ_{lv}, is given in (2.7), where h is the capillary rise, r is the tube radius, g is the acceleration constant of gravity, $\Delta\rho$ is the difference in density between the liquid and vapor and θ the contact angle. Its representation is in *Figure 2-13*.

$$\gamma_{lv} = \frac{r\Delta\rho g h}{2\cos\theta} \qquad (2.7)$$

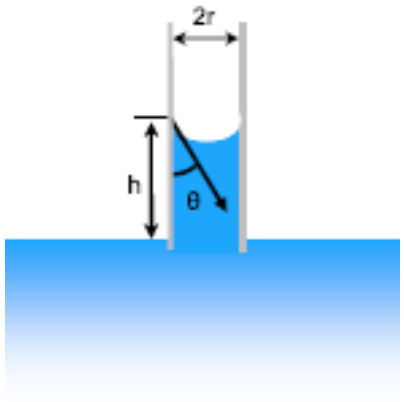

Figure 2-13: Illustration of a capillary tube immersed in a liquid (YUAN & LEE 2013)

In large-diameter tubes, this rise in the liquid level is unnoticeable. However, in very small-diameter tubes, the cohesive forces can draw the liquid upwards appreciable distances (STAVE & CHUAN-HUA 2014).

2.2.2 Wetting Time

Wetting time could be defined as the time that a drop needs to be completely absorbed in a surface. This state is reached when the contact angle measures θ=180º. The contact angle is measured using the same technique as in the goniometer-camera test (see section 0). The advantage of this variant is the

compensation of the rest of variables that can distort the outcome, when different tests are done.

One variant for this test can be found in (ROFFAEL ET AL. 2002), where the time of wood fibers are tested and compared. Different wood types were produced, and then calculated the time until the water drop is totally absorbed by them.

2.2.3 Klemm Method

This method determines the capillary rise of papers after clamping, suitable for papers with relatively high porosity. This test is carried out to calculate a relative wettability value through measuring the height achieved by distilled water.

First has to be cut 10 samples of papers of minimum 200 mm length and 15±1 mm wide. A line from 15 mm of one end is painted to subject them between this line and the end. The samples are dipped until the mark in a tank with distilled water at 23±1 ºC during 10 min ±10 s. After this time a Cathetometer or a measuring stick will measure the height in *mm* of the capillary rise (Norm DIN ISO 8787).

This test can be done with others materials and in two variants: calculate the achieved height, or the time needed to achieve a specific height. To obtain correct comparisons, the experiment conditions should be identical for all samples. The method is easy to do and not sophisticated to repeat. Some of this variants can be read in (SALGADO 2005), where it is used a blue ink made of a methylene solution through intern surface of a rock.

This method is besides being easy and non-demanding, appropriate to study the spreading of the electrolyte in layers. Although the procedure was done with a single sheet, it could be applied to more. The required montage is not as demanding as most methods.

2.2.4 Determination of Water Absorption by Norm ISO 5637

This method is described for all types of paper that had been treated to give some degree of resistance to water absorption. The agent applied is distilled or deionized water at 23±1 ºC in a tank of water large enough to hold at least

ten pieces in a vertical position and thermostatically controlled without circulation and conditioned in a relative humidity of about 50 %.

The test pieces shall be cut measuring 200±1 mm x 250±1 mm, and cut at least ten and select five randomly. Each dry-test-piece is weighted in a pre-weighed PE bag with an accuracy of ±0.01 g. Then, the test pieces are immersed vertically in the tank, with the longer side vertical and the upper edge 25±3 mm below the surface. The test pieces have to be removed from the water after 5 min ±15 s. of immersion. They are vertically held from one corner to allow the water to drain off for 2 minutes. After that, the tests are returned to their PE's bags and repeat the mass determination on each one.

Once both determinations are done, the water absorption comes in grams per square meter. With formula (2.8) the water absorption, where m_1 is the mass in grams of the test piece before the immersion, m_2 the mass in grams of the test piece after the immersion for the specified period, and 20 the number of test pieces per square meter (Norm ISO 4046).

$$(m_2 - m_1)\ x\ 20 \qquad (2.8)$$

The appliance of this test on cells is simple and not much effortless. The drawback remains on the impossibility to apply vacuum conditions and the evaporation of the liquid before weighting them.

2.3 Methods' Evaluation

The explained tests and methods have different positive and negative points. As mentioned in section 2.1.7, on the filling process of a cell a syringe introduces the electrolyte into the cell's case in vacuum conditions. The vacuum accelerates the process time, and avoids dry zones and the intrusion of undesirable particles (KORTHAUER 2013). The ideal would be to find a method that could perform like the real process does. For this reason, the explained methods have been rated based on different criteria that are crucial for the spreading phenomena in cell layers. The test has to achieve a high precision grade, as well as this cannot be extremely demanding in what refers to resources and simulation complexity. The results are expected to be concise and no much depending from uncontrollable factors. As the cells are composed for different sheets, the method has to be able to consider the whole pack. The samples will be tested under changing conditions of pressure and temperature. Finally, a quantity of electrolyte is introduced during the process. Therefore, the method has to be suitable for being tested with larger quantities than one single drop.

Table 1 shows a comparison among the methods explained on the previous chapter under different chosen criterions. In the Table 1 every method is grades from "--" to "++", being "++" the most favorable punctuation, and all methods enumerated from A to G as follows:

A. Goniometer and drop shape
B. Tilting plate
C. Wilhelmy balance tensiometry
D. Capillary tube
E. Wetting time
F. Klemm method
G. ISO 5637

LIBs are filled in vacuum conditions due to avoid air inside the pores and to shorten wetting's time. Thus, the developed method should be appropriate to simulate under vacuum conditions, with the layers under a compression case, resembling to the real assembly. Moreover, the layers have to be viewed during the whole wetting process due to study how the electrolyte spreads. As well as being feasible and not so much costly, in what time and money refers,

the method is also required to be accurate. The criterion “wetting process adaption” takes into consideration all the conditions that are in this work looked for.

Table 1: Methods‘ evaluation

	Methods						
Rating criteria	**A**	**B**	**C**	**D**	**E**	**F**	**G**
Accuracy	+	-	-	0	-	+	+
Setup Complexity	--	+	0	+	--	++	++
Variability	--	0	-	--	-	+	+
Demand to do the tests	0	-	+	+	-	+	++
Allows multilayer	-	--	0	--	-	+	++
More than one drop	--	++	++	++	--	++	++
Controllable conditions	0	--	-	0	0	+	-
Wetting evolution	+	-	-	--	+	++	0
Wetting process adaptation	-	-	0	-	-	+	+

After the evaluation for all the methods, it has been reached the conclusion that no existing method fits perfectly to the application in the field of batteries.

With the existence of two methods with favorable results, specifically the Klemm Method and ISO 5637, it was thought to find an alternative way, relied on these two, for the research on electrolyte’s diffusion. Therefore, the proposal for the applied method is relied on the principle of the Klemm method, which lets the liquid being soaked by the layers during a determined period. After that, the reached high of the liquid is measured.

The already developed method is presented in Chapter 4 and the improvements applied to this are in the 5th.

3 Design of Experiments and Statistical Interpretation

In any information-gathering process where variation is present, a design for the planned experimentation is needed, whether under the full control of the experimenter or not (JOHN WILLIAM MEREDITH, PETER 1998). A Design of Experiments (DoE) is a well selected a set of combinations that has to be performed by the experimenter. The aim of an experimental design is to optimize a process or system by performing each experiment and to draw conclusions about the significant behavior of the studied object from the analyzed data. Minimizing the amount of performed trials is always an aim in DoE, obtaining the maximal information with the minimum number of resources, meaning time, money, raw materials, and others. With DoE, the most informative combination of the levels' factors is chosen, hence DoE is an effective and economical solution (PRAT BARTRÉS 2004, ERIKSSON ET AL. 2000).

PRAT BARTRÉS (2004), ERIKSSON ET AL. (2000) and WU & HAMADA (2000) are the main three fonts of information that this chapter is based on.

3.1 Descriptive Statistics

The analysis of the responses acquired in a set of observations is a fundamental requirement in most research work. The most commonly used numerical measure to know the central tendency of a sample is the sample mean. The mean or average of a set of values is the total of the data values divided by the number of observations. Symbolically, if $y_1, y_2, \dots, y_n$ denote *n* data values, the sample mean, denoted $\bar{y}$, is

$$\bar{y} = \frac{\sum y_i}{n} = \frac{y_1 + y_2 + \cdots + y_n}{n} \qquad (3.1)$$

The most common dispersion measures for a set of values are the standard deviation (StDev) and the variance. The StDev, *s*, and the variance, s^2, of a set of data values $y_1, y_2, \dots, y_n$ are calculated as

$$s = \sqrt{\frac{\sum (y_i - \bar{y})^2}{n-1}} \qquad (3.2)$$

$$s^2 = \frac{\sum(y_i - \bar{y})^2}{n-1} \tag{3.3}$$

$$s_R^2 = \frac{(n_1 - 1) \cdot {S_1}^2 + (n_2 - 1) \cdot {S_2}^2 + \cdots + (n_N - 1) \cdot {S_K}^2}{n_1 + n_2 + \cdots + n_N - K} \tag{3.4}$$

When the number of replicas for each experimental condition are different, the variance s_R^2 is expressed as in (3.4), where $n_1 + n_2 + \cdots + n_N - K$ are the degrees of freedom, *K* the number of experimental conditions, and n_i the number of replicas for each experimental condition. StDev is more used than variance because the units from the first are the same as *y.*

Another concept to take into account is the confidence interval (CI). A CI consists of a range of values that acts as a proper estimator to express the degree of uncertainty associated with a sample. The interval within the parameter would be expected to misbelieve, represented in Figure 3-1 in gray. Assuming that *θ* is an unknown parameter, two statistics *L* and *U* are needed to find an interval estimation for *θ,* such that the probability statement (3.5) were true. The interval (3.6) is called a 100(1-α) percent confidence interval for the parameter *θ*.

$$P(L \leq \theta \leq \mathrm{U}) = 1 - \alpha \tag{3.5}$$

$$L \leq \theta \leq \mathrm{U} \tag{3.6}$$

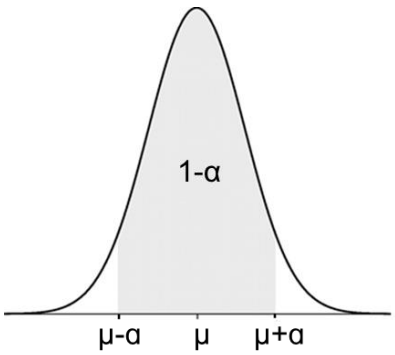

Figure 3-1: Theoretical distribution of a sample and its CI. The interval [μ-a,μ+a] covers 100(1-α)% of the sample means (CURRAN-EVERETT 2009)

The statistics *L* and *U* are called the lower and upper confidence limits, respectively, and *α* the significance level. A significance level of 0.05 reflects 95 % of confidence. (FIELD 2013, MONTGOMERY 2013)

Greater levels of variance yield larger confidence intervals and higher confidence percentage. A CI of 95 % has a larger range than a one of 90 %.

3.2 Factors and Responses

There are always two types of variables when experiments in the field of DoE are performed: factors and responses. Like represented in Figure 3-2, the responses or outputs give information about the investigated process, and the factors or inputs manipulate the responses. The process or system to study is a repeatable series of actions that results in an observable characteristic or measurement.

There is no existence of a totally determined system, meaning that when an action is repeated on a system, not always is the same result got. Then, any system could be represented with a determined part and a random part, or noise. In equation (3.7) is represented the equation for a model, where *Y* is the system's response, x_n the variables that explain the deterministic part, and ε the random part.

$$Y = f(x_1, x_2 \dots x_N) + \varepsilon \qquad (3.7)$$

When defining a relevant process of interest, the exact experimental conditions under which the observations are to be collected must be defined. Factors can be established in two or more values, also called levels (MASON ET AL. 2003). They are divided into three groups depending on different criteria.

3.2.1 Controllable and Uncontrollable Factors

Controllable factors are normal process factors that are easy to monitor and investigate. The experimenter can observe and change them. By contrast, an uncontrolled factor is hard to control because it is mostly a disturbance value or an external influence. Uncontrolled factors can have a high impact on the response and therefore should always be considered during the experiments.

The temperature inside a chamber is a good example of a controlled factor. In contrast, the ambient temperature is an uncontrollable factor, which is often not possible to completely eliminate its variations.

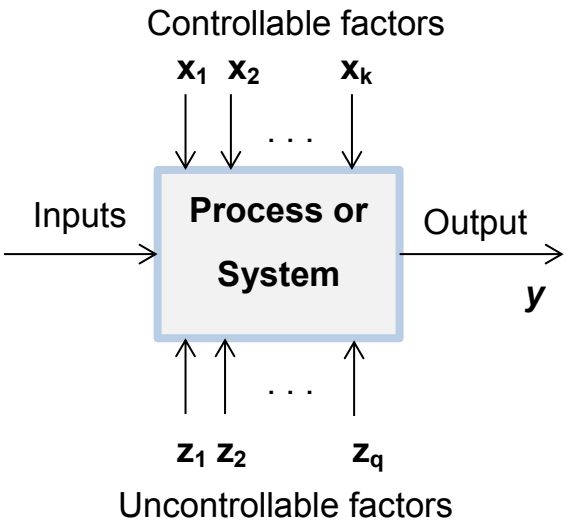

Figure 3-2: General modeling for a process or system

3.2.2 Quantitative and Qualitative Factors

The values of a quantitative factor have a given range and a continuous scale of values, whereas qualitative factors have only distinct values. For example, in a study of fuel economy, vehicle type and type of fuel are qualitative factors; ambient temperature and humidity are quantitative factors.

3.2.3 Process and Mixture Factors

Process factors can be changed independently and do not influence each other. They are normally expressed by an amount or level and can be seen as regular factors. Mixture factors stand from the amounts of ingredients in a mixture. They all are part of a formulation and add up to a value of 100 %. A mixture factor cannot be modified independently, so special designs are needed to deal with this type of factors.

3.2.4 Responses

A response is the general condition of a studied system during the change of the factors. It is possible and often useful to measure multiple responses that react differently to the factor adjustments. A response can be either a continuous or a discrete value. A discrete scale can be for example an ordinal measurement with three values (good, OK, bad). As these values are hard to process, it is always recommended to use a continuous scale.

3.3 Experimental Designs

As said above, the selected set of points in a DoE has the objective to gain maximal knowledge about the behavior of the system or processes with the minimum usage of resources. This selection seeks always to meet a commitment between experimental complexity and results accuracy.

A DoE approximates the reality with the help of a mathematical approach. Although this is never completely right, it helps to transport the complexity of the reality into an equation easy to handle, as the one showed in (3.7). The selection of the model is an important step during investigation. Aside from the linear approach, the simplest, there are other mathematical representations such as interactions or quadratics models.

3.3.1 Sequential

Traditionally, the experiments have been done through an intuitive approach, changing the levels of one single factor at a time until no further improvement was met. Figure 3-3 illustrates how complicate the acquisition of an optimum could be with the called COAT approach (*Change Only one Separate factor at a Time)*. This strategy is not the adequate, since the correct way would be to test all possible combinations, only by this could be detected the step's directions and achieve the peaks and the valleys. In the given situation from Figure 3-3, the experimenter does not know at which value of factor x_1 should be stopped because a further improvement cannot be observed with COAT. If this example had used a DoE, a special set of experiments would have been created around the so-called center-point.

The concept is to arrange a symmetrical distribution of experiments around a center-point, obtaining by this the tendencies of the response.

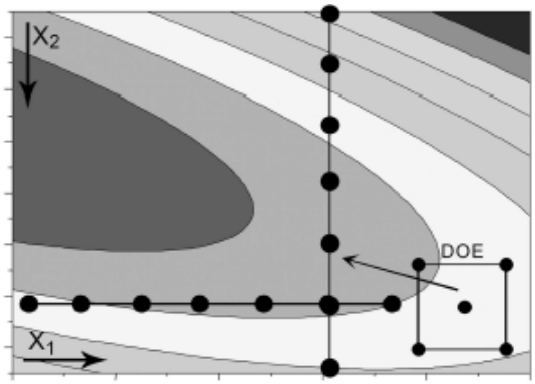

Figure 3-3: COST approach and DoE (ERIKSSON ET AL. 2000)

3.3.2 Full Factorial

In full factorial designs all the possible combination of variables and levels are included on the DoE. This type of designs has some advantages: it permits to approach an optimal point, to estimates interactions, and to provide estimations of the variable effects with a reduced variance. Even though it requires a huge amount of experiments, this drawback can be solved with the use of two-level factors (see page 32).

The total number of elemental experimentations to carry out on a factorial design is provided by the expression n^k, where *n* are the levels taken by each factor, and *k* the total number of factors. It can be also the case where the number of levels was not the same for all factors. For example, considering a study with four factors with two levels and five with three levels, the design would have $2^4 3^5$ elemental experimentations.

Two Level Factorial Design

The first cube showed in Figure 3-4 is a full factorial design with two levels of investigation, also represented as 2^k designs. 2^k designs are with wide difference among other designs, the most used designs. In this case, the level values are codified as *-1* for the low level and *+1* for the high level, being the

factor quantitative or qualitative. There are mainly three reasons why the 2^k designs are so diffused:

- They provide an excellent relation between the experimental effort and the information obtained
- are simple to build, to execute, to analyze and to interpret
- and can be easily combined to end up to more complex designs.

The models whose factors only have two levels are limited to lineal relations.

Once the factors and the levels for each factor are decided, it proceeds to create the design matrix. This contains all the combinations among all factors and levels, and is represented with standard order (see Table 2) to avoid an omission or repetition of any combination.

Table 2: Design matrix in standard order for a 2^3 design

EXP (y_i)	A	B	C
1	-1	-1	-1
2	1	-1	-1
3	-1	1	-1
4	1	1	-1
5	-1	-1	1
6	1	-1	1
7	-1	1	1
8	1	1	1

One of the most straightforward designs to implement is the completely randomized design, in which all the factor-level combinations in the experiment are randomly assigned to the sequence of test runs. Randomization is important in any experimental design because this protects the experimenter from the influence of not considered variables on the response, which possibly affects the evaluation and interpretation of results. Whenever it is possible and does not cause any serious problem or high additional cost, the experimentation order must be randomized.

3.3.3 Fractional Factorial Designs

Fractional designs allow to study designs with a big number of factors with a smaller number of experiments than a full factorial. Fractional designs do not consider all possible corners and reduce the number of designs choosing only a fraction of these. Figure 3-4 shows in the second cube an example, where

only four out of eight points are investigated. These experiments used the nomenclature n^{k-p}, where *n* is the number of levels, *k* the factors, and *p* the fraction's grade. Every added *p* grade reduces the number of experiments. Consequently, some factors' interactions are assumed to be zero, meaning a smaller resolution. For example, a design with seven two-level-factors and a fraction grade *p* equals 3, the third grade effects and greater and some of second grade are not taken into account.

3.3.4 Composite Designs

This last type combines the tests included in a factorial design, the corners and replicated center-points. The designs that include the center point are also names called "central composite designs". These allow the estimation of curvature, fitting full quadratic models. Figure 3-4 shows an example of three factors where axial experiments are placed on the six squares.

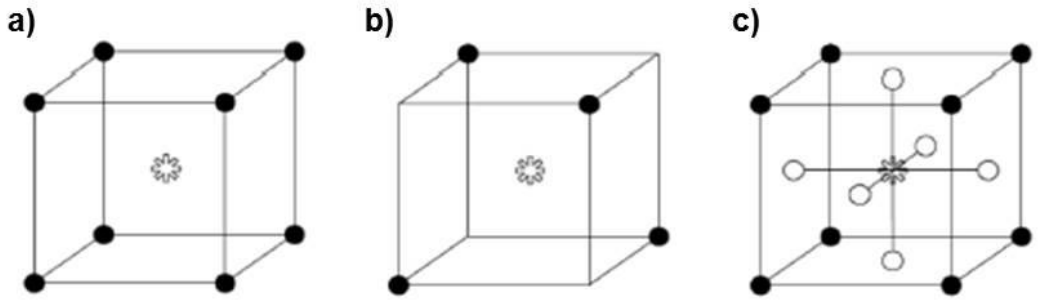

Figure 3-4: Comparison of statistical designs. Design (a) shows an example of a full factorial design, design (b) shows a fractional factorial, which considers only a fraction of design points, and design (c) shows a central composite design with six additional axial experiments (ERIKSSON ET AL. 2000)

3.3.5 D-Optimal Designs

The previous points were an introduction to basic principles of DoE and the purpose of three standard designs for regular experimental areas. Besides these designs, other alternatives are useful in certain situations. The present thesis deals with a D-optimal design, which is aimed to be used when the

experimental region is not regular in shape and when the number of runs is too large (TRIEFENBACH 2008).

A D-optimal design is a computer-aided approach containing the best subset of all possible experiments following a determinant criterion. First, the problem has to be established and the candidates points be known. Given a number of design runs and a selected criterion, a selection process creates the *best* possible design with all candidate points (TRIEFENBACH 2008). Mathematical criteria are useful to choose a good sets of candidates (AGUIAR ET AL. 1995), which will be explained in the section of page 37.

Matrix of Candidate Points

The candidate set is a matrix that contains all possible combinations, where each row represents an experiment and each column a variable. This so-called matrix of candidate points has *N* rows and is represented by ξ_N. From this matrix will be chosen the best combinations, resulting to a matrix represented by ξ_n for a set of *n* points. This selection is done following a criterion, which is explained at the page 36. (AGUIAR ET AL. 1995, TRIEFENBACH 2008)

Model Matrix

The design matrix *X* is a *(n x p)* matrix, where *p* is the number of coefficients in the model. With a given approach and a candidate matrix, the construction of the design matrix is simple. Each column contains a combination of the factors from the candidate set, depending on the terms in the model. The regressions can be either linear, linear with interactions, quadratic or quadratic with interactions, among others. Equations from (3.8) to (3.11) show the different models respectively for a two-factor design.

$$Y = b_0 + \sum_{i=1}^{k} b_i x_i + \epsilon \qquad (3.8)$$

$$Y = b_0 + \sum_{i=1}^{k} b_i x_i + \sum\sum_{i<j} b_{ij} x_i x_j + \epsilon \qquad (3.9)$$

$$Y = b_0 + \sum_{i=1}^{k} b_i x_i + \sum_{i=1}^{k} b_{ii} {x_i}^2 + \epsilon \qquad (3.10)$$

$$Y = b_0 + \sum_{i=1}^{k} b_i x_i + \sum_{i=1}^{k} b_{ii} {x_i}^2 + \sum\sum_{i<j} b_{ij} x_i x_j + \epsilon \qquad (3.11)$$

Consequently, it results a matrix with as many columns as regression coefficients, where all candidates from ξ_n are included. The first column of *X* represents the constant term b_0. The following columns represent the values that variables take for each coefficient b_i. The matrix that contains the *optimal* design points is called *optimal design matrix (X*) (AGUIAR ET AL. 1995, TRIEFENBACH 2008).*

Criterion

Another matrix needs to be defined to be used for the selection criterion. The information matrix *(X'X)* is the transposed design matrix multiplied by itself. The dispersion matrix as is defined as the inverse of the information matrix, $(X'X)^{-1}$. The more important criteria are D-optimality (determinant), G-optimality (maximum prediction variance), A-optimality (trace), and V-optimality (average prediction variance). All them maximize different functions of for *X'X. (AGUIAR ET AL. 1995, TRIEFENBACH 2008)*

The D-optimality is the most used criterion. This seeks to maximize |X'X|, i.e., the determinant of the information matrix of design, being equal to minimize the determinant of the dispersion matrix $(X'X)^{-1}$.

The optimal design matrix X* contains the *n* experiments which maximizes the determinant *(X'X).* In equation (3.12) is the selection of X* out of all possible design matrices chosen from ξ_N described (AGUIAR ET AL. 1995).

$$\left|X^{*\prime} X^*\right| = \max_{\xi_n \Xi_N} \left(|X'X|\right) \qquad (3.12)$$

Number of Points in the Design

The number of experiments that the experimenter wants to include into the design is freely chosen. The factor *n,* i.e., the number of runs expected to do,

is very significant because changing this number the model matrix is altered and another optimal design comes up. The selected model dictates the minimum number of runs, which is the quantity of regression's coefficients. The optimal number depends on the constraints imposed by the cost of the experiments, the time and the difficulty to perform them. The advantage of using the D-criteria is that there is no need to perform any experiment before choosing the best design (AGUIAR ET AL. 1995, TRIEFENBACH 2008).

3.4 Replication

When the regarded system is very unsettled, the experiment should have several replicate observations for each experimental combination. The principal reason to replicate is to reduce the variability on the response, thereby its effects' variability. Then, the experimental answer is the average value of all taken samples for a same set of levels. The replicas permit the measurement of a system's variability, which is employed to determine the effects' significations (MEAD 1988).

3.5 Best Fitting Model Selection

Statistics are concerns with what can be learned from any source of data. Building a model follows an iterative process, which is resumed in Figure 3-5.

Response surface methodology (RSM) is a collection of mathematical and statistical techniques useful for the modeling and analysis of problems, in which a response of interest is influenced by several variables. In most RSM problems, the relationship form is unknown (linear, quadratic, cubic…). The first step is to find a suitable approximation for the true functional relationship between *y* and the set of independent factors.

Most of the problems occurring during building a regression model can be divided into two groups:

1. Related to the model identification:
    a. Which variables have to be included in the model?
    b. Are transformations necessary? Which?
    c. How looks the function like ($Y = f(x_1, x_2 \dots x_N) + \varepsilon$)?

2. Related after the model is identified:
    a. How to adjust it?
    b. How to validate it?
    c. How to interpret it?

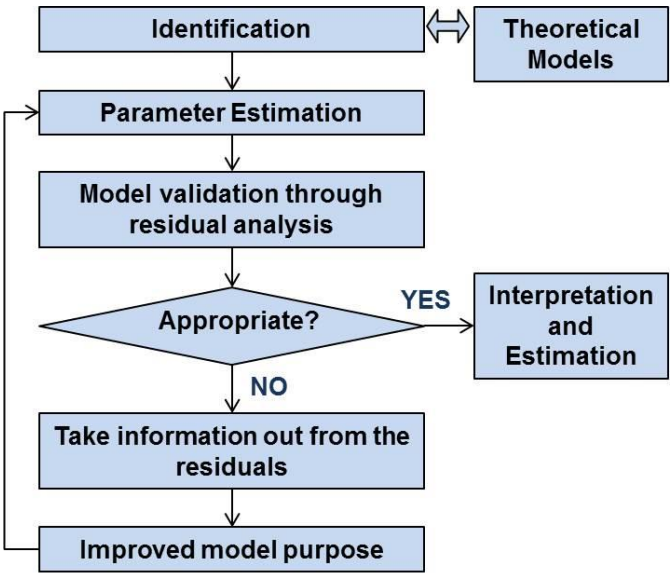

Figure 3-5: Course to build statistical models (according to PRAT BARTRÉS 2004)

The objective is to choose a subgroup of factors to introduce them to the approach. When the variables are chosen, there is a risk of choosing too many (over-fitting), or insufficient (under-fitting) factors. The model adjustment, according to least squares, predicts the model coefficients that minimizes the sum of the squares of the errors of the points from the curve. Because of the existence of a large number of possible models, some tools to notify the adjustment quality of the regression are needed.

3.5.1 Fitting Models

There are three possible ways to create a model via the statistical software Minitab. These are explained in the following sections.

Best Subsets

The Best Subsets regression identifies the sets of approaches that obtain the highest R^2 values from the full set of variables. It is an efficient way to identify

models that achieve good regression determinations without a large number of factors. Minitab examines all possibilities, beginning with all regressions containing one predictor, then those with two predictors, and so on. The output is a list of models with their R^2, R_a^2, and C_p values and the included variables for each model. (BARRY ET AL. 2015) The different indicators are explained in the next section.

Stepwise Regression

The Stepwise regression is a semi-automated process of building a model by successively adding or removing variables based solely on the *t*-statistics of their estimated coefficients. The Stepwise starts from a void model and it proceeds adding the most likely candidates , and then successively introduce other variables or omit existing ones at every step. The method provides two criteria for moving variables. They are based on the F-statistic, which is the square of the t-statistic. In order to remove a variable, the variable must have a higher F-statistic than the specified for removal, called *F-to-remove.* The criterion to add a variable is testing the significance (the F-statistic) that the coefficient would have if this were in the regression equation. If this value is above the one specified, *F-to-enter,* then the variable enters to the equation.

At each step, the program performs the following calculations: it enters the variable with the largest F-statistic, if this is greater than the *F-to-enter*. When there are no variables left to enter whose F-statistics were higher than the threshold, it checks whether the F-statistics of any variables added previously have fallen below the *F-to-remove*. If so, it removes the worst of them, and then tries to continue. It finally stops when no variables either in or out of the model have *F*-statistics on the wrong side of their respective thresholds. (BARRY ET AL. 2015)

In Minitab, the "*F-to-enter"* is represented with a α_e and the *"F-to-remove"* with a α_r.

All factors in

This procedure has no iterative sequence. Therefore are all the variables included to the regression and estimated their descriptive coefficients via the

table ANOVA (analysis of variance). The ANOVA table is explained in the section of page 43.

3.5.2 Model Selection Criteria

With the different ways to create a regression, Minitab delivers similar information for all them. The major challenge is to know which of the different coefficients and indicators fit better with the system requests. There are different criteria to decide among different models. More than a single criterion should be used not to leave relevant information behind. The different criteria are explained at the next points.

Coefficient of Determination (R^2)

This coefficient indicates how well data points fit to a line. This criterion seeks the approach that maximizes R^2. R^2 never decreases when a new variable is added. This is applied to sort models with equal number of variables. If this standard was the only to take into consideration, the chosen approach would always have all the variables.

Adjusted Coefficient of Determination (R_a^2)

The R_a^2 is an attempt to take into account the phenomenon that the R^2 automatically increases when extra variables are added to the model. Unlike R^2, R_a^2 penalizes the points that do not fit the model. R_a^2 is always less than or equal to R^2.

Mallows' Statistic (C_p)

This statistic is used as an aid on choosing between multiple regression models. Mallows' C_p compares the accuracy and bias of the full model to others with the best subsets of predictors. It helps to consider models with a more balanced number of variables in the design. A model with too many predictors can be relatively imprecise while one with too few can produce biased estimates. A Mallows' C_p value that is close to the number of predictors plus indicates that the model is relatively precise and unbiased in estimating

the true regression coefficients and predicting future responses (BARRY ET AL. 2015).

The statistic is calculated as in expression (3.13), where *p* is the number of variables chosen and *N* the sample size. C_p expects to equal nearly *p;* otherwise the expectation is *p* plus a positive bias term. The recommended model to be chosen, according to this statistic, is one that the C_p were similar to *p* and with the less number of variables. (DANIEL & WOOD 1999)

$$C_p = \frac{SS_r}{S_R^2} + 2p - N \qquad (3.13)$$

3.5.3 Quality Indicators

Once the model is selected, it has to be validated with some indicators. The indicators that are going to be used in this work are explained below.

Residual Analysis: Assumptions

Residuals are estimates of experimental error obtained by subtracting the observed responses from the predicted regression. Before taking for granted the confidence intervals, the four residual assumptions have to be fulfilled. More information that can be acquired from the residual analysis, is the detection of unusual observations.

Standard linear regression models with standard estimation techniques follow a number of hypotheses. The four premises made by regression models with ordinary least squares are:

1. Independence of errors: the errors of the response are uncorrelated with each other, i.e., they do not follow any trend
2. Expectancy: $E(e_i)=0$
3. Variance: $V(e_i)=\sigma^2(1-h_{ii})$).This means that different response variables have the same variance in their errors, regardless of the values of the predictor variables. h_{ii} measures the distance between X_i and $\bar{X}$
4. Normality: $N(0, \sigma^2(1-h_{ii}))$ the residuals should follow a normal distribution

Different type of residual plots can be illustrated to check the validity of the mentioned assumptions. Moreover, they are used to discover hidden

information on residuals, asses the quality of the regression, and achieve a better model for the response.

- Residual vs. Expected Values (e_i,$\hat{Y}$): if the suppositions are accomplished, it should not have any pattern. This is also useful to see if the variance is constant and detect anomalies. Two responses with different variance patterns are showed in Figure 3-6.

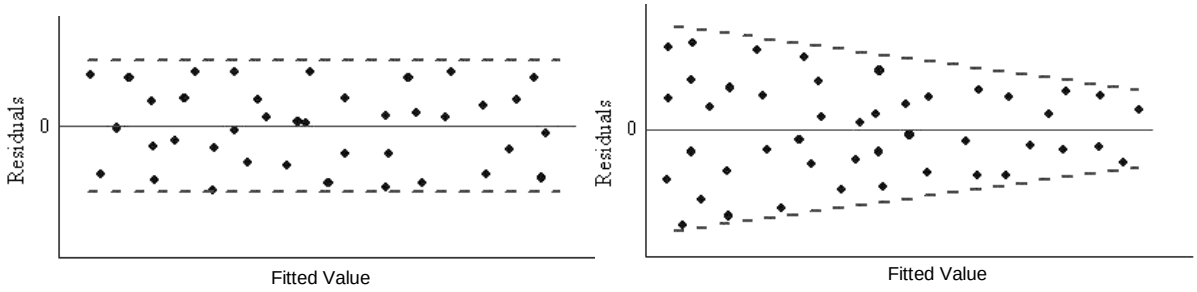

Figure 3-6: Example plots for residuals vs. expected values. While the left one presents a constant variance, the right one shows a decreasing trend (ORIGINLAB CORP.)

- Residual vs. Order of the Data: this plot will reflect the correlation between the error term and the order of data gathering. Two responses with different gathering correlations are showed in Figure 3-7.

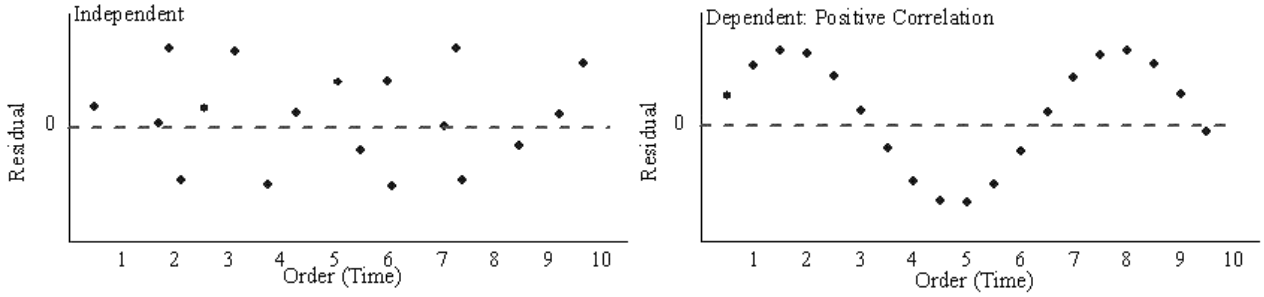

Figure 3-7: Example plots for residuals vs. collect order. The left one presents time-independence and the right plot has a high positive correlation (ORIGINLAB CORP.)

- Errors in probabilistic plot: it is employed to verify the requirement of normality and helps to detect error points. If the resulting plot is approximately linear, the error terms are normally distributed. Two

responses with different normal approximations are showed in Figure 3-8.

(PEÑA SÁNCHEZ DE RIVERA, DANIEL 2013, ORIGINLAB CORP.)

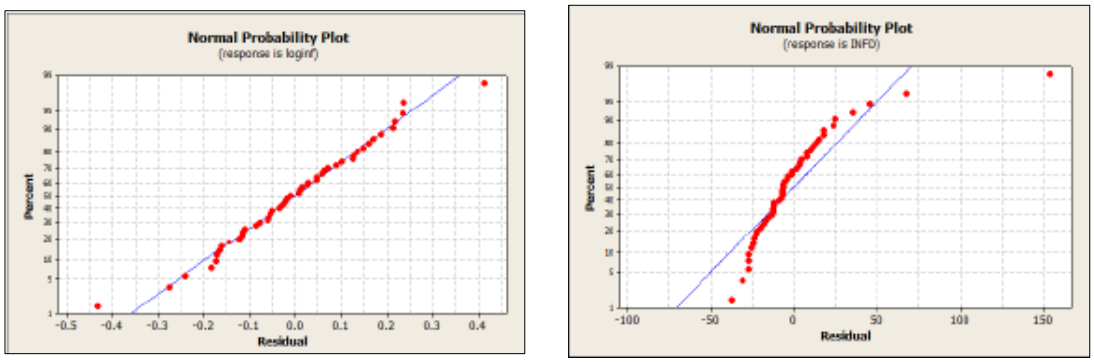

Figure 3-8: Example of residuals in normality plots. The left one fits to the normal line and the right needs further transformations (PRAT BARTRÉS 2004)

Analysis of Variance (ANOVA)

The analysis of variance is a quality tool that helps to explain how the adjusted model fits to the exploratory points in a resumed table. In Table 3 is represented an ANOVA, where *k* is the number of factors the model includes and *n* the total number of factors for the design.

Table 3: ANOVA table for a second-order model

Source of Variation	Sum of squares (SS)	Degrees of freedom (df)	Mean Square (MS)	F-Value
Regression	$SS_R = \sum(\hat{Y}_i - \bar{Y})^2$	*k*	$MS_R = \frac{SS_r}{p}$	$\frac{MS_R}{MS_E}$
Error	$SS_E = \sum(Y_i - \hat{Y}_i)^2$	*n-k-1*	$MS_E = \frac{SS_e}{n-2}$	
Total	$SS_T = \sum(Y_i - \bar{Y})^2$	*n-1*		

SS_T only depends on *Y*, meaning that while the response does not change, it changes neither. SS_R and SS_E depend on the model.

From the table can be extracted:

- $SS_R + SS_E = SS_T$
- The variance for the response: $s_R^2 = \frac{\sum(Y_i - \hat{Y}_i)^2}{n-2} = \frac{\sum {e_i}^2}{n-2}$
- Coefficient of Determination: $R^2 = \frac{explained sum\ of\ squares}{total\ sum\ of\ squares} = \frac{SS_R}{SS_T} = 1 - \frac{SS_E}{SS_T}$ indicates how the data fits to the statistical model, expressed as percentage

3.6 Effects and Interactions

An effect in the statistical context is the quantitative measurement of the impact that the variables have on the response.

Effects that involve comparisons among levels of only one factor are called main effects of that factor, and effects that involve comparisons for more than a single factor are called interactions. If smaller shifts in the mean of the response are wanted to be detected, replications are needed to be employed.

Principal effects indicate how the average response change when a factor takes the lowest (-1) or the highest (+1) level. Thereby, the principal effect of A from the Table 2 is the mean of the response values with A on +1, minus the mean of the ones with A on -1:

$$A = \bar{y}(A_{+1}) - \bar{y}(A_{-1}) = \frac{y_2 + y_4 + y_6 + y_8}{4} - \frac{y_1 + y_3 + y_5 + y_7}{4}. \qquad (3.14)$$

An interaction among two or more factors exists if the effect of one factor on a response depends on the levels of other factors (MASON ET AL. 2003). The way to quantify an interaction between A and B is:

$$\begin{aligned} AB &= \frac{1}{2}(effect\ A\ with\ B_{+1}) - \frac{1}{2}(effect\ A\ with\ B_{-1}) \\ &= \frac{1}{2}\left(\frac{y_4 + y_8}{2} - \frac{y_3 + y_7}{2}\right) - \frac{1}{2}\left(\frac{y_2 + y_6}{2} - \frac{y_1 + y_5}{2}\right). \end{aligned} \qquad (3.15)$$

When this difference is zero, means that the factor is independent from the other. The difference is divided by two to equal the interaction variance to the main effects ones. Analogously, three factors interact when the interaction from two of them depend on the level of one third. In most of the cases, the behavior of responses can be explained successfully without third or higher interactions.

3.6.1 Effects Significance

Once the effects are obtained, if these are sufficiently relevant to include them into the model has to prove.

When the estimation of an effect is different to zero, it does not imply that this factor had a meaningful outcome on the response. This question remains on the response's variability. The acceptance region of a two-sided hypothesis test for b_i, corresponds to a confidence interval for b_i. It may be detected whether zero lies inside the 100(1-α) % confidence interval for b_i. This CI comes with the expression (3.16), where $\mathrm{t}_{\frac{\alpha}{2};\mathrm{n_t-N}}$ is the probabilistic-value of both curve's tiles of the Student's t-distribution (see Appendix A), α the confidence level, n_T the total number of observations done, N the total number of experimental conditions and S_{b_i} the standard error of the coefficient. This standard error is a coefficient that indicates how precisely the model estimates the unknown effect (SMITH 1997).

$$\left[b_i - \mathrm{t}_{\frac{\alpha}{2};\mathrm{n_t-N}} S_{b_i}, b_i + \mathrm{t}_{\frac{\alpha}{2};\mathrm{n_t-N}} S_{b_i}\right] \qquad (3.16)$$

3.6.2 P-Value

P-value is a statistical coefficient used to determine the statistical significance in a regression analysis or hypothesis test. Technically, it gives the probability of getting an effect at least as extreme as the one in a sample data, assuming the truth of the null hypothesis.

In every experiment there is an effect or difference between groups that could be the effective or that the factors have no effect or no difference between the groups. This lack of a difference is called the null hypothesis. A P-value measures how compatible the data are with the null hypothesis. A low P-value suggests that a sample provides enough evidence to reject the null hypothesis.

For example, it is supposed that a vaccine study produced a P-value of 0.04. This P-value indicates that if the vaccine had no effect, the observed difference or more would have been obtained in a 4 % of studies due to random sampling error. (BARRY ET AL. 2015)

4 Former Work

In this chapter is described the method upon which this thesis is based and developed by BERGENGRUEN (2014). This section explains the principle of the method, the different components that has, the chosen experimental conditions, and a brief commentary of the obtained results and the extracted conclusions.

The principal extraction for the proposed method came from the Klemm method (2.2.3) to determine the absorption of different separators and electrodes in controlled conditions. As the isopropanol wets the layers, they get darker, enabling to observe the progression of those changes.

A clamping case is placed inside a vacuum chamber, where the sheets are compressed and the liquid is inserted. Then, a valve lets a specific quantity of electrolyte flow through the case while a camera records the entire process. Once the test is finished, the video is processed with MATLAB. The pressure and temperature inside the camera are under controlled conditions.

4.1 Experimental Setup

The setup is composed of various components: a vacuum chamber, a compression case, two valves, and a recording camera; all they are described on the following sections. A schematic representation of the setup is represented in Figure 4-1.

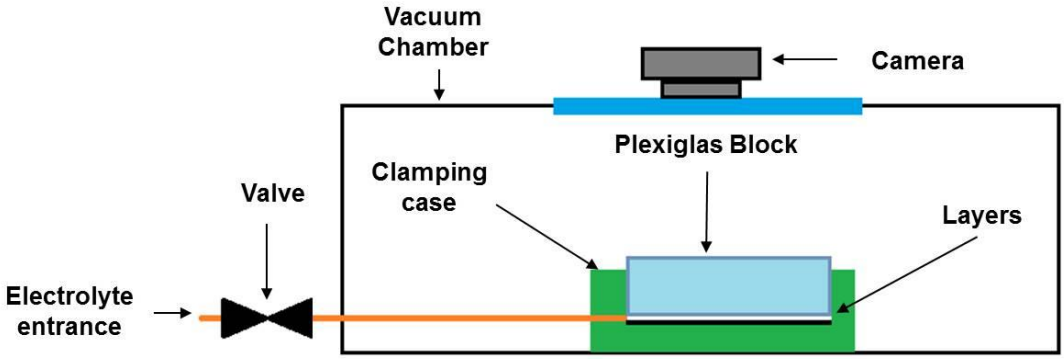

Figure 4-1: Schematic drawing of the setup

4.1.1 Vacuum Chamber

The employed vacuum chamber is a finished constructive diploma-work. It is comprised of a cylindrical case, which has a cover with two clamping braces. One relevant part of the chamber is its transparent window on the top, which permits to record what occurs inside. At the bottom a thermoelectric generator is installed, which uses the Peltier-effect[3], enabling the regulation of the temperature inside. Figure 4-2 shows the CAD representation of the vacuum chamber.

Around the cylindrical surface are placed eight sealed holes with flanges that content an O-Ring and a blind flange. Through one of the flanges, pass the conduct of the electrolyte. In a second hole is placed the hose of the vacuum pump, and in a third one goes the cables that control the thermoelectric generator through. With the appointed elements, the pressure and the temperature can be controlled inside the chamber. The temperature is controlled with an extern controller, and the pressure with a computer program.

The main parts of the vacuum chamber numbered in Figure 4-2 are the following:

a) Fast clamping fixture
b) Polycarbonate eyehole and combined overpressure valve
c) Handles
d) O-ring seal of EPDM[4]
e) Cylindrical screwed chamber of aluminum
f) ISO KF 16 – Standard flange
g) Glass-wafer as electronic isolation
h) Heat-transfer of aluminum
i) Peltier element for temperature regulation
j) High-adjustable floor

(HELLER 2013)

[3] Cooling or heating a junction when electric current is maintained in a circuit of material consisting of two dissimilar conductors.

[4] Ethylene propylene diene monomer

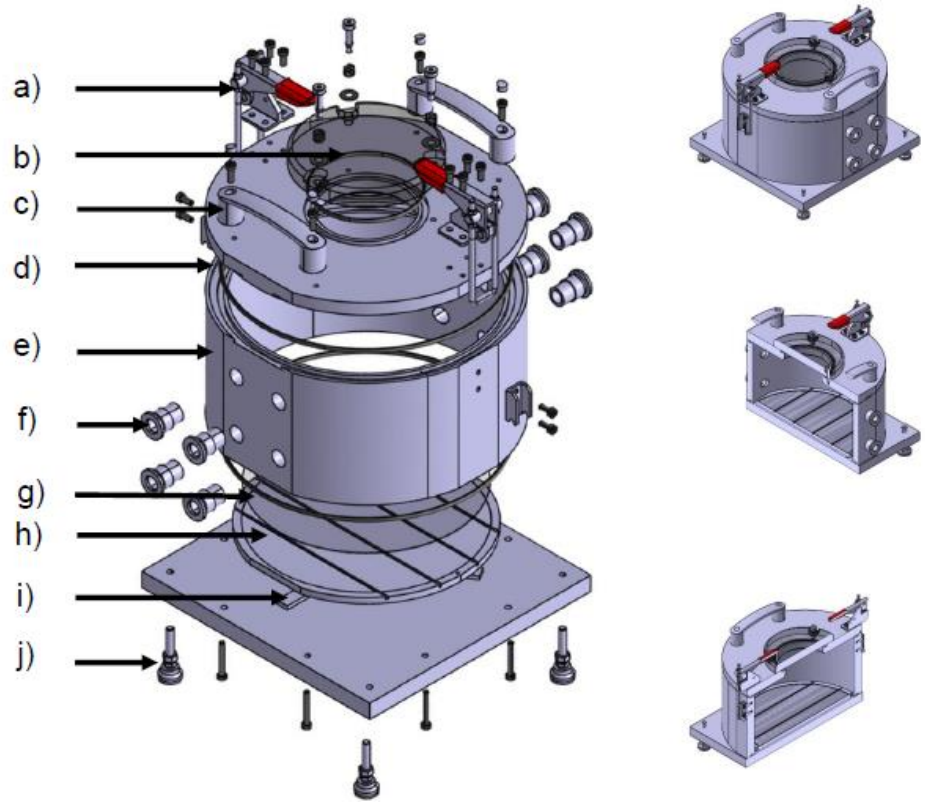

Figure 4-2: CAD Representation of the vacuum chamber (HELLER 2013)

4.1.2 Compression Case

A case was designed to place and to sustain the cell layers. This is composed with a shell base, a cover, a Plexiglas block and a thread to introduce the liquid. The cover is attached to the base with four screwed M5 bolts. In Figure 4-3 can be seen a CAD representation of the case.

The cover and the Plexiglas block play an important role in the setup, since they must let the camera see through them, to observe how the liquid spreads. The cover and the base are made of aluminum.

The electrolyte is introduced through a tube's connection on one face of the prismatic base. This tube's connection is from the company FESTO, being the same as in the real production line.

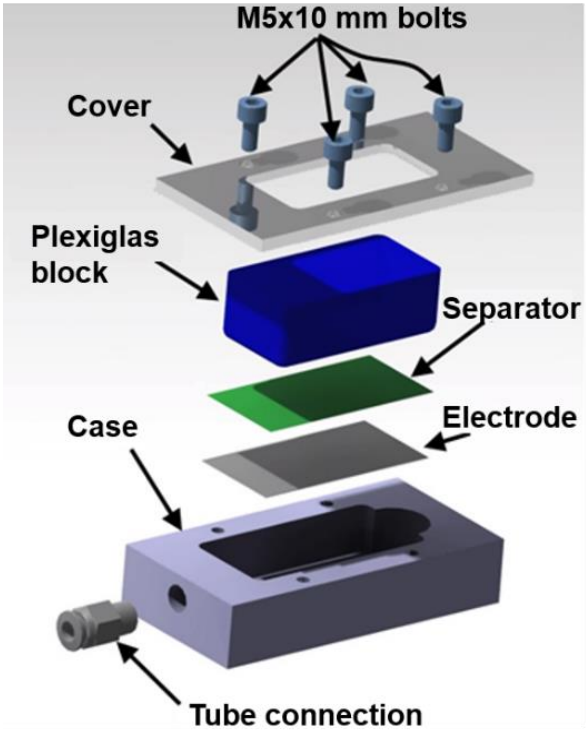

Figure 4-3: Exploded view of the compression socket (BERGENGRUEN 2014)

4.1.3 Valves

For the experiment are employed two valves from the company Bürkert. One is a two-way valve placed between the socked entrance and a three-way valve. This enables the flow of the liquid inside the vacuum chamber. The three-way valve has two entrances and one exit. The exit is connected to the two-way valve and in both entrances are attached two syringes, one empty and the other filled with the testing liquid. This three-way valve works in such a way, that when entrance *a* opens, entrance *b* closes, and vice versa. Both valves are controlled from a direct voltage source.

4.1.4 Recording Camera

One of the most demanded parts for the method is the recording of images for the later interpretation. The major trouble was the light that came from outside. To solve this fact, a diffusion sheet was placed on the chamber window, partially avoiding the light's distortions. In the middle of the sheet is cut a hole to insert the eyeglass of the camera.

4.2 Design of Experiments

The following sections explain the selection of factors. All the theory related to this is explained in Chapter 3.

4.2.1 Choice of Parameters and Variables

The first step was to determine the constant variables. To minimize the noise were selected as many as possible factors to lock their value, making the number of experiments lesser. The selected parameters are described in Table 4.

Table 4: Constant parameters in the former work (according to BERGENGRUEN 2014)

Parameter	Fixed Value	Observations/ Possible Influences
Room Temperature	27.2 ºC	Through room climate control
Separator/ Electrode Dimensions	30x60mm	Limited by the dimensions of the compression socket
Liquid	Isopropanol	For security reasons, a non-dangerous composition was used
Quantity of Liquid	1.2 ml	Determined in previous test and measured with a syringe
Vacuum-Chamber Pressure	45 mbar	Leakage losses are compensated by the vacuum pump
Humidity	Almost 0 %	Insignificant for the experiment. However it is controlled by the climate control
Illumination	Reproducible and steady	Very important. It is considered that the sunlight does not affect the indoor light.

In what variables refer, there were taken three categorical factors. One of them was a quantitative variable with fixed levels that was considered as categorical: the temperature in vacuum chamber. Table 5 shows the selected variables, their type and the chosen values.

Table 5: Variables in the former work (according to BERGENGRUEN 2014)

Variable	Type	Values
Temperature in Vacuum Chamber	Categorical	• Below room-temperature T_{R-} (19.2 ºC) • Room-temperature T_R (27.2 ºC) • Above room-temperature T_{R+} (35.2 ºC)
Separator	Categorical	• Evonik SEPARARION S240P30 • Celgrad 2325 • Separator from Brückner
Cell layers	Categorical	• Separator • Separator + Electrode

4.2.2 Establish a Test plan

Once the variables and their values were selected, a model design had to be chosen. As the work had three factors with two and three levels for each, a full factorial model was the only meaningful option. This had $3^2*2 = 18$ different combinations. There were also taken two and four replicas to reduce the variability of response. The table for the tests plan is presented together with the experimental results in Table 6 of page 54.

4.3 Experimental Procedure

Firstly, the layers had to be cut to the right dimensions and placed inside the case, which was closed with the Plexiglas block and the cover. The four bolts were screwed with a torque wrench. Once the case was placed inside the vacuum chamber, this was closed and the pump could be turned on. After that, the diffusion sheet and the camera were placed on the sight-window. One syringe was filled with 1.2 ml of Isopropanol and was connected to the

entrance *a* of one pipe and in the entrance *b* was attached an empty syringe, acting as a stopper.

When the wished temperature and the pressure of 50 mBar are reached, the two-way valve opens and the entrance *b* of the three-way valve opens too. This action creates the vacuum between both valves. Then, the two-way valve closes and the entrance *a* from the three-way valve opens simultaneously, letting the isopropanol being soaked by the vacuum established in the section. Before opening the two-way valve again, the camera starts to record. When the two-way valve is opened, the isopropanol flows through the layers. The recording stops 3 minutes after opening the two-way valve.

Once the test is completed, the syringe in *a* is uncoupled to rise chamber's pressure and blow some air to remove possible rests of isopropanol. The top of the vacuum chamber is not removed until the pressure reaches atmospheric values for security reasons.

4.4 Data Analysis and Results

Once the tests are performed and the necessary data is collected, the videos have to be analyzed to acquire the required information.

4.4.1 Data Analysis

First were extracted three photograms with the program VLC Player. The first one is extracted just at the moment that the aperture of the valve sounds, called t_0. The second image is taken 7 seconds later t_0, and the third one, 13 seconds after t_0. These time moments were not randomly chosen, since the separator achieves its critic phase during that period. From the second 13 the isopropanol starts to evaporate rather than spread, being the wet surface contracted. The images are processed with MATLAB to determine how many pixels are black, assimilating the obscured pixels as wet points. The employed code is attached in Appendix B.

After the RGB[5] images are converted into black and white, the number of black pixels are calculated for the three instants of time and compared with the ones found in the first picture, to obtain the number of obscured pixels during that time.

For the conversion from RGB to black and white, MATLAB needs a threshold value. The threshold was taken with the help of the software “Pixellineal”, which identified the brightest wet-pixel and the darkest non-wet-pixel from the third image.

4.4.2 Results

Table 6 shows the arithmetic mean value for the achieved results.

The runs are sorted in standard order. The values in columns “*mean wet surface at t_0 + 7 s.*” and “*mean wet surface at t_0 + 13 s.*” are the average black pixels among the replicas. The value from the replicas are the difference between the pixels at the specific time (*t_0 + 7 s. or t_0 + 13 s.)* to the ones at the time t_0. For runs 16, 17, and 18 was not possible to obtain consistent result because the wet pixels had a brighter tonality than the non-wet pixels in the gray-scale images.

4.5 Interpretation and Conclusions

A statistical analysis of the results was executed to extract conclusions about the influence of the variables conditions. The results from the experiments with the separator from Brückner were not analyzable, due to its critical evaluation. These levels were not taken into consideration for the rest of the study.

[5] RGB is an additive model color, in which red, green and blue light are added together to reproduce a broad array of colors.

Table 6: Tests results for the former work (according to BERGENGRUEN 2014)

Run	Separator	Cell Layers	Temperature	Replicas	Mean wet surface at t_0 + 7s [pixels]	Mean wet surface at t_0+ 13s [pixels]
1	Evonik SEPARARION S240P30	Separator	T_R	4	7717	15985
2			T_{R+}	2	40385	13437
3			T_{R-}	2	12455	19001
4		Separator + Electrode	T_R	4	10477	22966
5			T_{R+}	2	9550	12966
6			T_{R-}	2	13338	23011
7	Celgrad 2325	Separator	T_R	4	10687	14962
8			T_{R+}	4	4067	4197
9			T_{R-}	2	4417	18476
10		Separator + Electrode	T_R	4	9899	19958
11			T_{R+}	2	2298	7373
12			T_{R-}	2	6054	16017
13	Separator from Brückner	Separator + Electrode	T_R	2	9655	18849
14			T_{R+}	4	8114	12553
15			T_{R-}	4	7035	17471
16		Separator	T_R	2	3611	8992
17			T_{R+}	2	474	972
18			T_{R-}	2	4530	10593

4.5.1 Statistic Interpretation

Statistic helps to know which effects are significant to the response. The adopted abbreviations are *S* for Separator, *T* for temperature and *E* for cell layers. All necessary statistics background and formulas are explained on Chapter 3.

The main effects and interactions for both responses are calculated for the two specific times. The results for these are presented in Table 7. They are based on the formulas (3.14) and (3.15).

Table 7: Main effects and interactions (according to BERGENGRUEN 2014)

Main Effects and Interactions	S	T	E	ST	SE	TE
t_0+ 7 s.	4360.3	-2575.6	-371.22	-522.8	1196.1	-677.9
t_0+ 13 s.	4411.9	-9636.2	-2720.0	1825.5	-285.2	-782.2

After that, it was proceeded to find the CI every of them and to check if the interval [effect $\pm$ CI] contained the zero. The employed formulas were: (3.1), (3.3), (3.4) and (3.16); where

- n_T=31, total number of observations done
- N=12, total number of experimental conditions
- α= 0.05 significance level. Equal to 95 % of confidence
- t=2.093, having 19 degrees of freedom and a cumulative probability for two-tails of 0.05

The variances s^2 for each experimental condition obtained from the formula (3.3) are written down in Table 8. The three painted values in yellow were the ones with most variance and in green with the least variance.

Table 8: Variances of the replicas (according to BERGENGRUEN 2014)

Run	s_R^2 for t_0+ 7 s.	s_R^2 for t_0+ 13.s.
1	101778875	36251451
2	1162713118	120998
3	398961	396834
4	18651947	53307870
5	502143	4502582
6	3111575	3739099
7	34393558	11215610
8	2361753	93965
9	2089005	285000
10	24396117	4151658
11	65376	277845
12	4290504	611015

Consequently, the achieved CI's are in Table 9.

Table 9: Confidence Intervals (according to BERGENGRUEN 2014)

CI t_0+ 7 s.	CI t_0+ 13 s.
7988.37	2326.97

The study ends checking which interval does not include the zero, which would mean a significant effect. In this case, the only significant effects were S, T and E at the +13 s.

4.5.2 Conclusions

From the collected results from MATLAB and the statistical analysis, the conclusions and interpretations were:

- There is no significant effect for t_0+ 7 s., because the variance is much larger than for t_0+ 13 s. The reason why this variance is in general wider, lies on the fact that moments after that the isopropanol comes in, it wets with a big incertitude. Seconds later, the transient state is attenuated and the variance decreases, as noticed for the response at t_0+ 13 s.
- The only significant factors are the temperature, the separator type and the type of cell layers for the period from t_0 to t_0+ 13 s.

In reference to the period t_0 to t_0+ 13 s:

- Temperature is the most influent factor on the response (-9636), followed by the type of separator with approximately 50 % less effect (4411).
- In Figure 4-4 are represented the values of the wet surface at t_0+ 13 s with electrode for the three different room temperatures.
- As shows Figure 4-4, the quantity of wet pixels is smaller when the temperature is high. This phenomenon is due to the low boiling temperature of the isopropanol. As the pressure is fixed to 45 mBar, the correspondent temperature for that pressure is 20.68 ºC. This means that from that temperature the isopropanol begins to evaporate. The only instance that it should not evaporate would be for the lower temperature, since it is 19.2 ºC. Therefore, to get a reliable and comparable process, the temperature should remain lower than 20.68 ºC or increase the pressure. In the real process, this fact should not happen, because the electrolyte's boiling point is higher than isopropanol's point. (IFA 1997)

- The separator from Brückner is the least sensitive to react with temperature. Therefore, pixels suffer minor variations among the three temperatures.
- The variance is wider among the experiments with high temperatures. This fact is due to the evaporation and its unbalanced state.

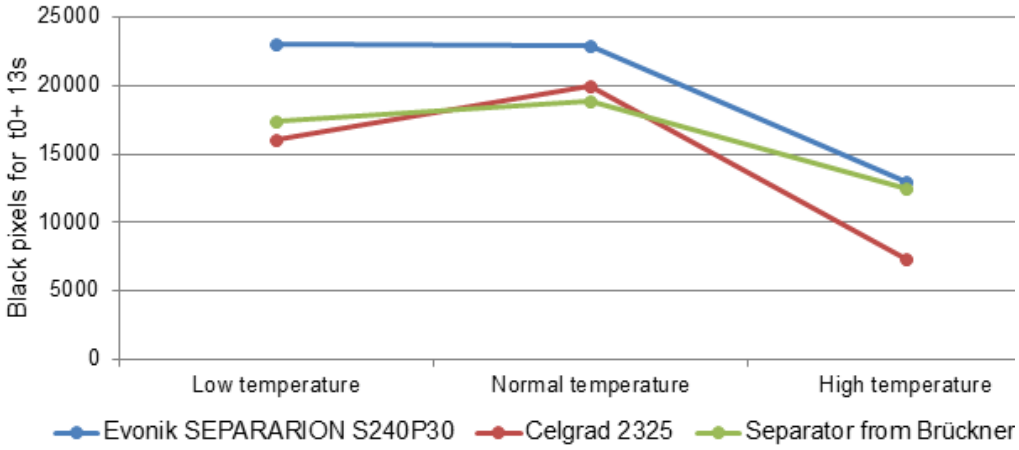

Figure 4-4: Comparison of the three separators with electrode at t_0+ 13 s. (according to BERGENGRUEN 2014)

4.6 Outlook

The described method has achieved its main goal: simulate the wetting process in vacuum conditions and extract a numerical response from graphic data. This work has been the first approach with this new developed method. It is very understandable that this has some lacks of precision and the simulation conditions were far from the ones applied for the real operation. For this reason, has been done the present master thesis to select some field of action, to improve the established method, and to prove the principle of this.

One of the upgrades will be focused to reduce the variation of light. This cause much incertitude for the threshold choice and the distortions of black pixels. Another redesigned field will be the DoE. The parameters and factors should be more similar to the real ones. This would help to extrapolate the results from one to the other. The last action field should be based on the video analysis.

5 Method Development

In this chapter are explained the modifications carried out in the established method. These are carried out to improve its accuracy and achieve closer simulation conditions to the real process.

As seen in section 4.5, the results obtained in the previous work were not convincing enough. The chosen field to apply modifications or add new components are:

- Clamping case
- Liquid's circuit
- Lighting
- Image capture
- Choice of parameters and factors

The new experiments are reproduced inside the same vacuum chamber that. Detailed information about this is found on section 4.1.1 or in HELLER (2013).

Due to the high evaporation of isopropanol, and to achieve realistic results, EC:EMC 3:7 is going to be the "fake" electrolyte used. From this chapter, the term electrolyte is associated to this salt and dissolvent ratio, which coincides with the compound employed in the real electrolyte. A normal liquid electrolyte is not used for safety reasons clarified in section 2.1.5.

5.1 Clamping Case

The functions of the case are to hold and compress the sheets, to maintain equal conditions for all experiments avoiding distortions among them, and to enable a camera to record the diffusion process.

In section 4.1.2 is briefly explained the case designed and used for the preceding work. That employed a case for layer with dimensions of 62.5 x 30 mm and closed with four M5-bolts. The vacuum chamber is big enough to comprise a case that could hold layers with the same dimensions as ones used for the manufactured cells at *iwb*. Therefore, the main change for this part is the enlargement of the old case from 62.5 x 30 mm to 100 x 73 mm.

The other evolution was about the way it closes and keeps the cover and the Plexiglas block fixed. On the previous work, the top was closed by four M5-

bolts tightened with a screw wrench. The pressure transmitted to the layers, was sometimes excessive and not equal for the different samples, bringing some disturbances to the outcome.

The solution for the fastening problem was the adoption of another technique that closes the set and ensures the same pressure on the cells for all runs. The first idea was to close the case with two elastic bands. They give a distributed force along their surface and they could have maintained it equal for runs. However, their drawback was the possible fast degradation, varying the elastic constant. The use of clamps to enclose the top was another solution, but the problems lied on the lack of space to embrace them inside the chamber and the unsteadiness of the case.

The best solution was the use of springs. They give a constant force, whenever the distance were the same. They are applied in a simple way, changeless, and metal's degradation is insignificant, within the project term.

The new case also has four passing holes on the top and on the base to ensure the same position of the cover on every test.

In Figure 5-1 are represented and enumerated all parts of the clamping case:

a) Aluminum top
b) 4 x Pin Ø8 mm
c) Plexiglas bock
d) Aluminum base
e) 4 x M4 endless-male
f) 4 x Spring RZ-055AI

5.1.1 Springs

The springs selected are the RZ-055AI of serial number from the company "Gutekunst Federn". The most relevant technical data is described in Table 10 and the rest is located at the technical sheet of Appendix C. With these parameters, the strength for each spring and the pressure to the layers can be measured.

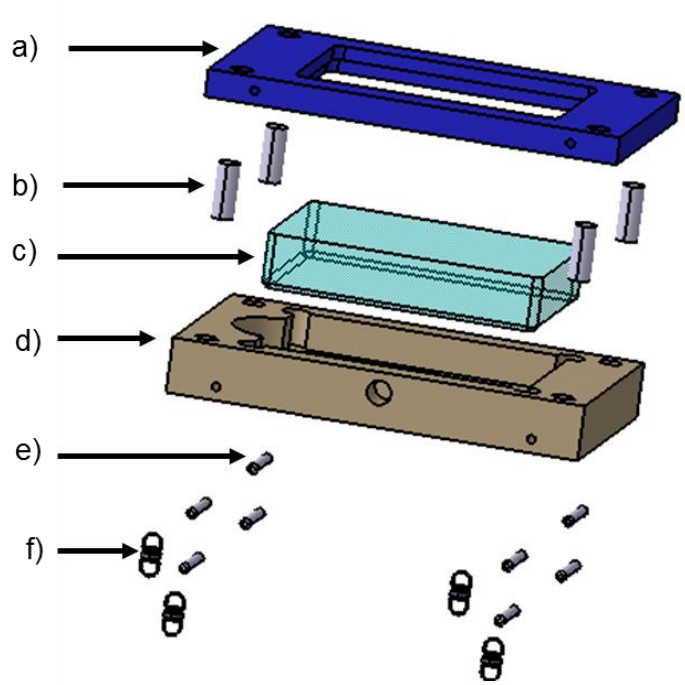

Figure 5-1: CAD representation of the clamping case. Exploded, isometric, vertical and horizontal views

Table 10: Main characteristics of the springs RZ-055AI

Unstressed length	14.8 mm
Spring rate	0.745 N/mm
Maximal Length	30.1 mm

As Hooke's law states, (5.1), the force depends on the spring's displacement, where *F* is the force, *k* the constant factor characteristic of the spring, and *X* the distance extended or compressed from the unstressed length. The distance between ends is 22.1 mm when the case is closed with an electrode and a separator sheet inside. The force in each spring is then 5.438 N, (5.2), meaning a total force of 21.754 N for the four. A pressure is defined as a force, divide to a surface, i.e., the Plexiglas block's surface, which is taken from the drawings attached in Appendix C. The resultant pressure is 3.544 kPa (5.3).

$$F = -kX \tag{5.1}$$

$$|F| = 0.745 * (22{,}1 - 14.8) = 5.438\ N \tag{5.2}$$

$$P = \frac{F}{S} = \frac{21.754\ \text{N}}{6138\ mm^2} = 3.544\ \text{kPa} \qquad (5.3)$$

5.2 Liquid's Circuit

The valve assembly employs a two-way and a three-way valve, two syringes, and tubes connections. The valves are from the company Bürkert with serial number 6628, being the same used for former work. The assemblage is mounted as shows in Figure 5-2: the two-way valve is between the entrance of the vacuum chamber and a tube; the three-way valve is attached at the entrance of this last tube. The three-way valve has a syringe at opened-by-defect entrance, which acts as stopper, and the other entrance is open.

The electrolyte is introduced between the valves, in the blue section of Figure 5-2. After some tests to study how much liquid remains inside the valve and the tubes after a pressure cycle, it has been determined that the best place to locate the liquid is between both valves. On one hand, if this is introduced after the two-way valve, the vacuum absorbs the liquid before being reached the wetting pressure. On the other hand, if this is placed before the tree-way valve, a significant quantity of electrolyte remains inside the valves, resulting a lesser effective quantity than the expected.

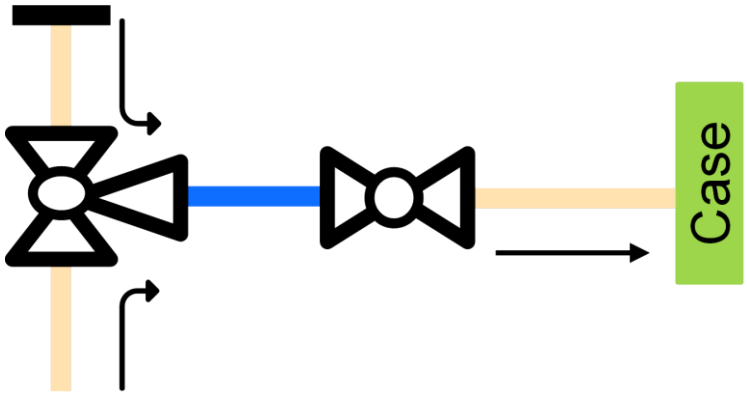

Figure 5-2: Schematic view of the liquid circuit

When the filling pressure is reached, the two-way valve opens letting the electrolyte enter into the clamping case. As the soaking force of the pressure difference is not enough to absorb all the liquid, the open second entrance of the three-way valve should open to push than remaining liquid into the case.

This operation has to be done rapidly, like a pulse signal; on the contrary it is blown too much air and the results are distorted. Then, the best solution is to open this way twice when the pressure reaches the 800 mBar for first time. After that, the valves remain closed for the rest of the simulation. This instant has been chosen to minimize the expelled liquid from the case. If the pressure-difference between chamber and outdoors is too high, the air throws out the liquid from the case, bringing a negative effect. The smaller this difference is, the smother the electrolyte flows throw the case. Furthermore, the 800 mBar moment is the single common state for all runs.

5.3 Lighting

In the previous study, the illumination came from the light of the controlled-environment-room, whose intensity was attenuated through a diffusion sheet, explained in section 4.1.4. Despite the diffusion sheet, the recorded videos suffered notable light's fluctuations. Shadows and tonality changes were noted on the recordings, distorting the number of black pixels at some times of the analysis. The solution involves the installation of a source of light inside the chamber, and the obstruction of the sight-window from any external light, leaving only a hole for the camera.

A flexible LED wire has been fastened around the inside face of the chamber (see Figure 5-3), providing a bright and constant illumination to the case. The features of the utilized LED strip are summarized in Table 11.

Figure 5-3: Flexible LED inside vacuum's chamber

The cable connection to the exterior of the chamber has to be done carefully not to lose vacuum conditions. Hence, it has adopted the same solution as for the Peltier element's connection already installed. It consists of an adapter connection ISO KF 16, that has 4 pins to let the current pass through it.

Table 11: Technical data of LED-strip

LED modules	30
Wire's length	50 cm
Power	2,4 W
Voltage	12 V
Luminous flux	170 lm

5.3.1 Sight-Window Cover

A cover made with paper and aluminum foil has been done to act as a cover for the eyehole (see Figure 5-4). The cover has been designed with three purposes:

- Avoid the incoming light
- Maintain the camera in a centered position for all trials
- Reflect the light from inside, acting as a continuation of chamber's faces

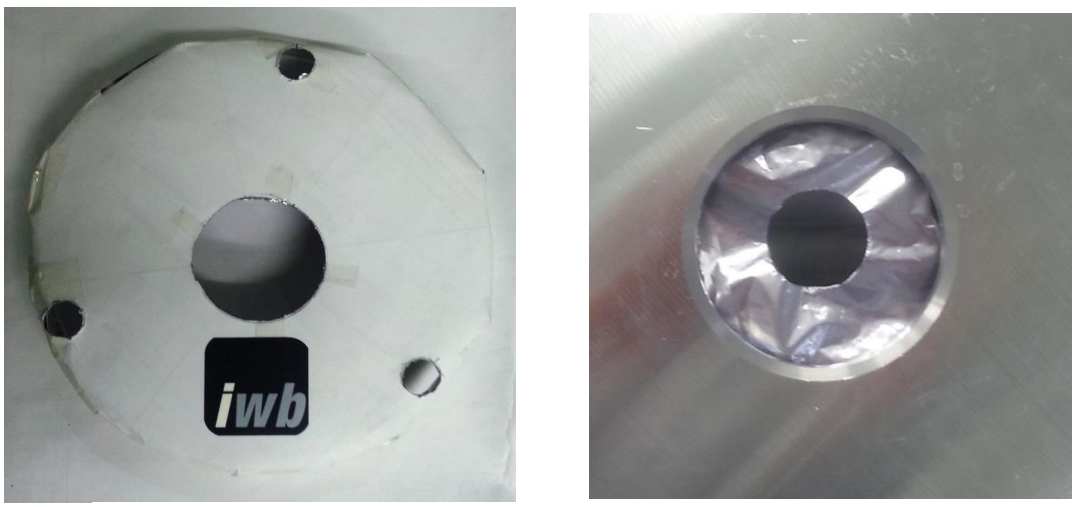

Figure 5-4: Self-made case's cover. Top and bottom views

5.4 Image Capture

The camera used to record all experiments is a GoPro® Hero3+ Black Edition. This device is controlled remotely via a Smartphone that shows simultaneously what the camera records. This functions permits to adjust the position of the camera, rotating this in most of the cases, to get a suitable video for the later crop with MATLAB. The captures settings are summarized in Table 12, after testing different configurations to obtain the most convenient setting. Further explanation about the meaning of every specification is found in (GOPRO).

To obtain the maximal possible clarity, the sight-window and the Plexiglas block are cleaned after every run, to remove the rest of electrolyte stuck on it.

Table 12: Image capture settings

Video resolution	1080 p
Frame rate	24 fps
Screen resolution	1920x1080
Field of view (FOV)	Narrow
White balance	3000 K
Color	Flat
ISO limit	400
Sharpness	High
Exposure	+ 0.5

5.5 Choice of Parameters and Factors

The first step was to determine the constant parameters that will remain unaltered during the tests. With the aim of minimizing the noise, so likely locked factors were selected to get results as unaltered as possible.

5.5.1 Choice of Parameters

In Table 13 presented and detailed the parameters choice.

Table 13: Constant parameters

Parameter	Fixed Value	Comments and Possible Influences
Room Temperature	20±1 ºC	Through room climate control
Dimensions of Layers	100 x 73 mm	Limited by the case dimensions
Fasten Pressure	3.544 kPa	Calculated with the spring force law
Electrolyte	EC:EMC/ 3:7	Solvent ratio used at *iwb*. It does not contain $LiPF_6$ for security reasons
Separator	Separion 240p30	Ceramic separator with 30 % porosity
Electrode	Anode	Current collector coated with graphite and 30 % porosity
Quantity of Electrolyte	1 ml	Proved to be the most convenient quantity
Electrolyte Introduction-Speed	Not specified	The electrolyte is automatically sucked, and always placed on the same position
Dew Point	-50 ºC	It is the combination of temperature and relative humidity (RH). The expected RH is about 3 %
Illumination	Reproducible and steady	Constant due to the LEDs and the aluminum cover

Quantity of Electrolyte

The quantity of electrolyte is calculated with the pores space of the cells. Knowing the dimension of the layers and their respective porosities, the total

available air to be filled with electrolyte can be calculated. For this work has been calculated the pore volume for two sheets; one electrode and one separator. The estimations are shown in Table 14:

Table 14: Layers characteristics

Layer	Square dimension	Thickness	Porosity (%)	Pore volume
Separator	100 x 73 mm	34 µm	30	74.46 mm^3
Anode	100 x 73 mm	110 µm	30	240.9 mm^3
				315.36 mm^3

The total volume to be soaked is 315.36 mm^3. After applying a security factor of 1.3, the volume becomes 409.97 mm^3. After doing a few tests with that quantity, the soaked volume was far from the half of the layer. Hence, it was decided to increase the amount until the surface was reasonably soaked. The chosen value that better fills the layers is 1 ml. These differences come from liquid losses inside the valve and during the way to the case.

5.5.2 Choice of Factors

Supported by the results of statistical and graphical analysis, and screening experiments, a critical set of factors has been identified for the modeling design. All of the factors are controllable and have adequate measurement systems, so they can be reliably set at wished values. The objective is to reproduce a pressure profile similar to the real filling stage. Details about filling profiles in the field of batteries can be found in patents such as (HOHENTHANNER & KLIEN 2012, RESCHKE 2011, THÖNNESSEN & NEUMANN 2014). In *Figure 5-5* is represented a pressure profile, where the green arrow is the aperture of the valve and the red arrow its closure. Both purple pointers represent the opening of the three-way valve to let air come in and push the remaining electrolyte inside the liquid circuit.

The chosen factors and their levels are in Table 15 annotated.

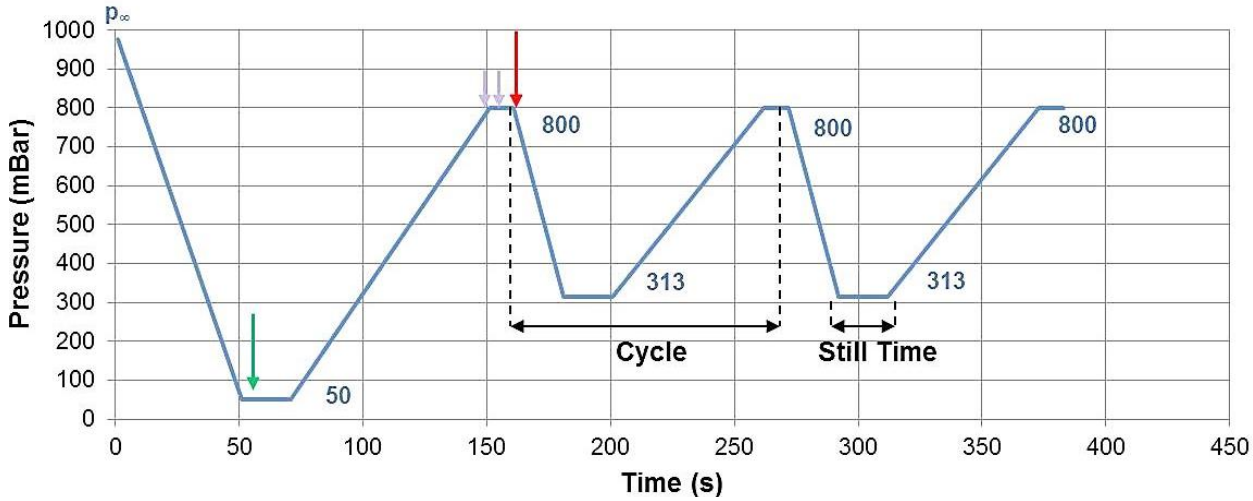

Figure 5-5: Pressure profile, with fillings pressure 50 mBar, wetting pressure 313 mBar, still time 20 seconds and 2 wetting cycles

Table 15: Factors and their selected levels

Factor	Type	Levels
Filling Pressure	Quantitative	• 50 mBar • 313 mBar • 607 mBar • 900 mBar
Wetting Pressure	Quantitative	• 50 mBar • 313 mBar • 607 mBar • 900 mBar
Still Time	Quantitative	• 10 seconds • 20 seconds • 30 seconds • 40 seconds
Number of Cycles	Quantitative	• 1 • 2 • 3

5.6 Video Evaluation

MATLAB is a full-featured technical computing environment. MATLAB allows matrix manipulations, plotting of functions and data, implementations of algorithms, creations of user interfaces and work with additional packages like Simulink (THE MATHWORKS C). For the manipulation of images, the toolbox "Image Processing" is used.

5.6.1 Image Processing

Image Processing Toolbox provides a comprehensive set of reference-standard algorithms, functions, and apps for image processing, analysis, visualization, and algorithm development. It can perform image analysis, image segmentation, noise reduction, and geometric transformations. This supports a diverse set of image types. Visualization functions and apps let explore images and videos, examine a region of pixels, adjust color and contrast, create contours or histograms, and manipulate regions of interest. (THE MATHWORKS B)

Digital Image

An image in MATLAB is a representation of a two dimensional matrix using a finite number of points, i.e., pixels. Each pixel is represented by one or more numerical values depending on the image type. An RGB image is represented using three 2D arrays of the same size, one for each color channel, i.e., a *m-by-n-by-3* data array that defines red, green, and blue color intensity in a scale of 256 unities.

A gray-level image is also encoded as a 2D matrix, usually with 8 bits per pixel. On each position is stored a value between 0 and 255, which represents the assorted shades of gray, being *0* a "*black*" pixel and *255* a "*white*" pixel. Finally, a black-and-white or binary image is a 2D array that uses one bit per pixel: *0* means "*black*", and *1,* "*white*". (MARQUES 2011)

Image Conversion

In this work a RGB image has to be converted to a black-and-white image. The ideal procedure is to convert firstly the RGB picture to a grayscale one, select a threshold value, and finally convert this grayscale image to a binary picture.

The first conversion is directly done using the function "*rgb2gray(image)".* This is followed by a study of the histogram, where the tonal distribution of the image is displayed. The threshold is the value that denotes the tonal separation between black pixels and white pixels. The function for transforming into a binary image is "*im2bw(image,threshold)".* In the arising image, all the pixels whose value is bigger than the thresholds are converted to white, otherwise converted to black pixels. (MARQUES 2011)

5.6.2 Script

Once the recording has ended, it has to be processed in order to extract all required data for a future analysis. The aim is to create a graph where the evolution of the wet surface was represented during the advance of video frames.

In the precedent work were extracted three samples from the video for their post-study. Particularly, those samples were taken on the seconds t_0, t_0+3 s. and t_0+7 s., being t_0 the opening of the valve which let the liquid flow. Then, the images were converted to binary ones and the number of black pixels were counted. This employed script is attached in Appendix B.

The key change regarding to the precedent investigation has been the consideration of the whole video instead of three images. With this suggested update the understanding of the wetting phase can be improved, the different stages it might suffer identified, and the effect that the chosen factors have on this quantified. The following sections are a brief explanation of the most significant actions the script performs and how it is organized. The entire script is attached in Appendix E.

Read and Create Variables

```
obj = VideoReader('18-2.mp4');
nFrames = obj.NumberOfFrames;
vidHeight = obj.Height;
vidWidth = obj.Width;
vidbw(1:nFrames)
=struct('cdata',zeros(vidHeight,vidWidth,1,'uint8'),'colormap',[]);
```

In this section, the video is read and the necessary properties are saved in variables for a later use. It follows the creation of a structure, in which all the frames will be stored with their convenient modifications. At the end, an unedited picture is shown with the aim of defining the zone to be cropped. Figure 5-6 illustrates the picture obtained with this last command.

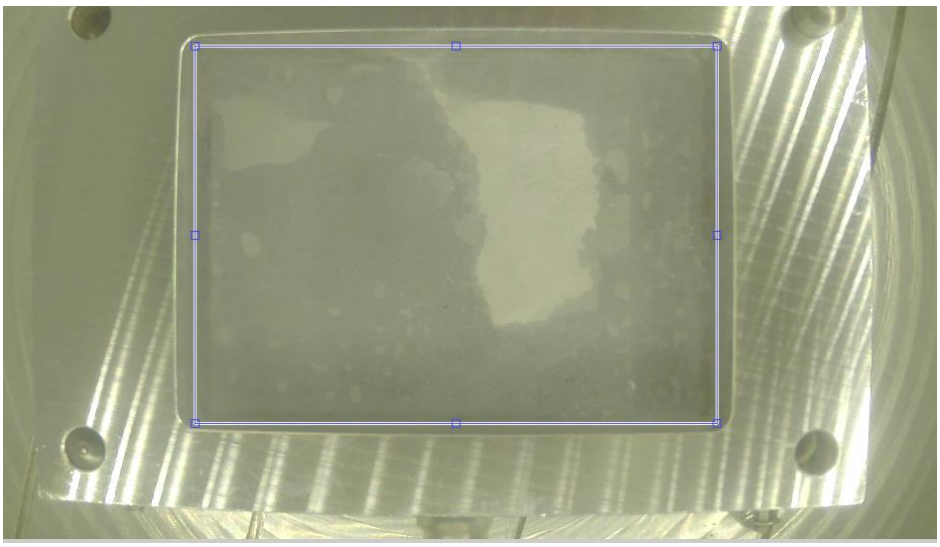

Figure 5-6: Original picture in the crop process of run 22, replica 1

Crop and Threshold Selection

```
imtool(read(obj,n2Frames));
x0=420;
y0=126;
xf=1451;
yf=864;
imtool(rgb2gray(imcrop(read(obj,n2Frames),[x0,y0,xf-x0,yf-y0])));
threshold=162;
imtool(im2bw(imcrop(read(obj,n2Frames),[x0,y0,xf-x0,yf-
y0]),threshold/255));
```

In this fragment are defined the corners' coordinates of the trim that delimitates the cell layers. Then, an image, already cropped, is transformed from RGB to gray scale and is shown to find a suitable threshold. This is the most difficult and demanding task to be done during the analysis, since the picture is inspected by eye. The technique is to observe three distinct frames (first, middle and last frames) and take the value that better fits to the split into wet and dry surface. This selected value is the same for all video's frames. This way was thought to be the most suitable manner, since after different automated strategies such as Otsu's method (THE MATHWORKS A), the mean or the median value of image's histogram were not appropriate to adjust properly those areas.

Figure 5-7 show the pictures obtained from MATLAB during this phase.

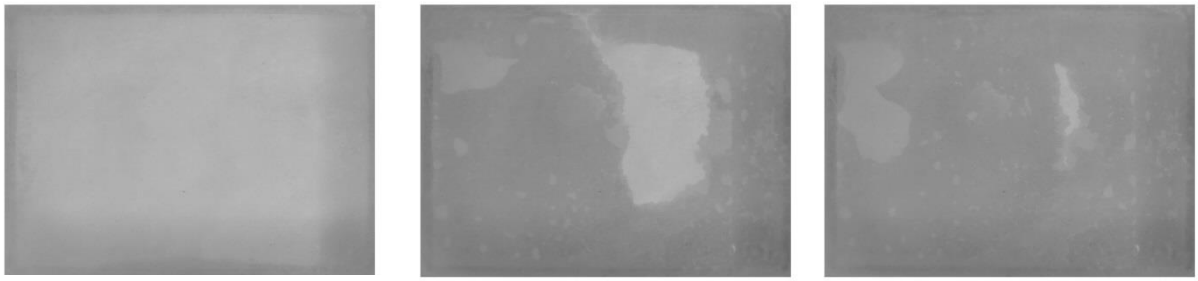

Figure 5-7: First, middle and last recorded frames in gray scale of run 22, replica 1

Video Conversion and Data Storage

```
for k = 1 : nFrames
    vidbw(k).cdata=im2bw(imcrop(read(obj,k),[x0,y0,xf-x0,yf-
y0]),threshold/255);
end

for k=1:nFrames
    blacks(k)=nnz(vidbw(k).cdata==0);
end
```

Each frame video is cropped and converted from RGB to black and white. All the new parts are stored into the structure created at the beginning. After that, the black pixels are counted for each frame and saved in a table, which is going to be the data base for the future chart. Figure 5-8 show the pictures achieved during this fragment.

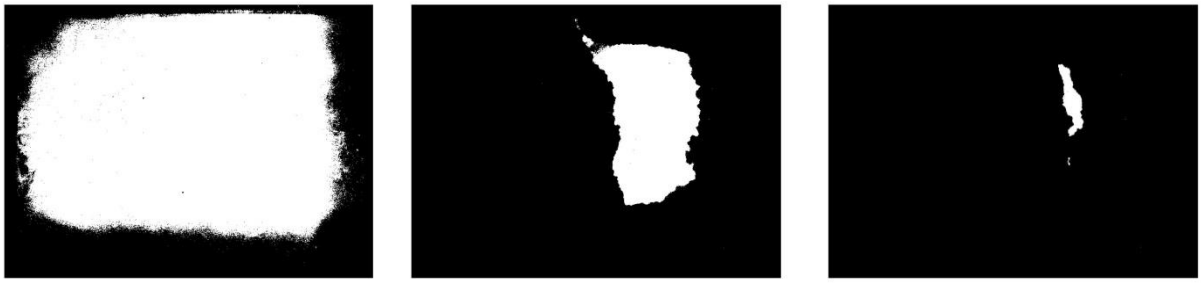

Figure 5-8: First middle and last recorded frames after black and white transformation of run 22, replica 1

```
plot(blacks);
hgexport(gcf, filename ,hgexport('factorystyle'), 'Format', 'jpeg');
imshow(rgb2gray(imcrop(read(obj,1),[x0,y0,xf-x0,yf-y0])));
filename=[num2str(fileimages) num2str(videofile) 'gray0.jpeg'];
xlswrite(num2str(excelfile),transpose(blacks),num2str(videofile))
```

The graph is created with its appropriate axis and saved as shown in Figure 5-9. The saved frames for every run are the first, middle, and last images in both gray scale and black and white. Finally, all the necessary data is exported to an Excel file and saved in a new page for each experiment. This information is:

- Table of black pixels for every frame
- Threshold value
- Number of frames
- Initial and ending number of black pixels

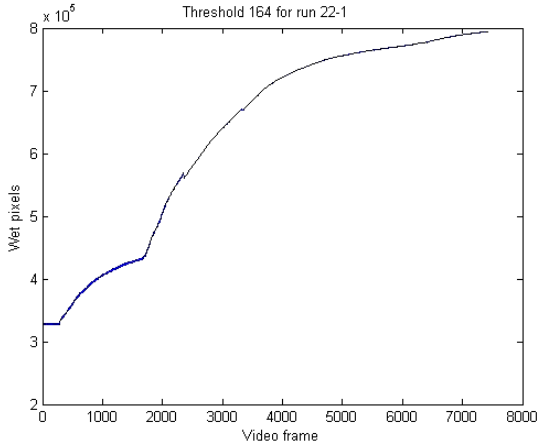

Figure 5-9: Plot created with MATLAB, showing the evolution of the black pixels in each frame for run 22, replica 1

6 Experimental Procedure

The actual chapter presents how the experimental phase is prepared and the methodic steps followed during the tests. Here is also explained the steps to choose a the DoE.

6.1 Pressure Profiles

The used vacuum pump in the experimentations comes from the company "*vacuumbrand*" and model MZ 2C NT VARIO. The main issue with this machine is the long transition times it needs to reach the objective value, due to its low maximal pumping speed of 2.8 m^3/h. With the aim of achieving the pressure's profiles alike each other, a simulation for all needed transitions was done, in which all the needed times for pressure changes were recorded. These transition times are going to be the ones used for every test.

With the help of a self-done Excel-VBA (Visual Basic for Application), the whole formation process has been automatized to ensure the same settings for every different profile and to simplify and to streamline a future labor execution. In Figure 6-1 can be seen an image of the file where this table is placed with all the possible transition values that may be found during the experimentations. On the left side are located the cells to write the conditions' values. When the square button is pushed, the program calculates automatically a table with the times and the pressures and refreshes the graph. The mentioned table is what the vacuum pump software needs to be

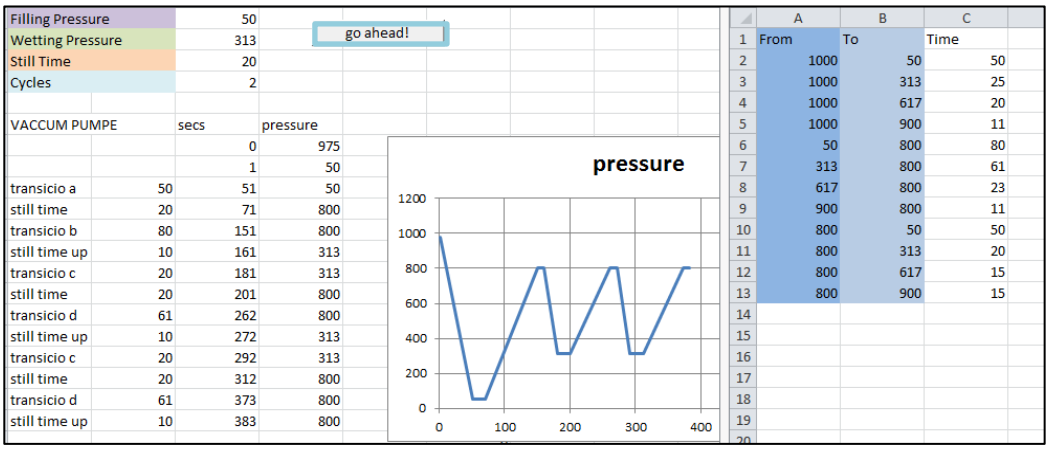

Figure 6-1: Screenshot of the macro to create the pressure profiles

introduced to achieve the desired pressure contour. The whole Visual Basic script is attached at Appendix D.

6.2 Experimental Procedure

First, the anode and the separator need to be cut to the wished dimensions, i.e., 100 x 73 mm. Then, the layers are placed inside the clamping case and it closed with the four mentioned springs. Images of the components and the procedure are shown in Figure 6-2. Second, the LED-wire is switched on and the whole set is placed inside the middle of the vacuum chamber, due to fit into camera's field of view. After that, the end of the tube has to be connected to the entrance of the clamping case, ensuring its proper tightness and then close the chamber afterwards. The syringe filled with 1 ml of electrolyte can now be evacuated into the intermediate tube-section like indicated in the previous Figure 5-2. During the tube is being filled, the two-way valve is opened, allowing a smooth circulation of both air and fluid thereby. When the 1 ml is introduced, the valve is closed and the three-way valve is attached behind at the tube entrance. The complete circuit has to lay on a high position to force the liquid to flow into the vacuum chamber. Otherwise, a higher quantity of electrolyte may remain inside the tubes. The profile data is adjusted to the pump-controller and the camera is positioned correctly. Via the GoPro App, a device controls remotely the camera, showing what the camera's sees. The case's sides have to be parallel to the sides of camera's image for the later analysis. MATLAB cannot rotate the image if this is decentered.

Once all the described adjustments are done, the trial can be started. All the valves rest closed at the beginning. The pump starts to work until the pressure reaches the "filling pressure". Now the camera starts to record, the two-way valve opens, and the electrolyte is sucked into the case. When the pressure reaches 800 mBar, the three-way valve opens shortly twice. After that, the valves will be closed for the rest of the simulation.

At the end of the profile, the video will be stopped. The total duration of the runs depend on the profile characteristics, which go between 90 to 720 seconds. When the pump is disconnected, both valves are switched on to blow the residual electrolyte inside the tubes, and bring the chamber to the atmospheric pressure conditions. Once those are reached, the cover can be

opened and the clamping case is unplugged. Before repeating the same procedure for the next run, the case and the Plexiglas block have to be cleaned to ensure that there are no electrolyte rests left.

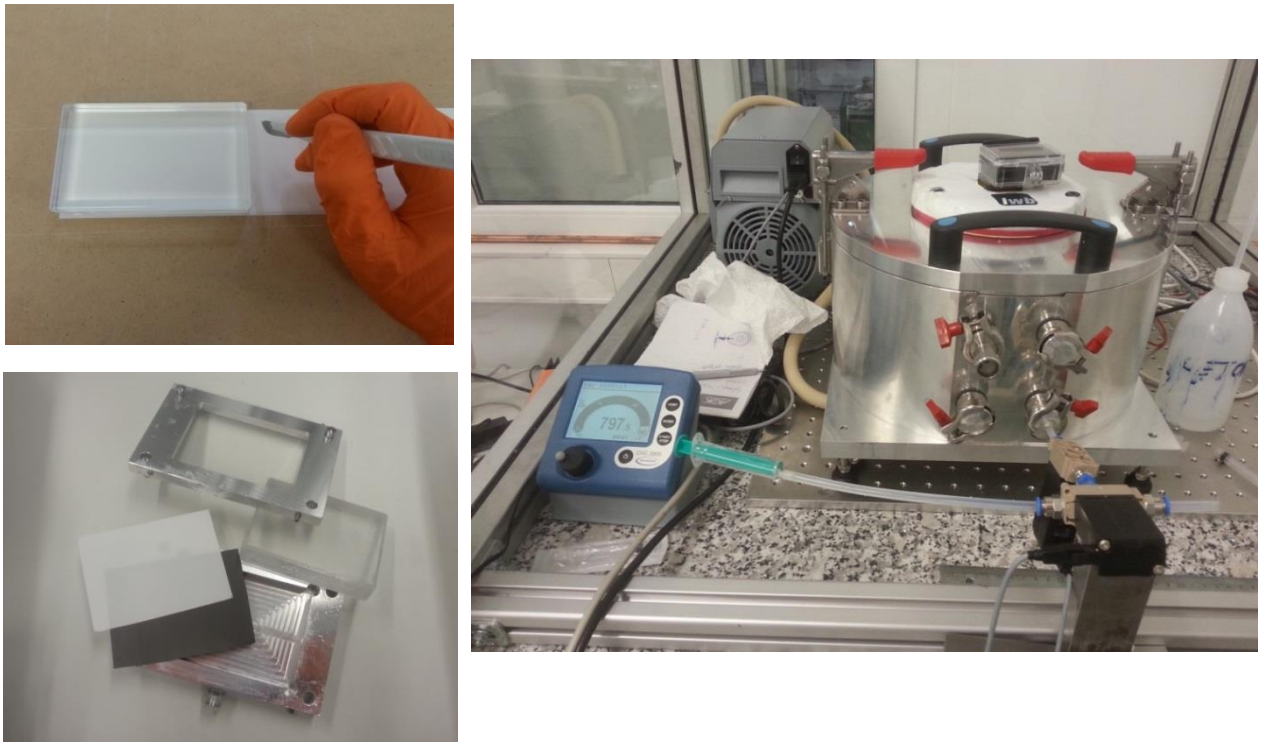

Figure 6-2: Photos of the experimental process

6.3 Design of Experiments

A design including the factors with greatest influence on the response needs to be created due to the experiment's optimization. The experimental goal is focused on the settings to create this optimal model.

In section 5.5.2 was explained the choice of factors and their levels. Now, with the support of the Design of Experiments (DoE), the most proper way to capture those influences has to be designed. With three four-level factors and one with three levels, the total number of runs without any replication rises to 192.

With the help of D-optimal designs, the minimum number of runs reduces to 16, having selected a quadratic model. In order to get a better explanation of the design surface, the decision was to take a total number of 42 matrix points for the basic design.

As described in section 3.3.5, the criterion of a D-optimal approach is to maximize the determinant of the information matrix. The DoE has been done with the statistical software called “Minitab 17”, in which the requested parameters to create the tests’ matrix are the quantity of wished runs. Starting from the whole design matrix, Minitab selects the number of runs to include in the optimal design and creates a new plan. The resulted determinant for the 42 selected points is 5.58E+18.

In order to reduce the variability in the response, two replicas for all runs are added to the design. A selected number of 18 runs have been complemented with two extra replicas. These 18 runs were chosen with another D-optimal design from the already 42 combinations, taking the points that provide more information to the factor influence. The resulting design matrix’s determinant with all replicas rises to 5.28E+25. Table 16 contains the complete design matrix with the replicas for each run.

Table 16: Design Matrix. Experiments from the number 27 are the later added

Run Number	Filling Pressure	Wetting Pressure	Still Time	Cycles	Replicas
1	50	607	10	1	2
2	50	313	40	3	4
3	607	50	20	1	2
4	50	50	10	3	2
5	50	900	40	2	2
6	900	607	20	2	2
7	900	50	40	1	4
8	50	607	40	3	4
9	50	50	30	1	2
10	900	900	10	3	4
11	900	50	10	1	4
12	50	900	20	1	4
13	900	900	40	3	4
14	313	313	20	3	4
15	50	313	40	1	2
16	607	900	30	1	2
17	313	900	10	2	4
18	900	900	40	1	4
19	50	900	10	3	4
20	900	50	30	3	2
21	313	607	10	3	4
22	607	313	30	2	2
23	900	900	10	1	4
24	313	50	40	2	2
25	900	50	10	3	4
26	607	50	40	3	2
27	50	50	10	1	4
28	50	607	30	1	2
29	50	50	30	3	4
30	313	50	10	3	4
31	313	313	30	2	2
32	313	313	40	1	2
33	313	900	20	3	2
34	607	50	40	1	2
35	607	607	20	2	2
36	607	900	10	1	2

37	607	900	30	3	2
38	900	50	40	3	2
39	900	313	20	1	2
40	900	313	40	3	4
41	900	607	40	1	2
42	900	900	40	2	2

The cubes in Figure 6-3 and Figure 6-4 map the position of all the design points in 3D spreadsheet planes. These drawings are helpful to visualize where the points at the first D-optimal design with 26 factors combinations are placed, and how this ends up with the 26 additional ones.

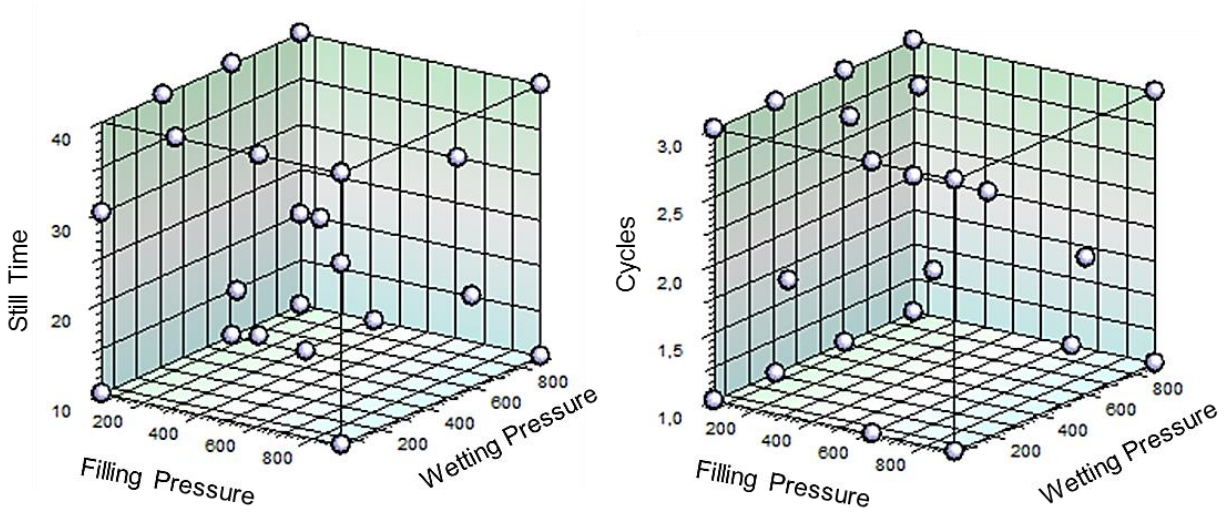

Figure 6-3: 3D representation for 26 design-points

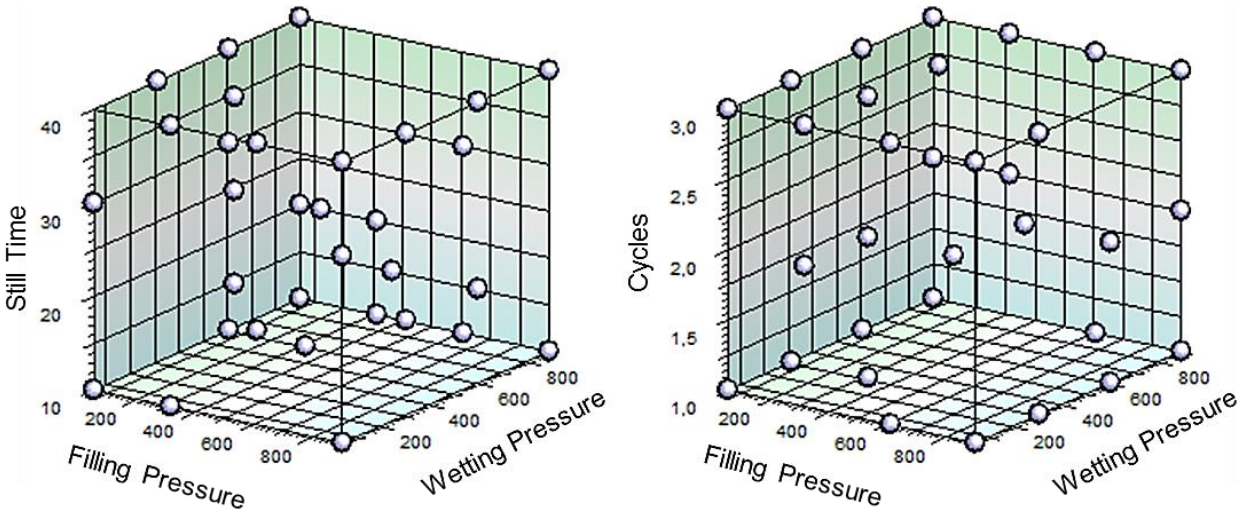

Figure 6-4: 3D representation for 42 design-points

7 Results

This chapter explains conversion from the graphic results obtained with the videos to a numerical result that explains the phenomena aimed to pattern. After that, comes the statistical analysis for the selected response through the choice of the right regression. All the statistical analysis has been done with a student license of the software Minitab 17.

7.1 Response Selection

Once the videos are converted into black and white and the plots are created, the primal query is not already solved: which would be the proper value that could be extracted from the videos and had a direct relation to the explanation of the electrolyte spreading process? Although the videos and plots are a helpful tool to reach and observe possible tendencies, all they should be summed up with a numerical value.

All the outputs stored from MATLAB were revised and drawn in single charts with their correspondent profile of pressure. Moreover, with the help of a VBA for Excel, a series of coefficients and relations were calculated to obtain a clear and helpful visualization of the desired information. All detailed information about the data processing is explained at Appendix F.

7.1.1 Wetting Speed

The first selected response was the point of time, at which every run reached an indicated percentage of pixels in relation with the last recorded value. This percentage was foremost selected, regarding as the value in which the trial's slope stabilizes, becoming a flat curve. The percentage value was carefully picked via the observation of the graphs adjusted to different percentages. Figure 7-1, Figure 7-2, and Figure 7- 3 show the adjustment of four runs to three different percentages.

After having attempted various percentages, the selected value was 95 %, because this was thought to be the fairest approximation and the one that adjust better to the expected response for all wetting profiles.

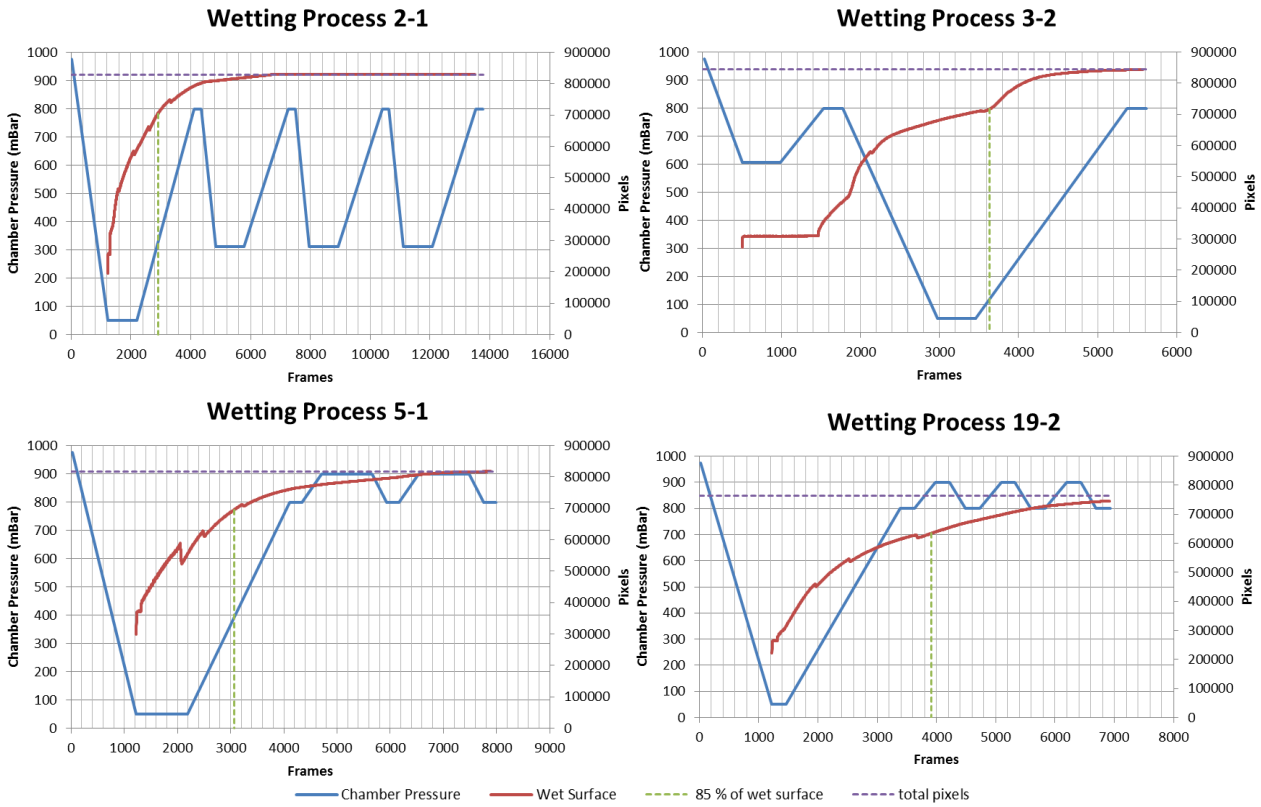

Figure 7-1: Plotted runs 2-1, 3-2, 5-1, and 19-2, with the 85 % mark

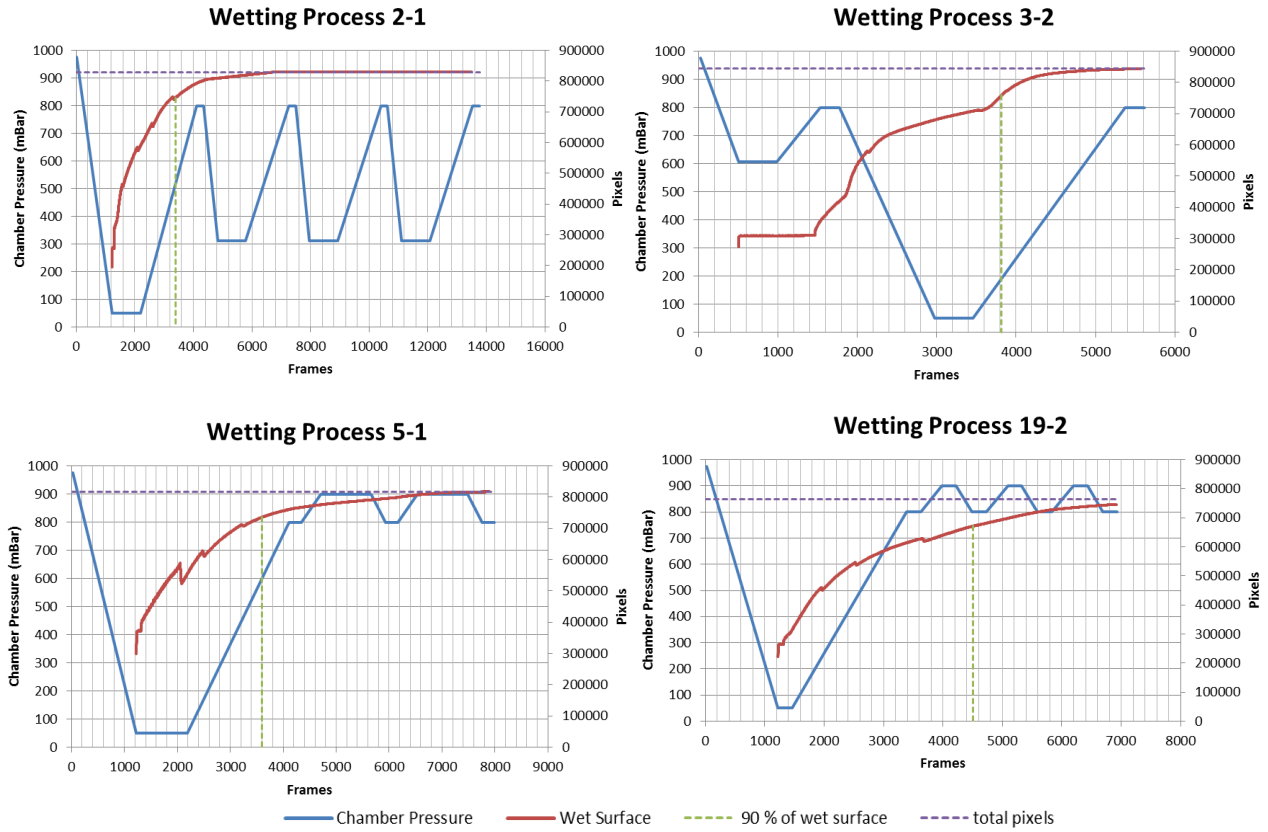

Figure 7-2: Plotted runs 2-1, 3-2, 5-1, and 19-2, with the 90 % mark

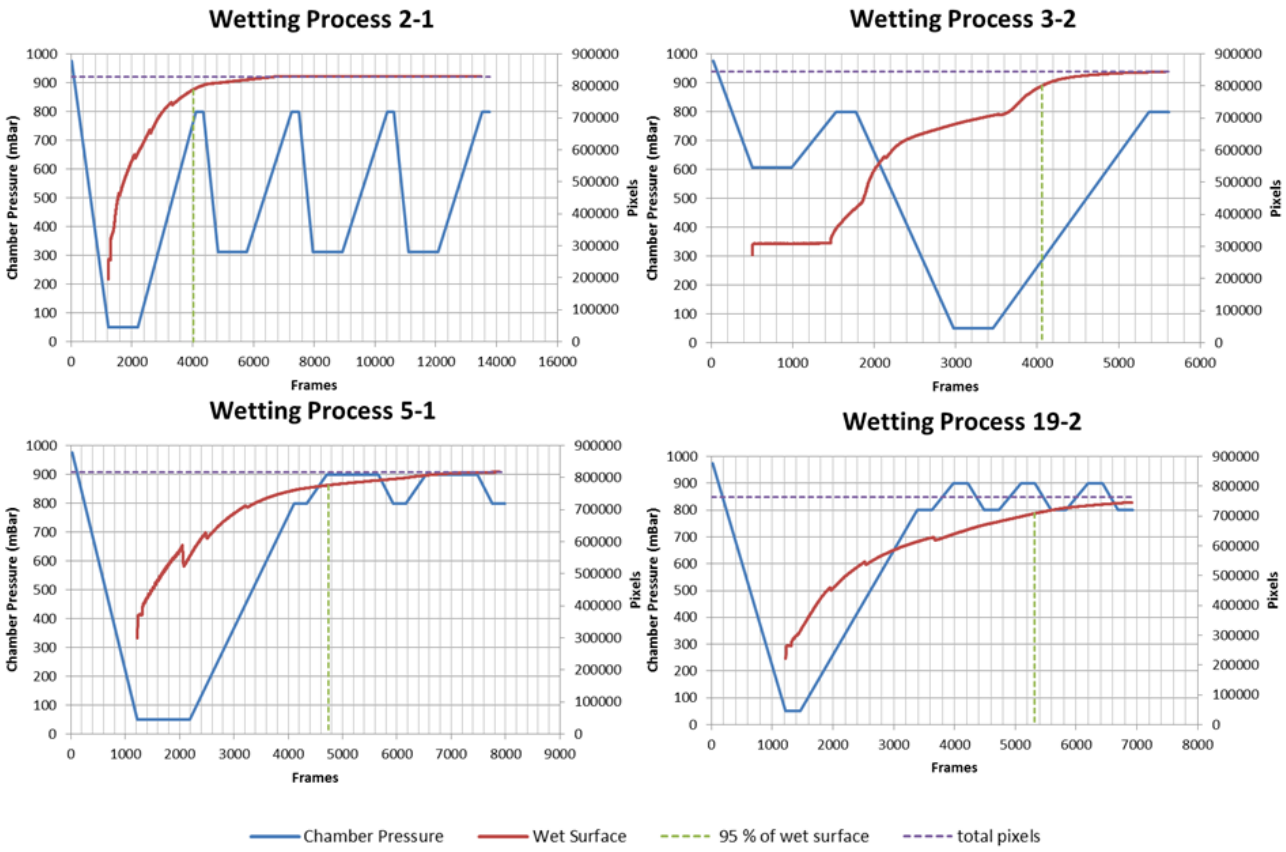

Figure 7-3: Plotted runs 2-1, 3-2, 5-1, and 19-2, with the 95 % signal

The obtained value from the Excel table, is the frame number from the start of the recording that corresponds to the indicated pixel percentage. In order to change the units into seconds, it is divided by a factor equal 24, corresponding to the quantity of frames per second. The major objection to this response was the high influence of the time that the vacuum pump needs for reaching deep pressures. These values are especially large for pressures of 50 and 313 mBar, as it can be seen in the blue table on the right side of Figure 6-1. While a transition from 800 to 50 mBar needs 50 seconds, one that goes from 800 to 617 mBar only takes 15 seconds. The respective inverse transition times, these differences are even more significant, lasting a total of 80 and 23 seconds respectively. The procedure to raise the pressure is done through a valve. With the aim of excluding part of that unwished time-influences, the time to reach the filling pressure was deducted from the total time. Therefore, the response relative time is the one from the open of the valve.

Table 17 gathers the replicas average relative times to reach a wet portion of 95 %, as well as their standard deviations (StDevs).

Table 17: Relative times to reach 95 % of the final value of pixels

Run	Replicas	Mean relative time to 95 % [s]	StDev relative time to 95 % [s]	Run	Replicas	Mean relative time to 95 % [s]	StDev relative time to 95 % [s]
1	2	68.1	53.92	**22**	2	169.3	50.71
2	4	199.5	82.79	**23**	4	65.1	7.34
3	2	155.3	9.87	**24**	2	210.6	40.51
4	2	236.5	3.33	**25**	4	246.1	97.68
5	2	126.6	28.23	**26**	2	195.6	99.79
6	2	118.6	16.00	**27**	4	151.8	39.79
7	4	157.4	25.59	**28**	2	117.4	23.31
8	4	190.4	38.15	**29**	4	180.2	102.17
9	2	116.5	82.32	**30**	4	282.3	76.82
10	4	123.4	6.49	**31**	2	226.7	45.28
11	4	122.1	19.44	**32**	2	173.3	12.61
12	4	118.9	22.57	**33**	2	194.2	7.07
13	4	169.1	47.41	**34**	2	195.8	9.02
14	4	218.0	59.98	**35**	2	145.2	10.37
15	2	156.9	6.66	**36**	2	79.3	2.80
16	2	111.4	9.34	**37**	2	159.7	6.51
17	4	125.9	14.80	**38**	2	340.0	85.18
18	4	112.1	3.25	**39**	2	108.8	3.56
19	4	166.3	15.10	**40**	4	217.2	72.72
20	2	151.4	1.62	**41**	2	121.2	3.18
21	4	178.7	22.11	**42**	2	146.5	5.27

After a study of the main effects (see Figure 7-4) and a comparison between the expected tendencies and the results achieved so far, it was realized that the chosen response was not the most appropriate to pattern the desired property. For example, the wetting pressure effect was expected to have an opposite influence as the predicted. The results are extremely distorted and highly influenced by the duration of those transition times. Figure 0-3 in

Appendix G shows the main effects for the response with complete simulation time from the recording's start.

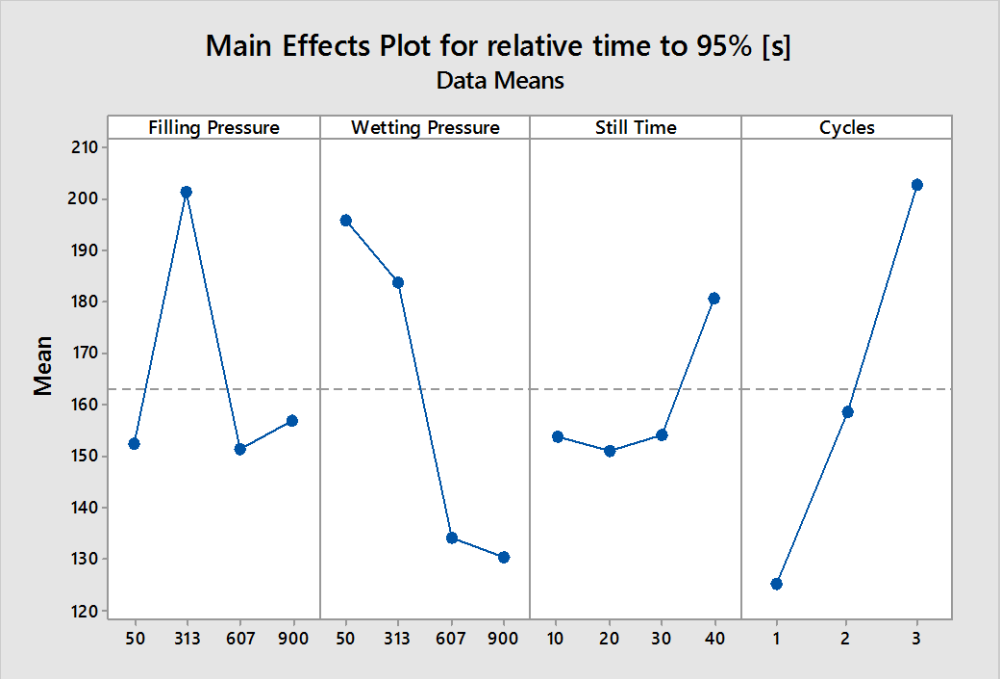

Figure 7-4: Main effects plot for relative time 95 %

In what StDevs refers, no visible pattern has been found. There is no relation to the number of replicas, neither to the simulation parameters. The only seen pattern is the correlation with the response. The bigger the response is, the wider the StDev is. However, it is not relevant enough.

With the aim of knowing whether the coefficients are significant, Stepwise regression was done, choosing a quadratic model with interactions and $\alpha_e = \alpha_r = 0.15$ (see all theory in Chapter 3). The results' summary obtained from Minitab is represented in Figure 7-5, where the wetting pressure and cycles are the most significant factors.

Coded Coefficients

Term	Effect	Coef	SE Coef	95% CI	T-Value	P-Value	VIF
Constant		164,5	11,0	(142,2; 186,7)	15,01	0,000	
Filling Pressure	-4,99	-2,50	6,04	(-14,76; 9,77)	-0,41	0,682	1,02
Wetting Pressure	-63,58	-31,79	5,95	(-43,86; -19,72)	-5,35	0,000	1,02
Still Time	22,81	11,41	6,02	(-0,81; 23,63)	1,89	0,066	1,03
Cycles	73,29	36,65	5,45	(25,58; 47,71)	6,73	0,000	1,01
Filling Pressure*Filling Pressure	-49,1	-24,5	11,8	(-48,5; -0,6)	-2,08	0,045	1,07
Still Time*Still Time	37,1	18,6	11,9	(-5,5; 42,6)	1,57	0,126	1,07

Figure 7-5: Stepwise coefficients for wetting speed at 95 %

Taking a second look at the got responses, they are highly correlated to the time the pressure profile takes to be completed. This direct relation can be seen for example in that the more cycles a profile has, the longer this lasts. Consequently, the more time the run takes to end with the profile, and the wider the electrolyte is spread, i.e., more black pixels.

The next section suggests another response with less time-dependence.

7.1.2 Wet Surface

After the rejection of the wetting speed as a response due to its high dependency of the transition times of the pump, a new numerical response that was less influenced by the slowness of the pump was searched for. In this case, the most appropriate response was thought to be the percentage of wet surface at the end of every video. This percentage is the division of the total number of black pixels at the end of the test by the pixels the cropped image contains, i.e., $\frac{final\ black\ pixels}{image\ pixels}\ x\ 100$.

The mean values of this percentage and their StDevs are shown in the Table 18. The values are estimated from the obtained results in all the replicas, attached in the Table 21 in Appendix H.

The response was obtained from the same datasheets of Excel as in the previous response. In Figure 7-6 are four selected processes' plots representing different pressure profiles.

The StDevs are noticeable smaller for this second response, because the ranges of values are narrower than the ones in the time response. The percentages range goes from 71.2 % to 100 %. The times have a range with more than 200 seconds between the slowest and the fastest result.

Table 18: Percentages of wet pixels and StDevs

Run	Replicas	Mean wet pixels [%]	StDev wet pixels [%]	Run	Replicas	Mean wet pixels [%]	StDev wet pixels [%]
1	2	79.9	11.51	**22**	2	99.6	0.59
2	4	94.9	8.17	**23**	4	71.2	7.10
3	2	95.1	6.74	**24**	2	99.9	0.09
4	2	91.9	4.96	**25**	4	89.3	9.75
5	2	99.9	0.15	**26**	2	99.4	0.85
6	2	91.6	9.69	**27**	4	91.4	11.98
7	4	97.4	3.05	**28**	2	98.6	0.27
8	4	91.4	8.03	**29**	4	99.7	0.60
9	2	98.9	1.59	**30**	4	98.4	1.95
10	4	89.8	6.83	**31**	2	97.9	2.85
11	4	95.5	6.13	**32**	2	97.3	0.34
12	4	94.6	3.17	**33**	2	92.9	7.48
13	4	78.5	15.67	**34**	2	97.8	1.72
14	4	88.0	14.71	**35**	2	95.9	4.82
15	2	96.6	0.10	**36**	2	73.7	1.89
16	2	72.3	7.34	**37**	2	98.6	1.37
17	4	89.0	9.13	**38**	2	96.4	4.45
18	4	84.2	9.52	**39**	2	88.0	9.41
19	4	93.6	3.37	**40**	4	96.9	4.63
20	2	100.0	0.00	**41**	2	80.2	13.07
21	4	87.0	13.57	**42**	2	97.6	0.55

Following the performed steps for the preceding response, the effects chart (see in Figure 7-7) is analyzed to acquire some tendencies for the main effects. This plot met the expectations. The layers are wider soaked when the pressures take lower values. The effects in Figure 7-7 agree with the behavior experimented up to now.

The tendency observed in the filling pressure is explained by the fact that when the pressure difference between the vacuum chamber and exterior is bigger, the electrolyte is pushed with more force.

For the wetting pressure, the explanation is similar. The more pressure

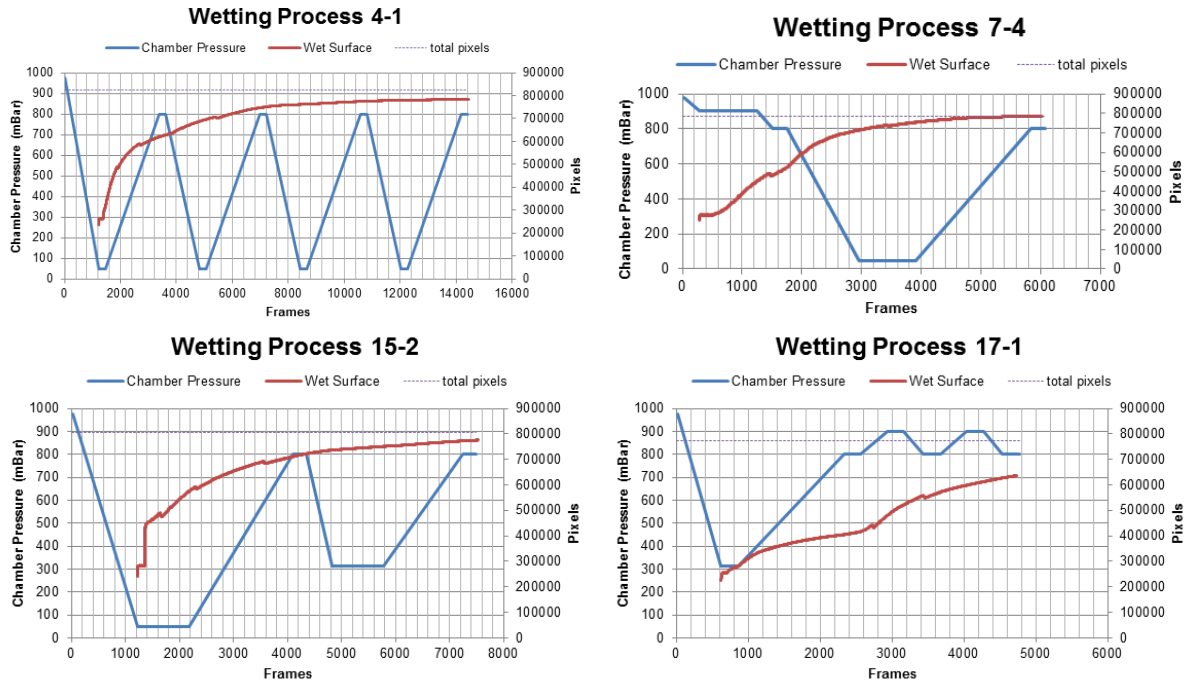

Figure 7-6: Plotted runs 4-1, 7-4, 15-2, and 17-1

difference the layers suffer during the cycles, the more dynamism is given to the liquid with the contractions and expansions of the block and among the sheets.

The still times show a maximum of wetting efficiency for 30 seconds. This characteristic could have the same reason as for the wetting pressure. The layers wet better the longer the time halts in the deep pressure, but too much time could result not dynamic enough for the proper liquid circulation.

Finally, one the one hand, the number of cycles rises because the process lasts longer and the liquid has more time to be soaked. On the other hand, this has an inflexion point for two cycles. This maximum could be explained by the evaporation of the electrolyte when the tests take too long times to be completed. This explanation could also be considered for the maximum found for the “still times”.

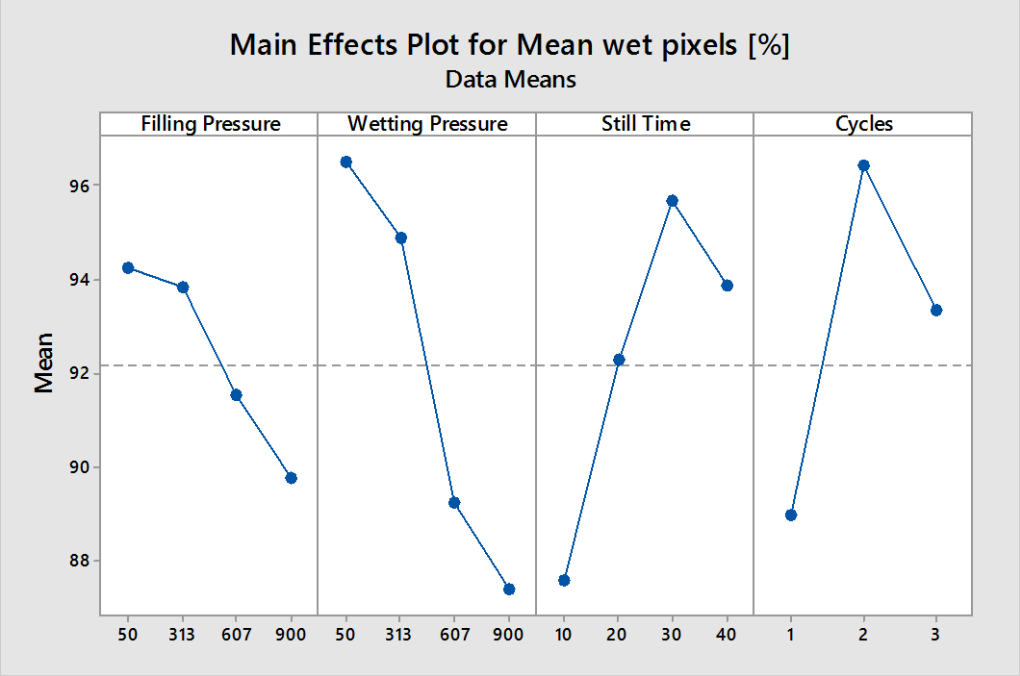

Figure 7-7: Main effects plot for wet pixels

7.2 Analysis Surface Response Design

As seen in section 3.5.1, there are three strategies to create a regressive model. In this study all three ways will be applied and the results will be compared among each other. The wetting surface is the selected response for the analysis.

7.2.1 Best Subsets

Figure 7-8 shows the Best Subsets indicators for the best models depending on the number of factors. The chosen variables that the program adds to the model on every step are considered the most significant for the response. Squared in an orange square are the most three interesting options, because are the ones with the smallest C_p-values and high R_a^2. The key determinant characteristic will be of how many parameters the model will be composed, due to over-fitting prevention. The Figure 7-9 plots the basic parameters that help to decide which model choose, and the progression of these parameters in relation to the number of factors in the model.

Response is Mean wet pixels [%]

Vars	R-Sq	R-Sq (adj)	R-Sq (pred)	Mallows Cp	S	Filling Pressure	Wetting Pressure	Still Time	Cycles	Filling^2	Wetting^2	Silltime^2	Cycles^2	Fill*wet	Fill*still	Fill*cycle	wet*still	Wet*cycle	Still*cycle
1	33,5	31,9	23,5	32,3	6,5415									X					
2	44,5	41,7	32,3	22,7	6,0520			X						X					
3	50,1	46,1	35,4	18,9	5,8187			X						X		X			
4	58,5	54,1	44,7	11,9	5,3722			X	X				X	X					
5	60,8	55,4	45,4	11,5	5,2955			X	X				X	X		X			
6	66,2	60,5	47,7	7,7	4,9839		X	X	X				X	X				X	
7	68,3	61,8	47,9	7,5	4,8984		X	X	X			X	X	X				X	
8	70,5	63,4	49,0	7,2	4,7971		X	X	X		X	X	X	X				X	
9	72,0	64,1	49,1	7,6	4,7464		X	X	X		X	X	X	X				X	X
10	72,8	64,0	48,2	8,8	4,7548		X	X	X		X	X	X	X		X		X	X
11	73,4	63,6	45,7	10,2	4,7791		X	X	X		X	X	X	X	X	X		X	X
12	74,3	63,7	44,4	11,2	4,7749	X	X	X	X	X	X	X	X	X		X		X	X
13	74,5	62,6	39,9	13,0	4,8448	X	X	X	X	X	X	X	X	X	X	X		X	X
14	74,5	61,3	32,2	15,0	4,9330	X	X	X	X	X	X	X	X	X	X	X	X	X	X

Figure 7-8: Best Subsets regression

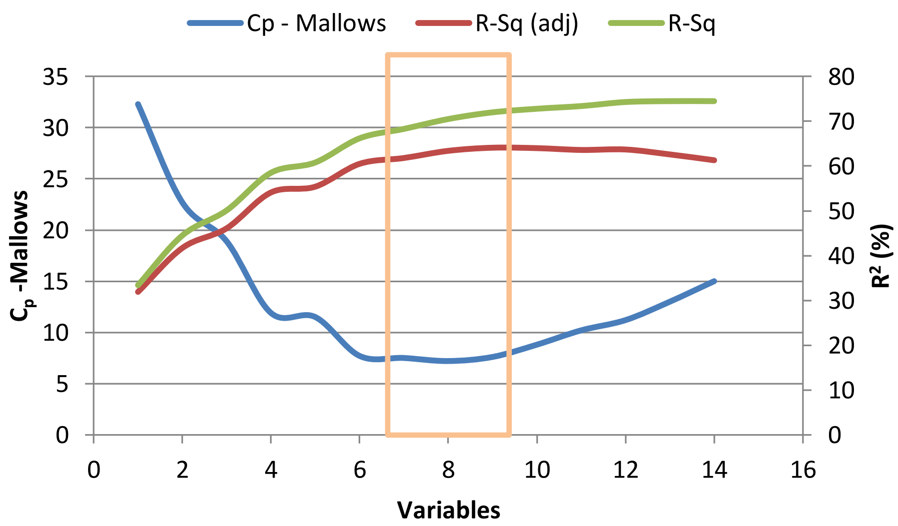

Figure 7-9: Evolution of C_p,R_a^2 and R^2 for Best Subsets regression

The designs for the models with 7, 8 and 9 variables are represented in Figure 7-10, Figure 7-11, and Figure 7-12 respectively to see whether the principal assumptions for the residuals are accomplished (see section 3.5.3).

Analysis of Variance

Source	DF	Seq SS	Contribution	F-Value	P-Value
Regression	7	1760,0	68,33%	10,48	0,000
Wetting Pressure	1	660,1	25,63%	8,42	0,006
Still Time	1	200,0	7,76%	3,64	0,065
Cycles	1	144,0	5,59%	8,19	0,007
Silltime^2	1	120,6	4,68%	2,23	0,144
Cycles^2	1	212,7	8,26%	8,80	0,005
Fill*wet	1	272,7	10,59%	10,40	0,003
Wet*cycle	1	149,9	5,82%	6,25	0,017
Error	34	815,8	31,67%		
Total	41	2575,7	100,00%		

Model Summary

S	R-sq	R-sq(adj)	PRESS	R-sq(pred)
4,89835	68,33%	61,81%	1342,43	47,88%

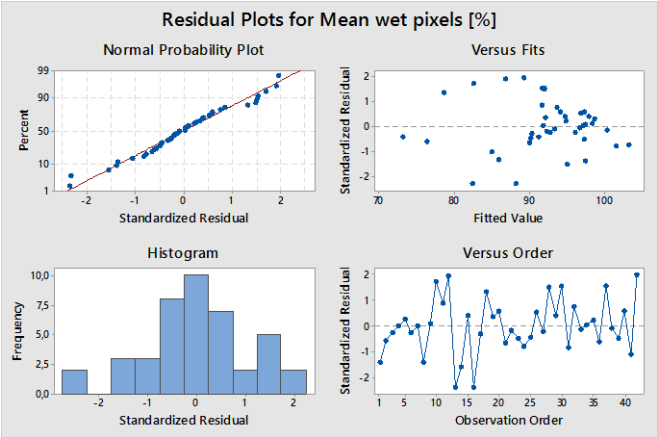

Figure 7-10: Best Subsets model for seven variables

Analysis of Variance

Source	DF	Seq SS	Contribution	F-Value	P-Value
Regression	8	1816,34	70,52%	9,87	0,000
Wetting Pressure	1	660,11	25,63%	8,25	0,007
Still Time	1	199,98	7,76%	4,77	0,036
Cycles	1	144,01	5,59%	9,44	0,004
Silltime^2	1	120,63	4,68%	3,03	0,091
Cycles^2	1	212,69	8,26%	10,15	0,003
Fill*wet	1	272,69	10,59%	12,18	0,001
Wet*cycle	1	149,85	5,82%	6,43	0,016
Wetting^2	1	56,38	2,19%	2,45	0,127
Error	33	759,41	29,48%		
Total	41	2575,74	100,00%		

Model Summary

S	R-sq	R-sq(adj)	PRESS	R-sq(pred)
4,79712	70,52%	63,37%	1313,56	49,00%

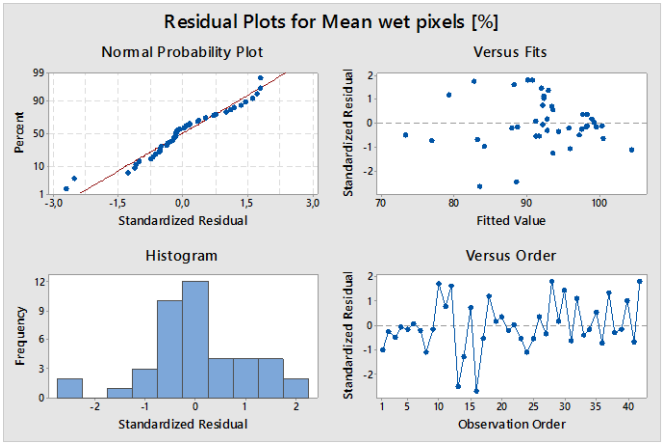

Figure 7-11: Best Subsets model for eight variables

The three represented models fulfill all the residual assumptions (3.5.3). The errors are independent of the run order, the variances do not follow any significant pattern, and the three of them are fitted to a normal law. However, the model that adjusts better to the normal law is the 7-variable regression.

Analysis of Variance

Source	DF	Seq SS	Contribution	F-Value	P-Value
Regression	9	1854,84	72,01%	9,15	0,000
Wetting Pressure	1	660,11	25,63%	8,14	0,008
Still Time	1	199,98	7,76%	6,37	0,017
Cycles	1	144,01	5,59%	11,01	0,002
Silltime^2	1	120,63	4,68%	3,30	0,079
Cycles^2	1	212,69	8,26%	10,38	0,003
Fill*wet	1	272,69	10,59%	12,37	0,001
Wet*cycle	1	149,85	5,82%	5,75	0,022
Wetting^2	1	56,38	2,19%	2,57	0,119
Still*cycle	1	38,51	1,49%	1,71	0,200
Error	32	720,90	27,99%		
Total	41	2575,74	100,00%		

Model Summary

S	R-sq	R-sq(adj)	PRESS	R-sq(pred)
4,74638	72,01%	64,14%	1311,00	49,10%

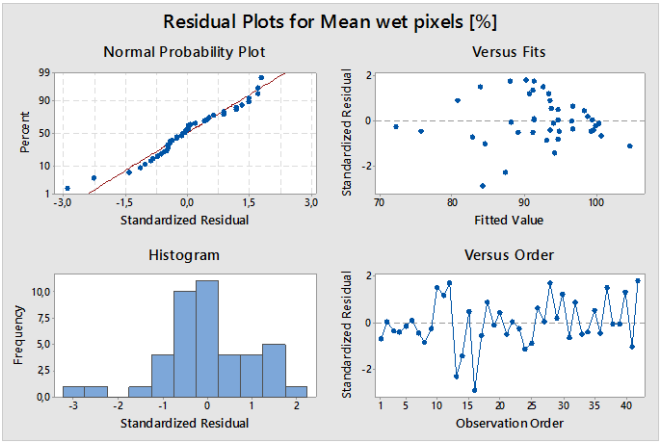

Figure 7-12: Best Subsets model for nine variables

7.2.2 Stepwise

The only needed parameters to enter in the Minitab are α_e and α_r. These parameters are the thresholds that let a variable enter to the model or force this to leave the model. Minitab recommends equal value of αs, proposing a default value of 0.15. Figure 7-13 shows the resultant model for $\alpha_e = \alpha_r = 0.15$. This first approximation has nine factors and the normal approach for the residuals is worse fitted than the models in the best subsets. Hence, the αs are reduced to acquire an approach with less parameters. The new parameters are $\alpha_e = \alpha_r = 0.1$ and $\alpha_e = \alpha_r = 0.05$, finding the same seven-factor model for both (Figure 7-14).

Stepwise Selection of Terms

α to enter = 0,15; α to remove = 0,15
The stepwise procedure added terms during the procedure in order to maintain a hierarchical model at each step.

Analysis of Variance

Source	DF	Seq SS	Contribution	F-Value	P-Value
Model	9	1817,14	70,55%	8,52	0,000
Linear	4	1167,70	45,33%	13,22	0,000
Filling Pressure	1	154,51	6,00%	7,46	0,010
Wetting Pressure	1	637,53	24,75%	23,56	0,000
Still Time	1	237,99	9,24%	9,78	0,004
Cycles	1	137,67	5,34%	6,72	0,014
Square	3	369,61	14,35%	5,06	0,006
Wetting Pressure*Wetting Pressure	1	13,28	0,52%	2,33	0,137
Still Time*Still Time	1	120,00	4,66%	2,94	0,096
Cycles*Cycles	1	236,33	9,18%	9,85	0,004
2-Way Interaction	2	279,83	10,86%	5,90	0,007
Filling Pressure*Wetting Pressure	1	131,74	5,11%	5,19	0,030
Wetting Pressure*Cycles	1	148,09	5,75%	6,25	0,018
Error	32	758,61	29,45%		
Total	41	2575,74	100,00%		

Model Summary

S	R-sq	R-sq(adj)	PRESS	R-sq(pred)
4,86893	70,55%	62,26%	1336,92	48,10%

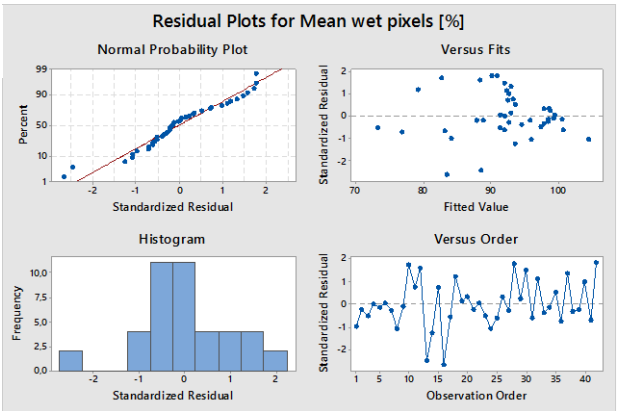

Figure 7-13: Stepwise model for $\alpha_e = \alpha_r = 0.15$

In this second model with seven significant factors, the normality assumption is accomplished with more precision than in the previous one.

Stepwise Selection of Terms

α to enter = 0,1; α to remove = 0,1
The stepwise procedure added terms during the procedure in order to maintain a hierarchical model at each step.
Analysis of Variance

Source	DF	Seq SS	Contribution	F-Value	P-Value
Model	7	1708,3	66,32%	9,57	0,000
Linear	4	1167,7	45,33%	11,81	0,000
Filling Pressure	1	154,5	6,00%	6,40	0,016
Wetting Pressure	1	637,5	24,75%	22,25	0,000
Still Time	1	238,0	9,24%	7,47	0,010
Cycles	1	137,7	5,34%	6,24	0,018
Square	1	258,0	10,02%	9,85	0,003
Cycles*Cycles	1	258,0	10,02%	9,85	0,003
2-Way Interaction	2	282,6	10,97%	5,54	0,008
Filling Pressure*Wetting Pressure	1	133,1	5,17%	4,88	0,034
Wetting Pressure*Cycles	1	149,5	5,80%	5,86	0,021
Error	34	867,5	33,68%		
Total	41	2575,7	100,00%		

Model Summary

S	R-sq	R-sq(adj)	PRESS	R-sq(pred)
5,05108	66,32%	59,39%	1376,23	46,57%

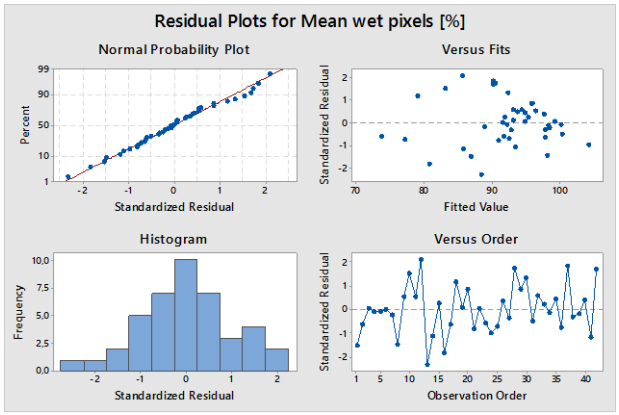

Figure 7-14: Stepwise model for $\alpha_e = \alpha_r = 0.10$ and 0.05

7.2.3 All in

For this technique, all the variables are present in the regression and their confidence p-values estimated (see Figure 7-15).

Analysis of Variance

Source	DF	Seq SS	Contribution	F-Value	P-Value
Model	14	1918,71	74,49%	5,63	0,000
Linear	4	1167,70	45,33%	12,60	0,000
Filling Pressure	1	154,51	6,00%	6,54	0,016
Wetting Pressure	1	637,53	24,75%	22,60	0,000
Still Time	1	237,99	9,24%	8,91	0,006
Cycles	1	137,67	5,34%	7,00	0,013
Square	4	386,13	14,99%	3,76	0,015
Filling Pressure*Filling Pressure	1	4,54	0,18%	0,99	0,330
Wetting Pressure*Wetting Pressure	1	13,68	0,53%	2,44	0,130
Still Time*Still Time	1	115,21	4,47%	3,22	0,084
Cycles*Cycles	1	252,70	9,81%	10,22	0,004
2-Way Interaction	6	364,88	14,17%	2,50	0,047
Filling Pressure*Wetting Pressure	1	131,37	5,10%	4,74	0,038
Filling Pressure*Still Time	1	2,15	0,08%	0,16	0,695
Filling Pressure*Cycles	1	22,38	0,87%	1,12	0,299
Wetting Pressure*Still Time	1	0,03	0,00%	0,01	0,933
Wetting Pressure*Cycles	1	149,36	5,80%	5,21	0,031
Still Time*Cycles	1	59,60	2,31%	2,45	0,129
Error	27	657,03	25,51%		
Total	41	2575,74	100,00%		

Model Summary

S	R-sq	R-sq(adj)	PRESS	R-sq(pred)
4,93300	74,49%	61,26%	1746,62	32,19%

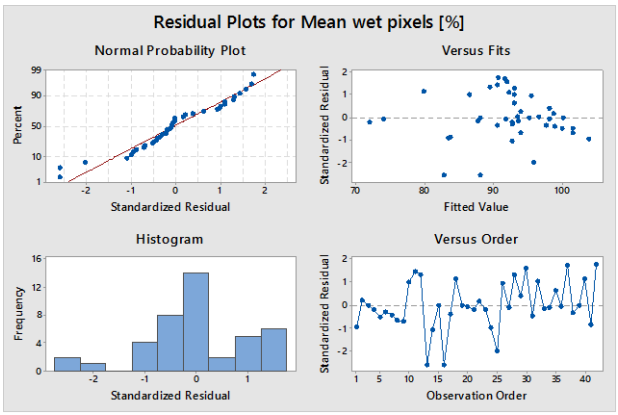

Figure 7-15: Model for all parameters in

7.2.4 Overview and Model Selection

To have an overview of the scores obtained for each strategy and take the most proper solution, number of variables, R^2, R_a^2, and C_p are ranked in Table 19.

Table 19: Models overview

Strategy / Model	No. Variables	R_a^2 [%]	R^2 [%]	C_p
Best Subsets	7	61.8	68.3	7.5
Best Subsets	8	63.4	70.5	7.2
Best Subsets	9	64.1	72	7.6
Stepwise $\alpha_e = \alpha_r$ =0.10	7	59.4	66.3	-
Stepwise $\alpha_e = \alpha_r$ =0.15	9	62.3	70.5	-
All in	14	61.3	74.5	-

The model with all the variables is over fitted. Despite owning the highest R^2, this has twice as many variables as the rest. When the models with nine factors are compared, the “best subsets” model explains the better response in both the R^2 and R_a^2 ratios than the Stepwise. In reference to the residual analysis, none of them differs from each other, taking all premises for granted.

The final choice was the model with seven factors from Stepwise. All regressions with more than seven factors were discarded because both models with seven have already an adjusted explication for the response. Taking models with more variables complicates the equation more than it improves the approach. Although the model with seven variables from the Best Subsets has a greater response determination than the one from the Stepwise, this last contemplate the four principal factors as significant variables. It is advisable to include the main factors if the interaction of any of these is in the model. When it comes to the residual plots, both have an adjusted normal probability chart.

In the following section, the chosen model is deeply studied.

7.3 Wetting Model

The selected approach is the Stepwise with $\alpha_e = \alpha_r = 0.10$, represented in Figure 7-14. In this chapter the residual assumptions will be verified, all available information will be extracted, and the phenomena will be interpreted.

7.3.1 Assumptions

The first step for extracting correct conclusions is to verify the residual hypotheses listed in 3.5.3. If these are fulfilled, the model will be reliable.

In the first plot the residuals vs. expected values are represented. As shown in Figure 7-16, there is neither a visible pattern in the variance nor a residual tendency. The red line is a linear tendency to determine if the residuals increase or decrease along the expected values. In this case, it is constant, accepting the assumption of constant variance.

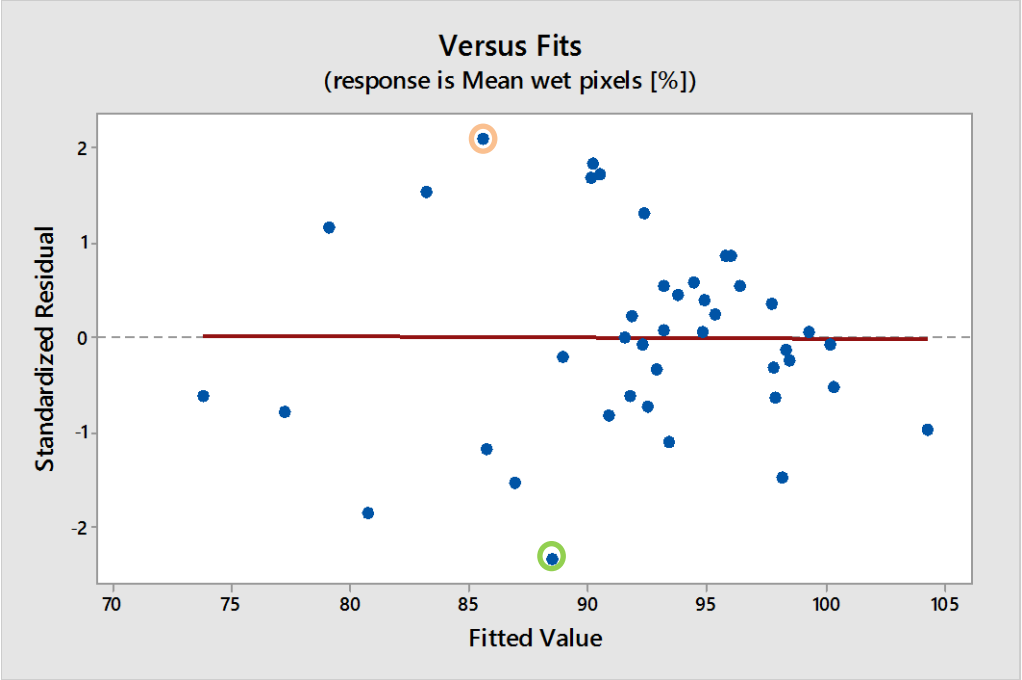

Figure 7-16: Standardized residual vs. expected values

The results include some responses with results equal 100 % of wet pixels. When the statistical approach is done, the fitted values reach percentages values greater than the maximum seen in the response. In this case, as the response is a percentage, obtaining results greater than 100 % has no sense. However, they cannot be limited.

The next plot is the independence of errors verified, with the illustration of residuals vs. order of the data. In Figure 7-17 can be seen that the errors have no correlation with the order of the collected response.

The last chart for the residual suppositions verifies the normality of these with an expectancy equal zero. As Figure 7-18 shows, the residuals follow a

normality law centered in zero with no necessity to carry out a transformation. In that figure can be seen that the points divert from the normality line. This deviation is not significant enough to apply a transformation of the response, because it does not imply any pattern change.

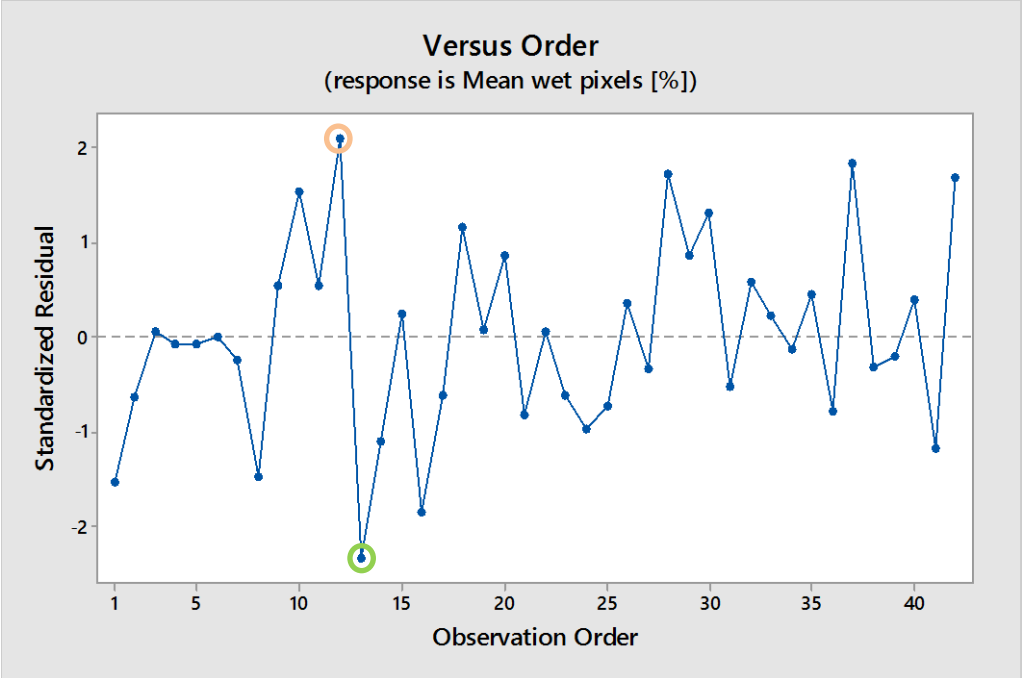

Figure 7-17: Standardized residual vs. observation order

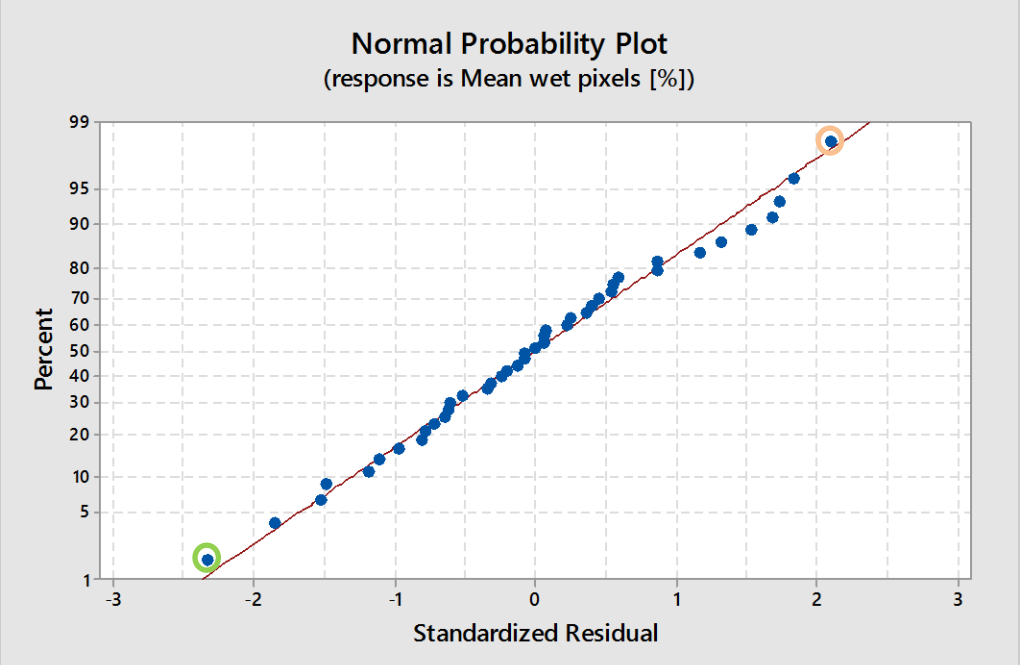

Figure7-18: Normal probability plot of residuals

After these three verifications, it is assumed that the model is appropriate, fulfilling all assumptions.

7.3.2 Model Coefficients and ANOVA

The model has been created using the Stepwise regression (3.5.1) in forward direction, starting with a void model. The two coefficients to allow the factors to be introduced to or removed from the model, namely α_e and α_r, are both equal to 0.10. Figure 7-19 shows the process that Minitab has followed to add and to remove factors.

The first added factors are the most influential, i.e., those that contribute more to the response's explanation. These factors are the wetting pressure and the number of cycles, providing overall two-thirds of the total explication. All factors' contributions are described in the ANOVA table of the Figure 7-20.

In last screenshot from Minitab, Figure 7-21, are detailed all the necessary information for the factors' coefficients such as effects, coefficients, confidence intervals (CI) for a confidence level of 95 %, and t- and p-values. Having this model consciously selected, the factors are all significant for the wetting progress. All them are achieved t-values greater than |2| and p-values smaller than 0.05. Below the table of the effects, the mathematical expression with the variables and their coefficients is located. This expression predicts the response given the characteristics of the pressure profile. Finally, the two listed runs are unusual observations detected for the model, i.e., the two worst predicted points. These runs are the number 12 and 13, and they do not fit accurately to the approached curve because the estimated wet percentage is far from the one measured. The difference between the fitted values and the real values is a 10 % and a 9 % for runs 13 and 12 respectively. In the previous figures the circled points in orange correspond to the run 12 and the green ones to the 13.

Stepwise Selection of Terms

Candidate terms: Filling Pressure; Wetting Pressure; Still Time; Cycles; Filling Pressure*Filling Pressure; Wetting Pressure*Wetting Pressure; Still Time*Still Time; Cycles*Cycles; Filling Pressure*Wetting Pressure; Filling Pressure*Still Time; Filling Pressure*Cycles; Wetting Pressure*Still Time; Wetting Pressure*Cycles; Still Time*Cycles

	----Step 1----		----Step 2----		----Step 3----	
	Coef	P	Coef	P	Coef	P
Constant	91,95		97,65		97,67	
Wetting Pressure	-4,79	0,001	-5,25	0,000	-5,31	0,000
Cycles			1,97	0,072	2,27	0,032
Cycles*Cycles			-7,06	0,007	-6,98	0,005
Wetting Pressure*Cycles					2,72	0,030
Still Time						
Filling Pressure						
Filling Pressure*Wetting Pressure						
S	6,92032		6,21115		5,90223	
R-sq	25,63%		43,09%		49,96%	
R-sq(adj)	23,77%		38,59%		44,55%	
R-sq(pred)	17,03%		30,57%		34,47%	
Mallows' Cp	40,72		26,24		20,97	

	----Step 4----		----Step 5----		-----Step 6----	
	Coef	P	Coef	P	Coef	P
Constant	97,01		97,06		97,13	
Wetting Pressure	-5,00	0,000	-4,89	0,000	-4,595	0,000
Cycles	2,325	0,022	2,270	0,019	2,187	0,018
Cycles*Cycles	-6,38	0,008	-6,37	0,005	-6,36	0,003
Wetting Pressure*Cycles	2,69	0,025	2,58	0,024	2,51	0,021
Still Time	2,33	0,036	2,57	0,016	2,642	0,010
Filling Pressure			-2,31	0,029	-2,442	0,016
Filling Pressure*Wetting Pressure					-2,57	0,034
S	5,62475		5,32340		5,05108	
R-sq	55,78%		61,49%		66,32%	
R-sq(adj)	49,64%		54,89%		59,39%	
R-sq(pred)	38,48%		42,85%		46,57%	
Mallows' Cp	16,80		12,76		9,65	

α to enter = 0,1; α to remove = 0,1

The stepwise procedure added terms during the procedure in order to maintain a hierarchi model at each step.

Figure 7-19: Stepwise: selection of terms

Analysis of Variance

Source	DF	Seq SS	Contribution	Adj SS	Adj MS	F-Value
Model	7	1708,3	66,32%	1708,3	244,04	9,57
Linear	4	1167,7	45,33%	1205,0	301,25	11,81
Filling Pressure	1	154,5	6,00%	163,2	163,17	6,40
Wetting Pressure	1	637,5	24,75%	567,6	567,60	22,25
Still Time	1	238,0	9,24%	190,5	190,51	7,47
Cycles	1	137,7	5,34%	159,1	159,14	6,24
Square	1	258,0	10,02%	251,4	251,36	9,85
Cycles*Cycles	1	258,0	10,02%	251,4	251,36	9,85
2-Way Interaction	2	282,6	10,97%	282,6	141,29	5,54
Filling Pressure*Wetting Pressure	1	133,1	5,17%	124,4	124,39	4,88
Wetting Pressure*Cycles	1	149,5	5,80%	149,5	149,50	5,86
Error	34	867,5	33,68%	867,5	25,51	
Total	41	2575,7	100,00%			

Figure 7-20: Model's ANOVA table

Coded Coefficients

Term	Effect	Coef	SE Coef	95% CI	T-Value	P-Value
Constant		97,13	1,82	(93,43; 100,82)	53,37	0,000
Filling Pressure	-4,883	-2,442	0,965	(-4,404; -0,480)	-2,53	0,016
Wetting Pressure	-9,190	-4,595	0,974	(-6,575; -2,615)	-4,72	0,000
Still Time	5,284	2,642	0,967	(0,677; 4,607)	2,73	0,010
Cycles	4,374	2,187	0,876	(0,407; 3,967)	2,50	0,018
Cycles*Cycles	-12,72	-6,36	2,03	(-10,48; -2,24)	-3,14	0,003
Filling Pressure*Wetting Pressure	-5,14	-2,57	1,16	(-4,94; -0,20)	-2,21	0,034
Wetting Pressure*Cycles	5,01	2,51	1,04	(0,40; 4,61)	2,42	0,021

Regression Equation in Uncoded Units

Mean wet pixels [%] = 73,16 + 0,00101 Filling Pressure - 0,01585 Wetting Pressure
+ 0,1761 Still Time + 24,83 Cycles - 6,36 Cycles*Cycles
- 0,000014 Filling Pressure*Wetting Pressure
+ 0,00590 Wetting Pressure*Cycles

Fits and Diagnostics for Unusual Observations

Obs	Mean wet pixels [%]	Fit	SE Fit	95% CI	Resid	Std Resid	Del Resid	HI	Cook's D	DFITS	
12	94,62	85,61	2,67	(80,18; 91,03)	9,01	2,10	2,22	0,279510	0,21	1,38235	R
13	78,50	88,49	2,67	(83,06; 93,92)	-10,00	-2,33	-2,51	0,279955	0,26	-1,56314	R

Figure 7-21: Model Coefficients, Effects, 95 % CI, and unusual observations

7.3.3 Principal Effects and Interactions

In the table of Figure 7-21 the numerical values for main effects and interactions are annotated. Figure 7-22 are represented the effects in plots. In these charts are shown the impact of the response when the value of factors are changed inside the experimental range.

The digits for the coefficients and effects are different, even though both explain the same information. On one side, the effects indicate the absolute change that is suffered by response from the low to the high level. On the other side, the equation's terms are adapted values that express those response's changes, relying on the contribution and the range value of that factor.

Coefficients signs match to the slope's direction of the effects. The higher the slope's grade is, the more impact a factor has on the response. As the model includes a squared cycle (cycle^2), its profile is parabolic, achieving a maximum wetting around two cycles. Filling and wetting pressures are decreasing regressions, which perform their bests wetting percentages at low pressures. The still time describes an upward curve.

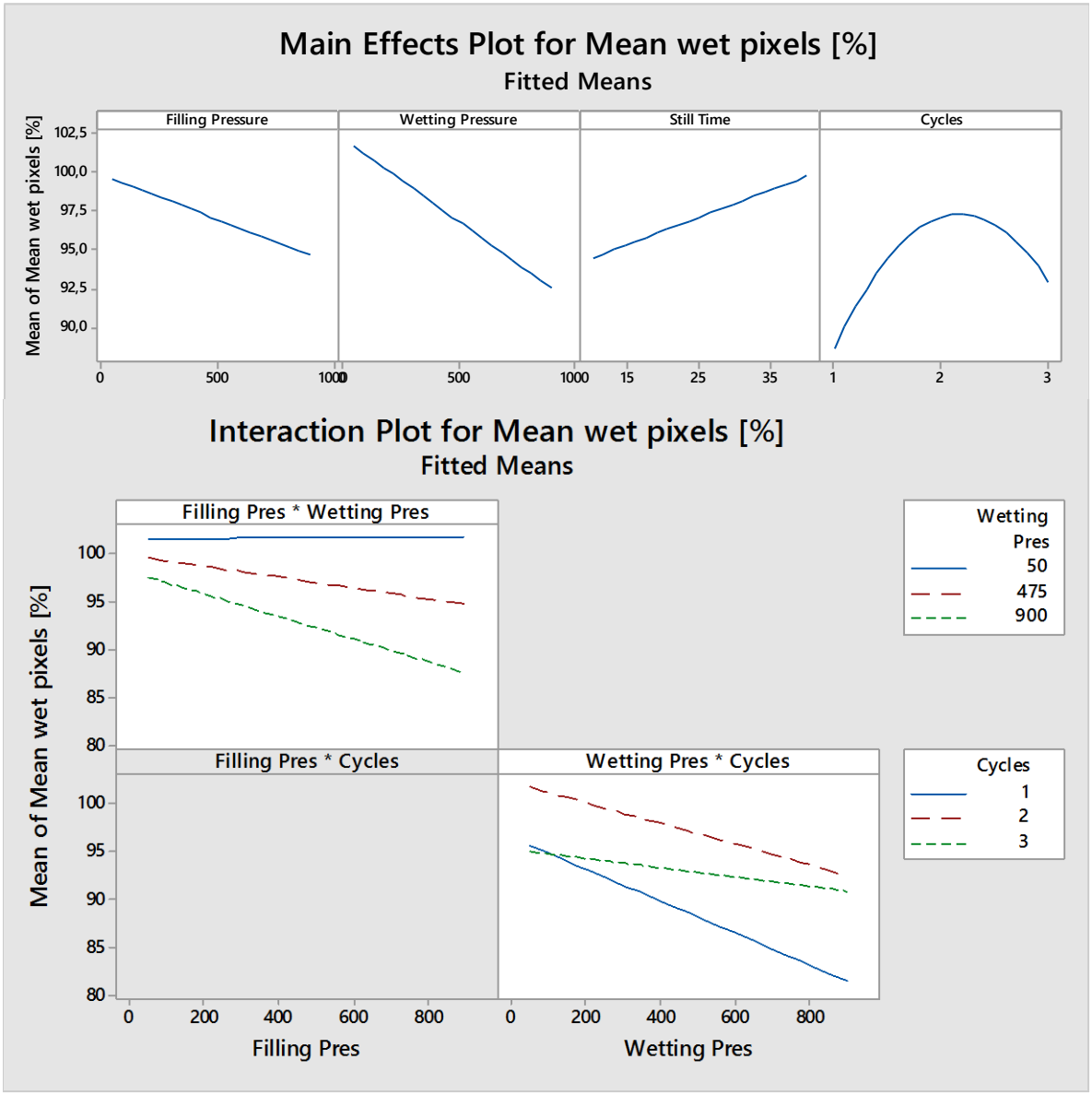

Figure 7-22: Main effects and interaction plots

8 Discussion

The main target of this thesis was to find a pattern to describe and predict the behavior of the electrolyte during the wetting process for the manufacture of LIBs. In this chapter the developed model and the achieved results will be discussed. The implication of the findings will be explained and possible future work on the field suggested.

8.1 Review of MATLAB Analysis

All tests have been analyzed and the most proper thresholds selected throughout the mentioned procedure in section 5.6. Figure 8-1 contains the most significant descriptive statistics, a threshold histogram, and the data gathering order for all the selected thresholds.

The figure states that the most used threshold is 162, the mean 163.5, and the range within all thresholds are comprised is [160,169]. This range represents less than 5 % of the possible value dispersion that could have been chosen ([0,255]). This difference of thresholds has had an insignificant influence to the spreading tendencies. The unique effect that might have caused this divergence, is reduced on a few tens of pixels, which it is considered irrelevant for the response. To change the surface percentages a single 0.1 %, it would be needed around 780[vi] pixels to differ from their value. With this certainty, it is concluded that the response is not sensitive to the threshold.

8.2 Unusual Observations

All the information derived from MATLAB has been studied and taken some commentaries to explain the observed patterns and possible problems.

Table 18 on page 85 shows the standard deviation for all the runs. The samples 13, 14, 21, and 41 present the greatest StDevs, with values between 13 % and 15 %, far behind from the mean of 5.5 %. Two of these tests coincide with the unusual observations detected by Minitab, 13 and 14, as the

[vi] Analyzed frames have an average of 782.000 pixels

Variable	Total Count	Mean	SE Mean	StDev	Variance	Minimum	Q1	Median	Q3	Maximum	Range
thresholds	120	163,46	0,204	2,23	4,99	160,00	162,00	162,00	165,00	169,00	9,00

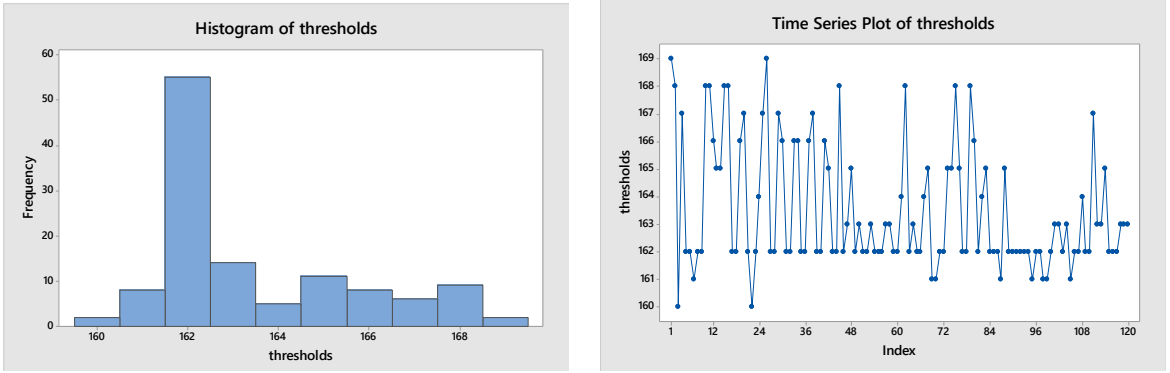

Figure 8-1: Descriptive statistics, histogram and time series plot obtained with Minitab for the chosen thresholds

ones with higher residuals. Taking a look at the Table 21 on page 144, both wide StDevs come from the tests 13-2 and 14-3, whose results are rather different from the other replicas. This might be either an experimental error or an atypical conduct of the electrolyte during those experiments. Nonetheless, no data has been excluded from the study.

Figure 8-2 and Figure 8-3 show the four replicas for the runs 13 and 14. In them, the pressure profile, and wet surface progression are plotted. The abnormal test is squared in red.

8.3 Factors Effects

The results declare significant the four factors, i.e., they have an influence on the response.

The most contributive factor for the regression is the “wetting pressure”, explaining one fourth of the answer. Its effect is equal to -9.2, what means that a test with a wetting pressure of 50 mBar wets 9.2 % more surface than one at 900 mBar. This factor owns the wider number of standard errors from its non-zero estimated parameter until the null hypothetical effect, precisely, a distance of 5.35 times its error. Furthermore, the effect on the cell’s wetting is totally supported by the trends observed. The relative maximum is obtained at the pressure of 50 mBar.

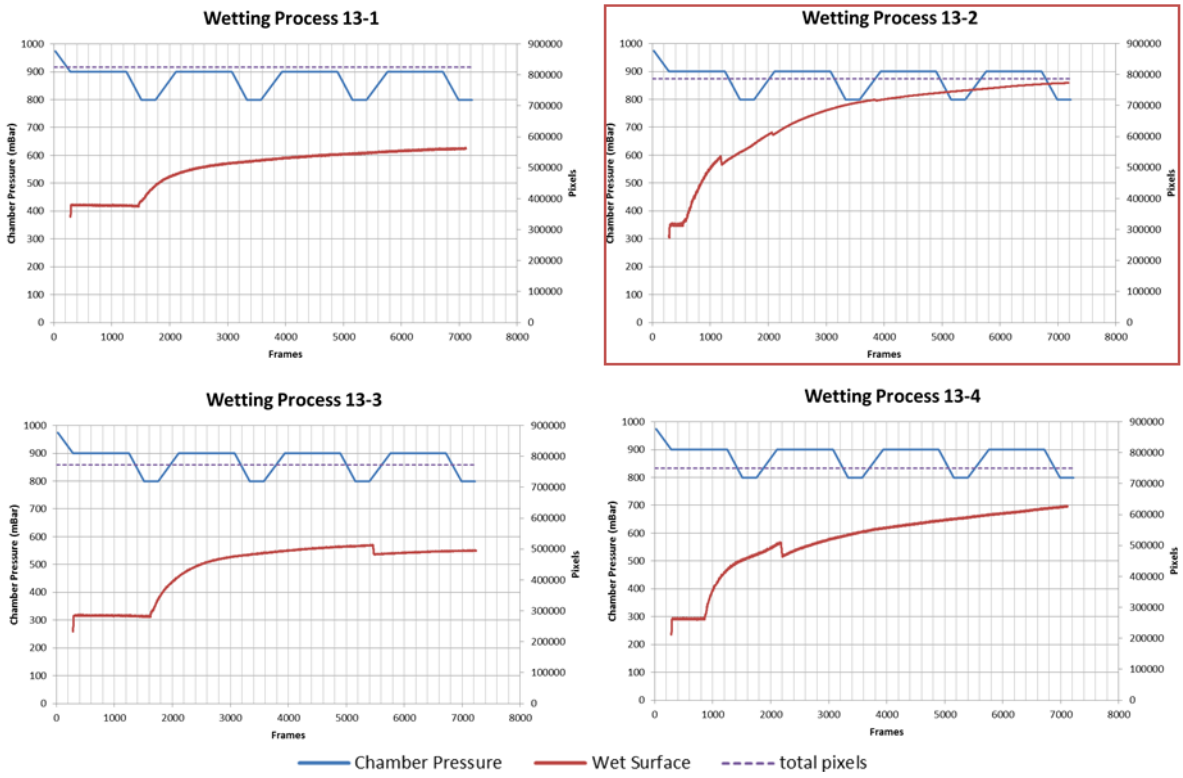

Figure 8-2: Plotted replicas for run 13

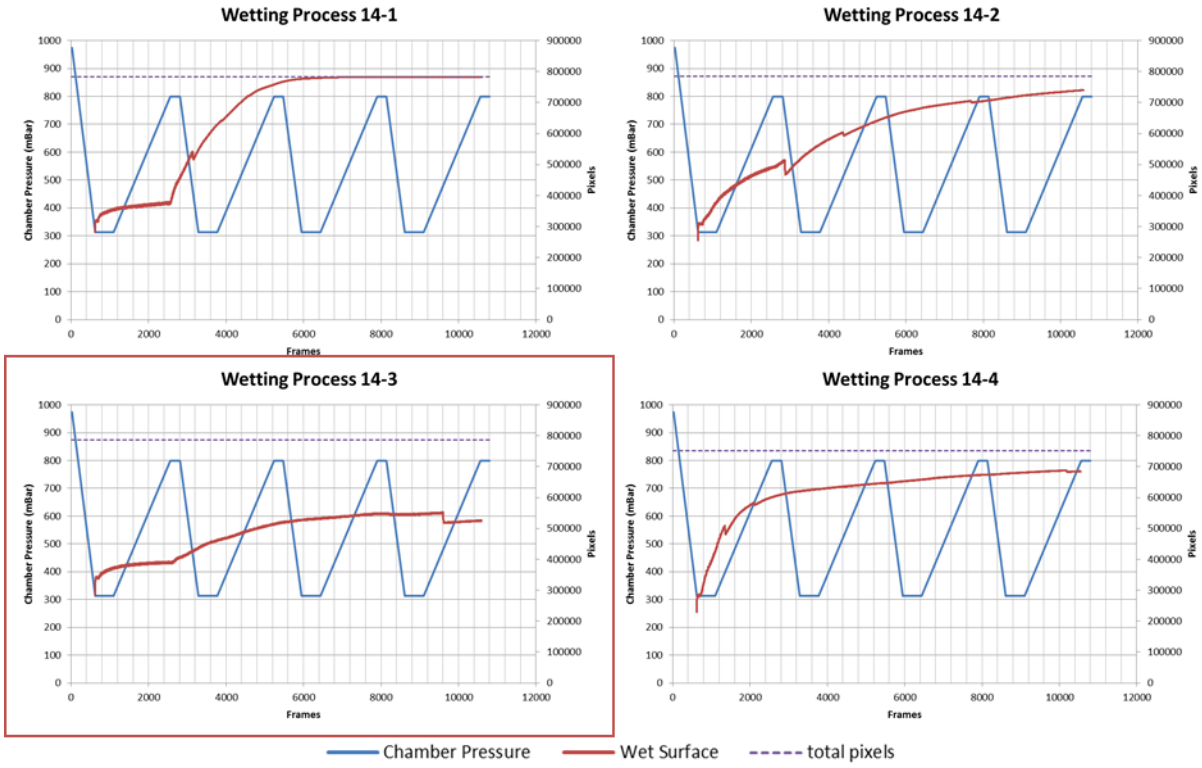

Figure 8-3: Plotted replicas for run 14

The better wetting cannot be demonstrated for lower pressures. However,

variations in pressure are thought to be helpful for the electrolyte propagation.

The “number of cycles” is found in second position in descendant order of contribution with a 15.4 %. This factor presents a second order term. Both coefficients, the lineal and quadratic, have a wide confidence margins to accept their hypothesis of significance. The t-values for the respective terms of “cycles” and “cylces^2” are 2.5 and 3.1. The significance is of 95 %. Hence, the frontier value of significance is two. This factor presents a concave curve with a maximum for two cycles. This finding is of relevant importance because the optimal performance of the wetting is restricted, leaving behind the uncertainty over the maximal potential outside the tested boundaries.

The two left factors are the “still time” and the “filling pressure”, which provide respectively 9.2 % and 6 % of contribution to the approach. The “filling pressure” has a decreasing direction, like the “wetting pressure”, giving a total effect of 4.9 unities and a maximal relative performance for 50 mBar. The “still time” has a positive tendency and an effect of 5.3 unities to the response from the 10 seconds to the 40 seconds. This factor does not follow the same tendency as the response effect (see Figure 8-4). The first one is the effect extracted from the statistical model and taking into consideration the significance of each coefficient. The response effects, already seen in page 98, are extracted directly from the response and calculated as shown in formulas (3.14) and (3.15). In the model has not been included the second order term because is not significant enough. The statistics indexes have considered more relevant to include other terms before the squared still time.

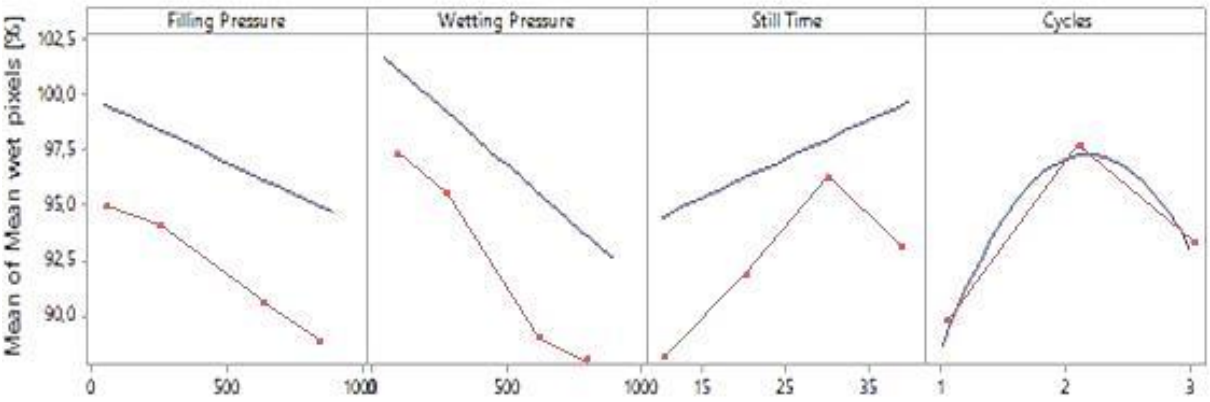

Figure 8-2: Effects comparison. Model and response effects plot. Blue contour represents the model effects and the red one the response effects

What refers to interactions, the two of them that seem to be meaningful in the model are the “filling pressure” with the “wetting pressure”, and the “wetting pressure” with the “cycles”. Both have a similar weight of 5 % in the overall response. There are two singular behaviors to highlight for these (see Figure 7-22):

- When the “wetting pressure” takes low values, the impact of the “filling pressure” on the response is smaller. Interestingly, when the “wetting pressure” is 50 mBar, the “wetting pressure” has no effect on the response.
- When the cycles are one or two, the “wetting pressure” has a more inclined slope. This fact changes the correlation between the “wetting pressure” and the response, which is dependent on how many cycles the profile has.

The correlations take into consideration the change of one factor’s effect, directly related to other factors levels. These are important and useful when a compromise must be chosen among factors levels, time of simulations, the efficiency of the wetting, and the costs of operations.

The following set of graphs in Figure 8-3 shows the predictions for the electrolyte’s spread. The previously commented patterns are displayed in these plots.

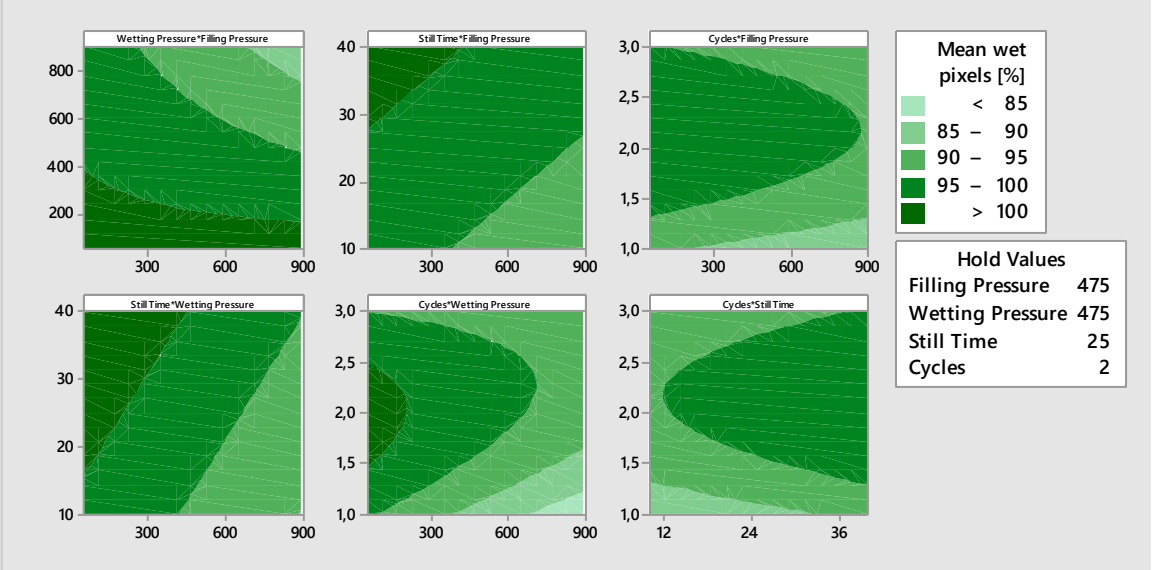

Figure 8-3: Response contour plots

8.4 Time Dependency

In section 7.1.1 was rejected a possible response, i.e., the time to reach a concrete wet portion, due to its huge correlation with time. The choice of that response would have misinterpreted the obtained conclusions, since the hidden factor was the “experiment length”. In Figure 8-4 the runs durations and their relatives times for the 95 % of wet surface are plotted. The expected trend is justified with the indicator of the t-value for a regression with the time. The coefficient of determination is 42 % and the t-value 7.9, justifying a doubtless high time-dependence. When this is compared to the same response including the time to reach the filling pressure, the correlation is steeper and the regressive percentage increases until 46 %.

When the same evaluation is executed with the selected response, the wet surface percentage, the results are not as evident as for the former. In this case, the tendency is flatter, with a correlation of 15 % and the t-value is 3.7. In spite of being still significant, it is not as decisive as for the wetting speed.

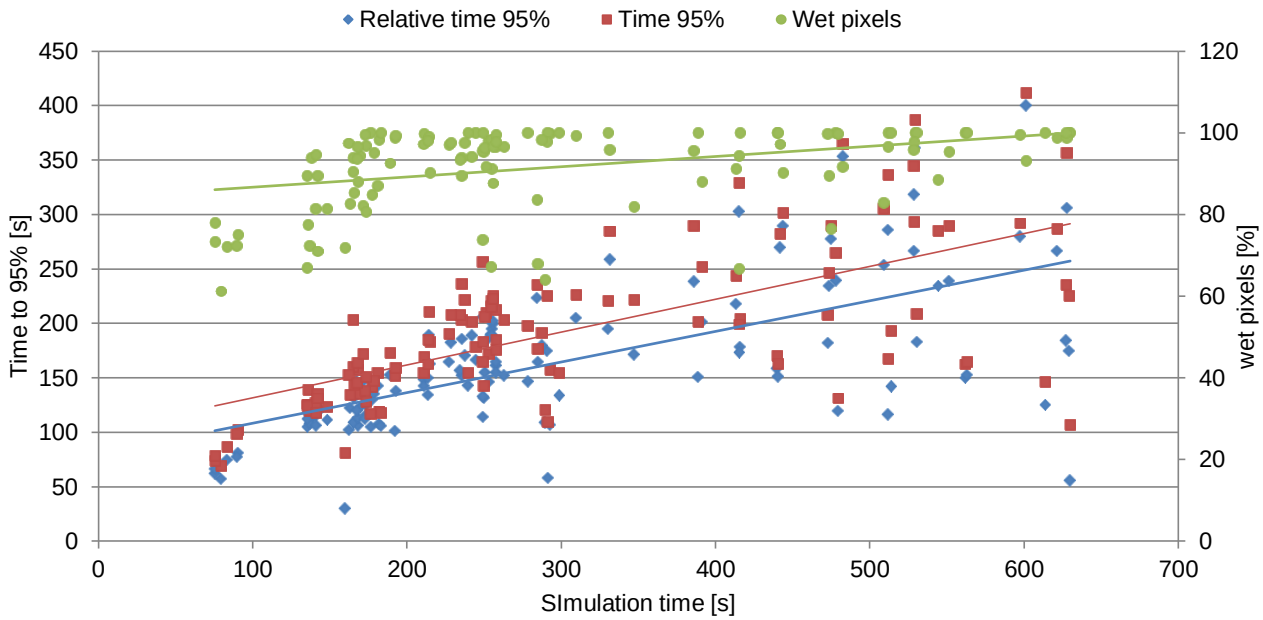

Figure 8-4: Scatterplot with simulation time and indicated responses with their linear regressions

8.5 Limitations

The major limitation for this work was the vacuum pump (see section 6.1 for model information). This pump was already used for the previous work, in which the pressure was maintained in 50 mBar. In the present work, the pressure is the main factor to be fluctuated. In order to get a proper assimilation to the process taking place in the manufacture, these changes should be done in similar conditions. As the pump could not extract more than 780 cm^3 of air per second, the necessary time to extract half the air of the vacuum chamber, with a total approximated volume of 45000 cm^3, is estimated in half a minute. This time is far from the time that the filling system in production line needs, being this no more than few tenths of seconds. With this drawback, the select response was not affected for the simulations time at all. With the employment of a turbo pumping station with pumping speed's ranges around 20 l/s, the time to bring the whole chamber to vacuum would be about three seconds. The transition in which the pressure was increased were also slow. The air was sucked through a valve attached to the pressure controller. These facts have been tough to be minimized.

A second limitation, and possible source of variations, has been the liquid's circuit. The unique certainty was the volume of electrolyte injected into the tube. Depending on the filling pressure, this volume was sometimes instantly soaked (for 50 mBar), at times advanced progressively to the case (for 313 mBar), and the other times, remained almost the whole quantity inside the tubes (for 607 and 900 mBar), not reaching the layers until the aperture of the three-way valve. The purpose of this action is to solve the liquid's introduction problem, ensuring an equal volume inside the case for all the tests.

After every test the valves opened to the atmospheric conditions, recovering the initial pressure inside the chamber and removing simultaneously the rests of electrolyte along the circuit. Those rests of electrolyte were noticeably more abundant in profiles with higher filling pressures. These differences on the reached electrolyte to the sheets, is thought to be a possible font of errors.

8.6 Range of Validity

The results obtained for this work are delimited for the range of selected values in the DoE and the described conditions of section 5.5. The response is not ensured to behave like seen in the results, when the conditions were outside the established ranges and the used materials were different, i.e., liquid and cell layers.

All tests have been systematically executed as explained in section 6.2. The procedure was selected after the simulation of some trials; in order to choose the most appropriate and accurate method. The runs have been randomized and replicated two and four times.

For the statistical validation, a significance level of 0.05 has been used, since it is the most convenient cutoff level to reject the null hypothesis (HEALEY 2010). The probability that a value could lay outside the confidence interval is 5 %.

9 Conclusions

The most relevant changes and findings for the obtained results are listed below:

- The former proposed method has been successfully upgraded. The main sources of errors seen in the previous work have been solved, and other new components have been added to the setup. The achieved targets are: the constant and clear illumination inside the vacuum chamber, a bigger case that uses the same cells dimensions as in the production line, and a precise liquid circuit, a used electrolyte-like liquid, and an accurate quantity of that liquid introduced.
- The principle of the method has been proved. This has accomplished the purposed goal of describing the advancing front of the electrolyte through the sheets of a battery's cell.
- An elaborated analysis for the entire process of wetting has been created. The functionality of all the obtained data has been the expected, saving useful information in form of videos, images, and graphs.
- The first chosen response was discarded after being highly influenced by the time. The conclusions taken from this would have been wrong.
- The studied response describes the wetting quality. This measures the percentage of wet surface at the end of the simulations.
- The statistical model explains 66 % of the response. The most influential factor is the "wetting pressure", contributing to the regressive model more than one third.
- Both the "filling pressure" and the "wetting pressure" are linear decreasing effects. As the pressures take lower values, the liquid spreads wider though the surface. Although most efficient pressures were the lower ones, i.e., 50 mBar, there are still pressures to be reached, which could improve the wet surface.
- The factor of "still time" has a linear increasing tendency that has a relative maximal point at the time of 40 seconds. The parabolic contour found in the response effect is a relevant finding. However, the second order term is not included in the model because it is not significant enough in the selected statistical pattern.

- The “number of cycles” follows a quadratic norm, where the optimal wetting point is situated at two cycles.
- The maximums detected on the “cycles” and on the response effects of the “still time”, might be caused by the evaporation of the liquid when the wetting process lasts too long.
- When the “wetting pressure” takes a value of 50 mBar, the “filling pressure” has no more effect on the answer, suffering no alteration when “filling pressure” changes.

10 Summary and Outlook

In the manufacture of batteries, like in any operation, the efficiency of the complete chain is an unquestioned ambition. The filling and wetting of the cells is an important phase, in which the electrolyte has to be rapidly soaked and completely wet the cell layers. In other words, the objective of this phase is to imbibe the whole pore's volume. Otherwise, the cell will be defective. Hence, the process must ensure a complete wet.

Being started out with a method from which could hardly extract any significant proposition about that wetting phenomena in LIBs, this work has dealt with its main deficits. With an upgraded setup, a completely new DoE, and a redesigned video analysis, the present work has overcome the weaknesses of the previous one. The chosen factors define a pressure profile, which is employed during the stage in the manufacturing process. The factors are the filling and wetting pressures, the time the deep pressures are maintained, and the number of pressure cycles. The response to be adjusted was the portion of wet surface at the end of every test. The most significant patterns have been identified with a statistical model.

The selected statistical approach explains the 66 % of the wetting pattern, in which the four main factors are significant. The found trends that maximize the response are with filling and wetting pressure at 50 mBar, 40 seconds of hold time, and two wetting cycles. The interactions have also shown that the filling pressure has no influence on the response when the wetting pressure is around 50 mBar.

These conditions need to be evaluated in the process of the production line. In a possible succeeding development of this method, a more powerful vacuum pump is aimed to be used to avoid long transition times. The use of a sensor is also recommended to know the exactly amount of electrolyte introduced into the case. The study of the behavior with more than two layers would be a worthy step forward for the later extrapolation of results.

This thesis provides useful foundations to develop new ideas and to do further research into this investigation field. The method has been demonstrated to be consistent and feasible, achieving its purpose of characterizing the wetting phenomena in the battery cells

Bibliography

ABDALLAH ET AL. 2007
Abdallah, W.; Buckley, J. S.; Carnegie, A.; Edwards, J.; Fordham, E.;Graue, Arne; Hussain, Hassan; Montaron, Bernard; Ziauddin, Murtaza: Fundamentals of Wettability. Schlumberger (2007).

AGUIAR ET AL. 1995
Aguiar, P. F. de; Bourguignon, B.; Khots, M. S.; Massart, D. L.; Phan-Than-Luu, R.: D-optimal designs. Chemometrics and Intelligent Laboratory Systems 30 (1995) 2, S. 199-210.

AL-SHAREEF ET AL. 2013
Al-Shareef, A.; Neogi, P.; Bai, B.: Force based dynamic contact angles and wetting kinetics on a Wilhelmy plate. Chemical Engineering Science 99 (2013), S. 113-117.

ANDERSON 1986
Anderson, W. G.: Wettability literature survey. Society of Petroleum Engineers 38 (1986) 10, S. 1125-1144.

ARMAND & TARASCON 2008
Armand, M.; Tarascon, J.-M.: Building better batteries. Nature 451 (2008) 7179, S. 652-657.

BARRY ET AL. 2015
Barry, C.; Runkel, P.; Smith, J.; Rudy, K.; Frost, J.;Fox, Greg; Heckman, Eric; Keller, Dawn; Martz, Estom; Meldrum, Karen; Scibilia, Bruno; Santiago, Eduardo; Steele, Cody: Minitab Blog. <http://www.minitab.com/en-us/support/> - 03/2015.

BERGENGRUEN 2014
Bergengruen, N.: Methode zur Messung des Benetzungsverhaltens von Zelllagen in Lithium-Ionen-Batterien. TUM. München (2014).

BESENHARD 1999
Besenhard, J. O.: Handbook of battery materials. Weinheim, Cambridge: Wiley-VCH 1999. ISBN: 3-527-29469-4.

BESENHARD & EICHINGER 1976
Besenhard, J. O.; Eichinger, G.: High energy density lithium cells. Journal of

Electroanalytical Chemistry and Interfacial Electrochemistry 68 (1976) 1, S. 1-18.

BIRKE & SCHIEMANN 2013
Birke, P.; Schiemann, M.: Akkumulatoren. Vergangenheit, Gegenwart und Zukunft elektrochemischer Energiespeicher. München: Utz 2013. ISBN: 978-3-831-60958-1.

BONN ET AL. 2009
Bonn, D.; Eggers, J.; Indekeu, J.; Meunier, J.; Rolley, E.: Wetting and spreading. Reviews of Modern Physics 81 (2009) 2, S. 739-805.

BRAIN 2006
Brain, M.: How Lithium-ion Batteries Work- HowStuffWorks. <http://electronics.howstuffworks.com/everyday-tech/lithium-ion-battery1.htm> - 02/12/2014.

COUSSEAU ET AL. 2006
Cousseau, J.-F.; Siret, C.; Biensan, P.; Broussely, M.: Recent developments in Li-ion prismatic cells. Journal of Power Sources 162 (2006) 2, S. 790-796.

DANIEL & WOOD 1999
Daniel, C.; Wood, F.: Fitting Equations to Data. Revised Edition. New York: John Wiley & Sons, Inc. 1999. ISBN: 978-0-471-37684-2.

DIN ISO 8787
DIN ISO 8787: Testing of paper and board; Determination of capillary rise; Klemm method. DIN-Taschenbuch 275: 1986.

DIN 55660-1
DIN 55660-1: Paints and varnishes - Wettability - Part 1: Terminology and general principles. Berlin: Beuth 2012.

DINGER ET AL. 2010
Dinger, A.; Martin, R.; Mosquet, X.; Rabl, M.; Rizoulis, D.;Russo, M.; Sticher, G.: Batteries for Electric Cars: Challenges, Opportunities, and the Outlook to 2020. The Boston Consulting Group. 2010. <http://www.bcg.de/documents/file36615.pdf> - 01/2015.

ERBIL 2014
Erbil, H. Y.: The debate on the dependence of apparent contact angles on

drop contact area or three-phase contact line: A review. Surface Science Reports 69 (2014) 4, S. 325-365.

ERIKSSON ET AL. 2000
Eriksson, L.; Johansson, E.; Kettaneh-Wold, N.; Wikström, C.; and Wold, S.: Design of experiments. Principles and applications
Learbways AB. Umea: Umetrics 2000. ISBN: 978-9-197-37300-5.

FIELD 2013
Field, A.: Discovering statistics using IBM SPSS statistics. 4th edition Aufl. Los Angeles, CA: Sage 2013. ISBN: 978-1-446-27457-6.

GOPRO
GoPro: HERO3+ Black. Technical Specifications. <http://shop.gopro.com/cameras/hero3plus-black/CHDHX-302-master.html> - 15/02/2015.

HEALEY 2010
Healey, J. F.: The essentials of statistics. A tool for social research. 2nd ed Aufl. Australia, Belmont, CA: Wadsworth/Cengage Learning 2010. ISBN: 0-495-60143-8.

HELLER 2013
Heller, B.: Aufbau eines Dichtigkeitsprüfstandes für Lithium-Ionen-Zellen. iwb TUM. Garching (21/07/2013) - 14/01/2015.

HOHENTHANNER & KLIEN 2012
SCHUTZRECHT US 20130312869 A1 Patent (24.11.2010) US 13/989,664.Hohenthanner, C.-R.; Klien, A.: Method and apparatus for filling an electrochemical cell.

IFA 1997
IFA: Institute for Occupational Safety and Health. (Hrsg.): 2-Propanol. <http://www.ifa-arbeitsmappedigital.de/7970> - 04/2015.

ISO 4046
ISO 4046: Paper, board, pulp and related terms - Vocabulary. Genève, Switzerland: International Organization for Standardization 1978.

IWB 2014A
iwb: ExZellTUM - Exzellenz-Zentrum für Batterie-Zellen an der Technischen Universität München. <http://www.iwb.tum.de/ExZellTUM.html> - 9/12/2014.

IWB 2014B
iwb: Produktionstechnik für Lithium-Ionen-Zellen. <http://www.iwb.tum.de/ProLIZ.html> - 9/12/2014.

IWB 2014C
iwb: Produktionstechnisches Demonstrationszentrum für Lithium-Ionen-Zellen - DeLIZ. <http://www.iwb.tum.de/DeLIZ.html> - 9/12/2014.

JOHN WILLIAM MEREDITH, PETER 1998
John William Meredith, Peter: Statistical design and analysis of experiments. Philadelphia, Pa.: Society for Industrial and Applied Mathematics 1998. ISBN: 978-0-898-71427-2. (Classics in applied mathematics 22).

JOSSEN & WEYDANZ 2006
Jossen, A.; Weydanz, W.: Moderne Akkumulatoren richtig einsetzen. 36 Tabellen. Neusäß, Untermeitingen: Ubooks; Reichardt 2006. ISBN: 3-939-35911-4.

KAHN RIBEIRO ET AL. 2007
Kahn Ribeiro, S.; Kobayashi, S.; Beuthe; J. Gasca; D. Greene;D. S. Lee; Y. Muromachi; P. J. Newton; S. Plotkin; D. Sperling; R. Wit; P. J. Zhou: Transport and its infrastructure. In Climate Change 2007: Mitigation. Contribution of Working Group III to the Fourth Assessment Report of the Intergovernmental Panel on Climate Change [B. Metz, O.R. Davidson, P.R. Bosch, R. Dave, L.A. Meyer (eds)]. Cambridge University Press, Cambridge, United Kingdom and New York, NY, USA. (2007).

KNOCHE 2012
Knoche, T.: Large-scale lithium-ion cells seen from the point of view of production technology. Electrical energy storage. Garching: 14.11.2012.

KNOCHE 2013
Knoche, T.: Elektrolytbefüllung grossformatiger lithium-ionen-zellen. Präsentation. Garching: 17.10.2013.

KORTHAUER 2013
Korthauer, R.: Handbuch Lithium-Ionen-Batterien. Berlin, Heidelberg: Imprint: Springer Vieweg 2013. ISBN: 978-3-642-30653-2. (SpringerLink : Bücher).

KURFER ET AL. 2012
Kurfer, J.; Westermeier, M.; Tammer, C.; Reinhart, G.: Production of large-

area lithium-ion cells – Preconditioning, cell stacking and quality assurance. CIRP Annals - Manufacturing Technology 61 (2012) 1, S. 1-4.

LIENKAMP 2014
Lienkamp, M.: Auslegung von Elektrofahrzeugen. Batterie Einleitung. Diss. Technische Universität München. Garching: 2014.

LINDEN & REDDY 2002
Linden, D.; Reddy, T. B.: Handbook of batteries. 3rd ed Aufl. New York: McGraw-Hill 2002. ISBN: 0-071-35978-8.

LIU 2012
Liu, R.-S.: Electrochemical technologies for energy storage and conversion. Weinheim: Wiley-VCH 2012. ISBN: 978-3-527-32869-7.

LOVE 2011
Love, C. T.: Thermomechanical analysis and durability of commercial micro-porous polymer Li-ion battery separators. Journal of Power Sources 196 (2011) 5, S. 2905-2912.

LUO ET AL. 2014
Luo, Z.; Gao, M.; Ye, Y.; Yang, S.: Wettability studies of reduced-charge montmorillonites modified by quaternary ammonium salts using capillary rise test. Powder Technology 266 (2014), S. 167-174.

MARQUES 2011
Marques, O.: Practical image and video processing using MATLAB. Hoboken, NJ: Wiley-IEEE Press 2011. ISBN: 978-0-470-04815-3.

MASON ET AL. 2003
Mason, R. L.; Gunst, R. F.; Hess, J. L.: Statistical design and analysis of experiments. With applications to engineering and science. 2nd ed Aufl. New York: J. Wiley 2003. ISBN: 0-471-37216-1.

MEAD 1988
Mead, R.: The design of experiments. Statistical principles for practical applications. Cambridge, New York: Cambridge University Press 1988. ISBN: 0-521-24512-5.

MIRET 2011
Miret, S.: Storage Wars: Batteries vs. Supercapacitors.

<http://berc.berkeley.edu/storage-wars-batteries-vs-supercapacitors/> - 02/12/2014.

MONTGOMERY 2013
Montgomery, D. C.: Design and analysis of experiments. Eighth edition Aufl. Hoboken, NJ: John Wiley & Sons, Inc. 2013. ISBN: 978-1-118-14692-7.

NAZRI & PISTOIA 2009
Nazri, G.; Pistoia, G.: Lithium batteries. Science and technology. New York: Springer 2009. ISBN: 978-0-387-92674-2.

OHZUKU & BRODD 2007
Ohzuku, T.; Brodd, R. J.: An overview of positive-electrode materials for advanced lithium-ion batteries. Journal of Power Sources 174 (2007) 2, S. 449-456.

ORIGINLAB CORP.
OriginLab Corp.: Graphic Residual Analysis. <http://www.originlab.de/doc/Origin-Help/Residual-Plot-Analysis> - 17/03/2015.

PEÑA SÁNCHEZ DE RIVERA, DANIEL 2013
Peña Sánchez de Rivera, Daniel: Fundamentos de Estadística. Madrid: Alianza Editorial op 2013. ISBN: 978-84-206-8380-5.

PRAT BARTRÉS 2004
Prat Bartrés, A.: Métodos Estadísticos. Control y mejora de la calidad. Barcelona: Edicions UPC 2004. ISBN: 8-48301-786-5.

REDDY 2010
Reddy, T. B.: Linden's handbook of batteries. Set 2. 4th ed Aufl. New York, London: McGraw-Hill Professional; McGraw-Hill 2010. ISBN: 978-0-071-62421-3.

REINHART ET AL. 2013
Reinhart, G.; Zeilinger, T.; Kurfer, J.; Westermeier, M.; Thiemann, C.;Glonegger, M.; Wunderer, M.; Tammer, C.; Schweier, M.; Heinz, M.: Research and Demonstration Center for the Production of Large-Area Lithium-Ion Cells. In: Schuh, G. et al. (Hrsg.): Future Trends in Production Engineering. Berlin, Heidelberg: Springer Berlin Heidelberg 2013, S. 3-12. ISBN: 978-3-642-24490-2.

RESCHKE 2011
SCHUTZRECHT US 8047241 B2 (26.03.2008) US 12/078,022.Reschke, B.: Method for filling electrolyte into battery cell and apparatus for carrying out the method.

RITCHIE & HOWARD 2006
Ritchie, A.; Howard, W.: Recent developments and likely advances in lithium-ion batteries. Journal of Power Sources 162 (2006) 2, S. 809-812.

RODRÍGUEZ GARCÍA-CEBADERA 2010
Rodríguez García-Cebadera, Á.: Estudio del ángulo de contacto y de la mojabilidad a alta temperatura de fases líquidas en la sinterización de metales.Universidad Carlos III. Madrid (2010) - 01/2015.

ROFFAEL ET AL. 2002
Roffael, E.; Dix, B.; Schneider, T.: Methode zur Erfassung der Benetzung von Holzfasern. Holz als Roh- und Werkstoff 60 (2002) 5, S. 347-348.

ROSANO ET AL. 1971
Rosano, H.; Gerbacia, W.; Feinstein, M.; Swaine, J.: Determination of the critical surface tension using an automatic wetting balance. Journal of Colloid and Interface Science 36 (1971) 3, S. 298-307.

SALGADO 2005
Salgado, B. M.: Efecto de la Mojabilidad en las Propiedades Petrofísicas y Operaciones de Recobro Secundario. Facultad de Ingenierias Fisicoquimicas Universidad Industrial de Santander. Santander, Spain (2005) - 12/2014.

SANTHANAGOPALAN & ZHANG 2012
Santhanagopalan, S.; Zhang, Z.: Rechargeable Batteries rechargeable battery, Separators for. In: Meyers, R. (Hrsg.): Encyclopedia of Sustainability Science and Technology: Springer New York 2012, S. 8715-8757. ISBN: 978-0-387-89469-0.

SAUER 2010
Sauer, U.: Produktionstechnik für die Batterieproduktion. Messe Düsseldorf. (Produktionstechnik auf dem Weg zur Elektromobilität - METAV 2010). <http://www.produktion.nrw.de/uploads/media/Vortrag_Herr_Prof_Sauer.pdf> - 12/2014.

SCHMITT ET AL. 2014
Schmitt, M.; Hempelmann, R.; Ingebrandt, S.; Munief, W.; Durneata, D.;Groβ, Katja; Heib, Florian: Statistical approach for contact angle determination on inclining surfaces: “slow-moving” analyses of non-axisymmetric drops on a flat silanized silicon wafer. International Journal of Adhesion and Adhesives 55 (2014), S. 123-131.

SCHUH ET AL. 2012
Schuh, G.; Neugebauer, R.; Uhlmann, E.: Future trends in production engineering. Proceedings of the WGP Conference, Berlin, Germany, 8th-9th June 2011. Berlin: Springer 2012, c2013. ISBN: 978-3-642-24490-2.

SIEMENS AG 2014
Siemens AG: Battery Manufacturing Process. <http://www.industry.siemens.com/topics/global/en/battery-manufacturing/process/Pages/default.aspx#> - 01/2015.

SMITH 1997
Smith, P. J.: Into statistics. A guide to understanding statistical concepts in engineering and the sciences. Berlin, New York: Springer 1997. ISBN: 978-9-813-08320-2.

STAVE & CHUAN-HUA 2014
Stave, J.; Chuan-Hua, C.: Lesson: Capillarity—Measuring Surface Tension. <https://www.teachengineering.org/view_lesson.php?url=collection/duk_/lessons/duk_surfacetensionunit_lessons/duk_surfacetensionunit_less2.xml> - 12/2014.

THE MATHWORKS A
The MathWorks: Global image threshold using Otsu's method. <http://de.mathworks.com/help/images/ref/graythresh.html> - 01/2015.

THE MATHWORKS B
The MathWorks: Image Processing Toolbox. <http://www.mathworks.com/products/image/index.html?s_tid=gn_loc_drop> - 08/01/2015.

THE MATHWORKS C
The MathWorks: MATLAB. <http://www.mathworks.com/products/matlab/> - 09/01/2015.

THÖNNESSEN & NEUMANN 2014
SCHUTZRECHT WO2014048918 A1 (25.09.2012)
PCT/EP2013/069842.Thönnessen, T.; Neumann, G.: Method for filling electrochemical cells.

TIRADO 2003
Tirado, J. L.: Inorganic materials for the negative electrode of lithium-ion batteries: state-of-the-art and future prospects. Materials Science and Engineering: R: Reports 40 (2003) 3, S. 103-136.

TRIEFENBACH 2008
Triefenbach, F.: Design of Experiments: The D-Optimal Approach and Its Implementation As a Computer Algorithm. Department of Computing science Umea University. Sweden (15.01.2008).

WAKIHARA 2001
Wakihara, M.: Recent developments in lithium ion batteries. Materials Science and Engineering: R: Reports 33 (2001) 4, S. 109-134.

WAKIHARA & YAMAMOTO 1998
Wakihara, M.; Yamamoto, O.: Lithium ion batteries. Fundamentals and performance. Tokyo, Weinheim, New York: Kodansha; Wiley-VCH 1998. ISBN: 3-527-29569-0.

WOLLERSHEIM & PFLEGING 2012
Wollersheim, O.; Pfleging, W.: Battery Research: Bionics Reduces Filling Time. ATZelektronik worldwide Edition (2012), S. 39-41.

WOOD ET AL. 2015
Wood, D. L.; Li, J.; Daniel, C.: Prospects for reducing the processing cost of lithium ion batteries. Journal of Power Sources 275 (2015), S. 234-242.

WOODBANK 2014
Woodbank: Battery and Energy Technologies. Lithium Battery Manufacturing. <http://www.mpoweruk.com/battery_manufacturing.htm> - 01/2015.

WU & HAMADA 2000
Wu, C.-F.; Hamada, M.: Experiments. Planning, analysis, and parameter design optimization. New York: Wiley 2000. ISBN: 978-0-471-25511-6. (Wiley series in probability and statistics).

YOSHIO ET AL. 2009
Yoshio, M.; Brodd, R. J.; Kozawa, A.: Lithium-ion batteries. Science and technologies. New York, NY: Springer 2009. ISBN: 0-387-34445-4.

YUAN & LEE 2013
Yuan, Y.; Lee, T. R.: Contact Angle and Wetting Properties. In: Bracco, G. et al. (Hrsg.): Surface Science Techniques. Berlin, Heidelberg: Springer Berlin Heidelberg 2013, S. 3-34. ISBN: 978-3-642-34242-4.

Appendices

Appendix A

Student's t-Distribution

***t* Table**

cum. prob	$t_{.50}$	$t_{.75}$	$t_{.80}$	$t_{.85}$	$t_{.90}$	$t_{.95}$	$t_{.975}$	$t_{.99}$	$t_{.995}$	$t_{.999}$	$t_{.9995}$
one-tail	0.50	0.25	0.20	0.15	0.10	0.05	0.025	0.01	0.005	0.001	0.0005
two-tails	1.00	0.50	0.40	0.30	0.20	0.10	0.05	0.02	0.01	0.002	0.001
df											
1	0.000	1.000	1.376	1.963	3.078	6.314	12.71	31.82	63.66	318.31	636.62
2	0.000	0.816	1.061	1.386	1.886	2.920	4.303	6.965	9.925	22.327	31.599
3	0.000	0.765	0.978	1.250	1.638	2.353	3.182	4.541	5.841	10.215	12.924
4	0.000	0.741	0.941	1.190	1.533	2.132	2.776	3.747	4.604	7.173	8.610
5	0.000	0.727	0.920	1.156	1.476	2.015	2.571	3.365	4.032	5.893	6.869
6	0.000	0.718	0.906	1.134	1.440	1.943	2.447	3.143	3.707	5.208	5.959
7	0.000	0.711	0.896	1.119	1.415	1.895	2.365	2.998	3.499	4.785	5.408
8	0.000	0.706	0.889	1.108	1.397	1.860	2.306	2.896	3.355	4.501	5.041
9	0.000	0.703	0.883	1.100	1.383	1.833	2.262	2.821	3.250	4.297	4.781
10	0.000	0.700	0.879	1.093	1.372	1.812	2.228	2.764	3.169	4.144	4.587
11	0.000	0.697	0.876	1.088	1.363	1.796	2.201	2.718	3.106	4.025	4.437
12	0.000	0.695	0.873	1.083	1.356	1.782	2.179	2.681	3.055	3.930	4.318
13	0.000	0.694	0.870	1.079	1.350	1.771	2.160	2.650	3.012	3.852	4.221
14	0.000	0.692	0.868	1.076	1.345	1.761	2.145	2.624	2.977	3.787	4.140
15	0.000	0.691	0.866	1.074	1.341	1.753	2.131	2.602	2.947	3.733	4.073
16	0.000	0.690	0.865	1.071	1.337	1.746	2.120	2.583	2.921	3.686	4.015
17	0.000	0.689	0.863	1.069	1.333	1.740	2.110	2.567	2.898	3.646	3.965
18	0.000	0.688	0.862	1.067	1.330	1.734	2.101	2.552	2.878	3.610	3.922
19	0.000	0.688	0.861	1.066	1.328	1.729	2.093	2.539	2.861	3.579	3.883
20	0.000	0.687	0.860	1.064	1.325	1.725	2.086	2.528	2.845	3.552	3.850
21	0.000	0.686	0.859	1.063	1.323	1.721	2.080	2.518	2.831	3.527	3.819
22	0.000	0.686	0.858	1.061	1.321	1.717	2.074	2.508	2.819	3.505	3.792
23	0.000	0.685	0.858	1.060	1.319	1.714	2.069	2.500	2.807	3.485	3.768
24	0.000	0.685	0.857	1.059	1.318	1.711	2.064	2.492	2.797	3.467	3.745
25	0.000	0.684	0.856	1.058	1.316	1.708	2.060	2.485	2.787	3.450	3.725
26	0.000	0.684	0.856	1.058	1.315	1.706	2.056	2.479	2.779	3.435	3.707
27	0.000	0.684	0.855	1.057	1.314	1.703	2.052	2.473	2.771	3.421	3.690
28	0.000	0.683	0.855	1.056	1.313	1.701	2.048	2.467	2.763	3.408	3.674
29	0.000	0.683	0.854	1.055	1.311	1.699	2.045	2.462	2.756	3.396	3.659
30	0.000	0.683	0.854	1.055	1.310	1.697	2.042	2.457	2.750	3.385	3.646
40	0.000	0.681	0.851	1.050	1.303	1.684	2.021	2.423	2.704	3.307	3.551
60	0.000	0.679	0.848	1.045	1.296	1.671	2.000	2.390	2.660	3.232	3.460
80	0.000	0.678	0.846	1.043	1.292	1.664	1.990	2.374	2.639	3.195	3.416
100	0.000	0.677	0.845	1.042	1.290	1.660	1.984	2.364	2.626	3.174	3.390
1000	0.000	0.675	0.842	1.037	1.282	1.646	1.962	2.330	2.581	3.098	3.300
z	0.000	0.674	0.842	1.036	1.282	1.645	1.960	2.326	2.576	3.090	3.291
	0%	50%	60%	70%	80%	90%	95%	98%	99%	99.8%	99.9%
	Confidence Level										

Appendix B

MATLAB Script from the former work:

```
A1=imread('bild1.jpg');
B1=rgb2gray(A1);
hist1=imhist(B1);
C1=im2bw(B1,0.359375);
nblack1=(nnz(C1==0);
A2=imread('bild2.jpg');
B2=rgb2gray(A2);
hist3=imhist(B2);
C2=im2bw(B2,0.359375);
nblack2=(nnz(C2==0);
A3=imread('bild3.jpg');
B3=rgb2gray(A3);
hist3=imhist(B3);
C3=im2bw(B3,0.359375);
nblack3=(nnz(C3==0);
```

Where:

- Bild1= image taken at the open of the valve
- Bild2= image taken 7 seconds after the first
- Bild3= image taken 13 seconds after the first
- 0,359375 is the threshold taken for this test

Appendix C

NEW CASE

The drawings for each component are presented below.

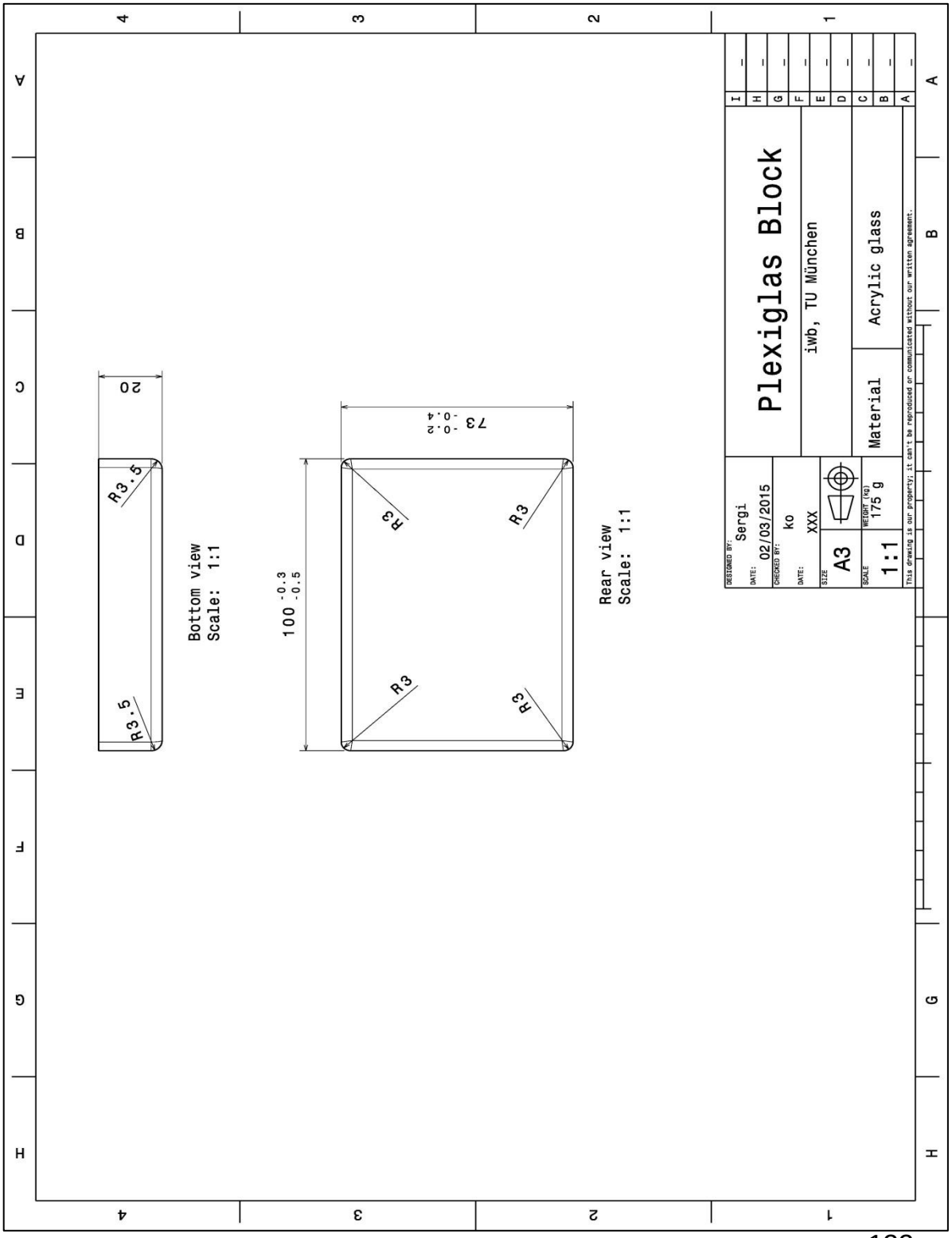

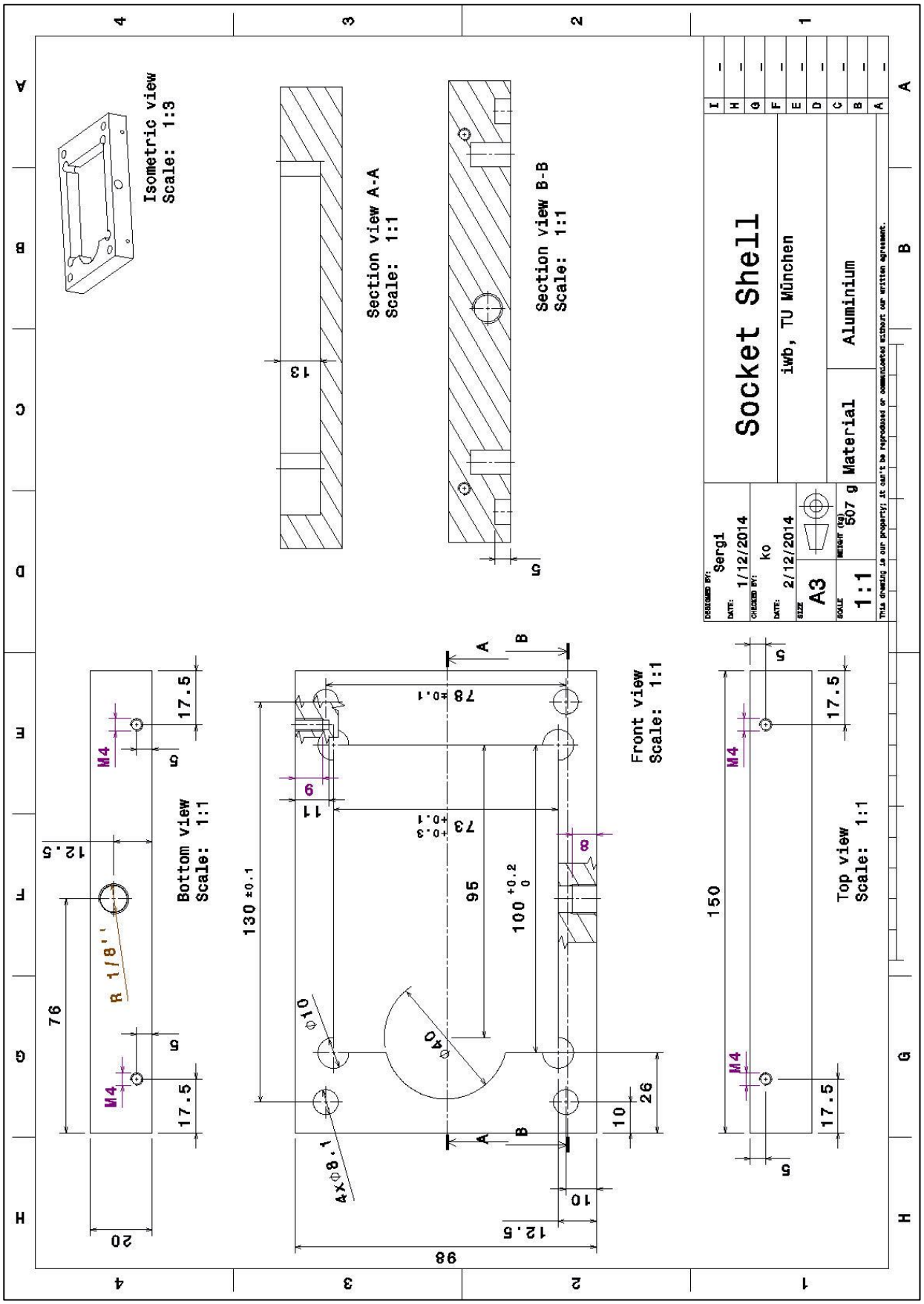
Isometric view
Scale: 1:3
Section view A-A
Scale: 1:1
Section view B-B
Scale: 1:1
Socket Shell
iwb, TU München
Material
Aluminium
Sergi
1/12/2014
ko
2/12/2014
A3
1:1
507 g
Bottom view
Scale: 1:1
Front view
Scale: 1:1
Top view
Scale: 1:1
M4
R 1/8''
4x⌀8.1
⌀10
⌀40
130 ±0.1
100 +0.2 0
78 ±0.1
73 +0.3 +0.1
95
150
98
76
20
12.5
17.5
26
10
11
9
8
5
13

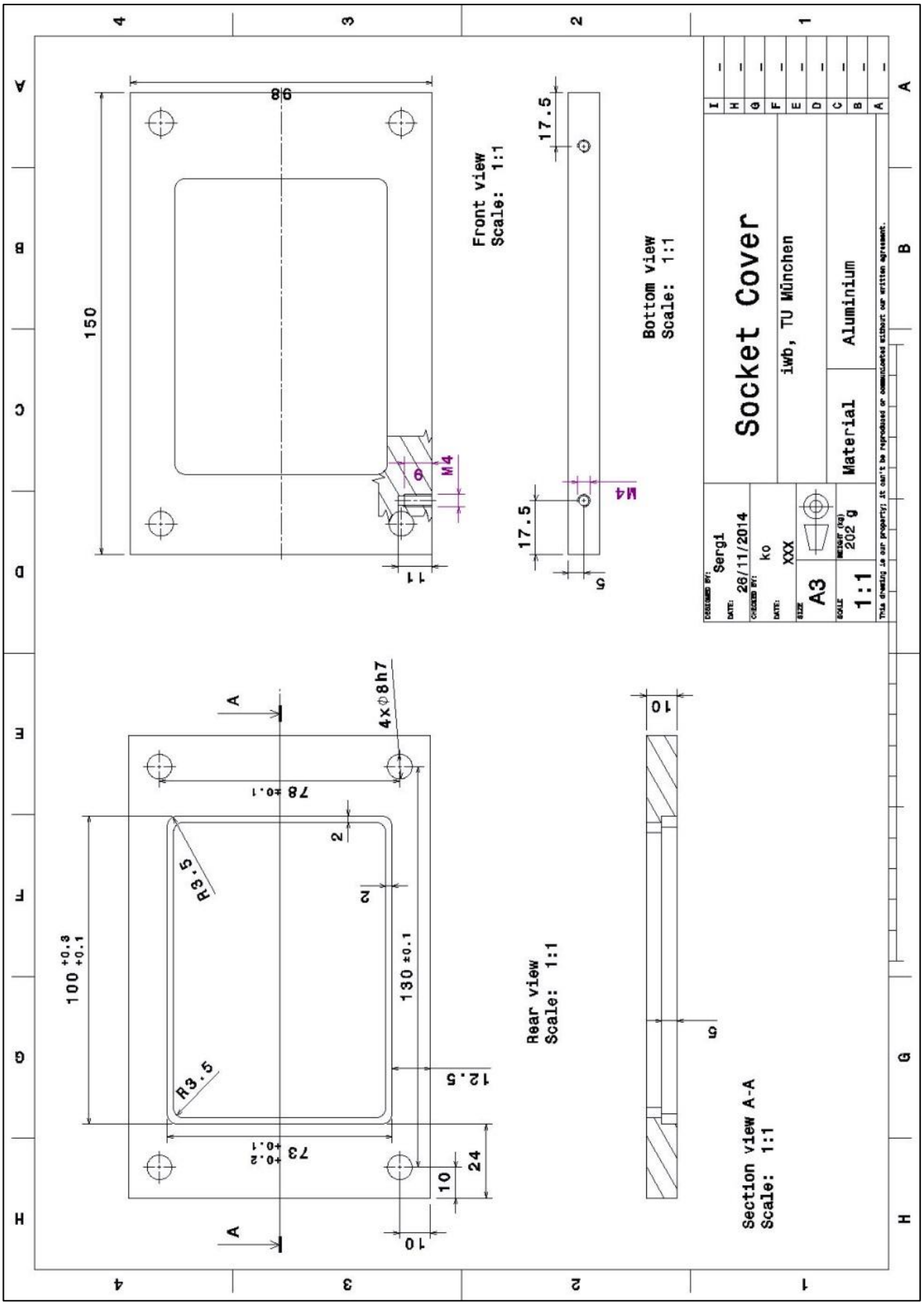
Socket Cover
iwb, TU München
Material
Aluminium
Sergi
26/11/2014
ko
XXX
A3
1:1
202 g
Front view
Scale: 1:1
Bottom view
Scale: 1:1
Rear view
Scale: 1:1
Section view A-A
Scale: 1:1
4xØ8h7
M4
150
98
17.5
78 ±0.1
100 +0.3 +0.1
130 ±0.1
73 +0.2 +0.1
R3.5
24
10
12.5
2

Data sheet Extension spring : RZ-055AI

GUTEKUNST FEDERN

d	mm	Wire diameter	L1	mm	Prestressed spring length	Weight	g	Weight of one spring
D	mm	Mean coil diameter	L2	mm	Loaded spring length			
De	mm	Outer coil diameter	Ln	mm	Maximum spring length			
Dh	mm	Minimum diameter of bush	m	mm	Loop opening width			
F0	N	Initial tension	n	pc.	Number of aktive coils			
F1	N	Prestressed spring force	nt	pc.	Total number of coils			
F2	N	Loaded spring force	s1	mm	Prestressed spring deflection			
Fn	N	Maximum spring force	s2	mm	Loaded spring deflection			
Lh	mm	Loop height	sn	mm	Maximum spring deflection			
Lk	mm	Lenght of unstressed spring body	sh	mm	Excursion			
L0	mm	Unstressed spring length	R	N/mm	Spring rate			

03.2015

*Loops are stocked without openings (m = 0,00). However it is possible to have an opening cut into the loop at an extra cost, without causing any delay.

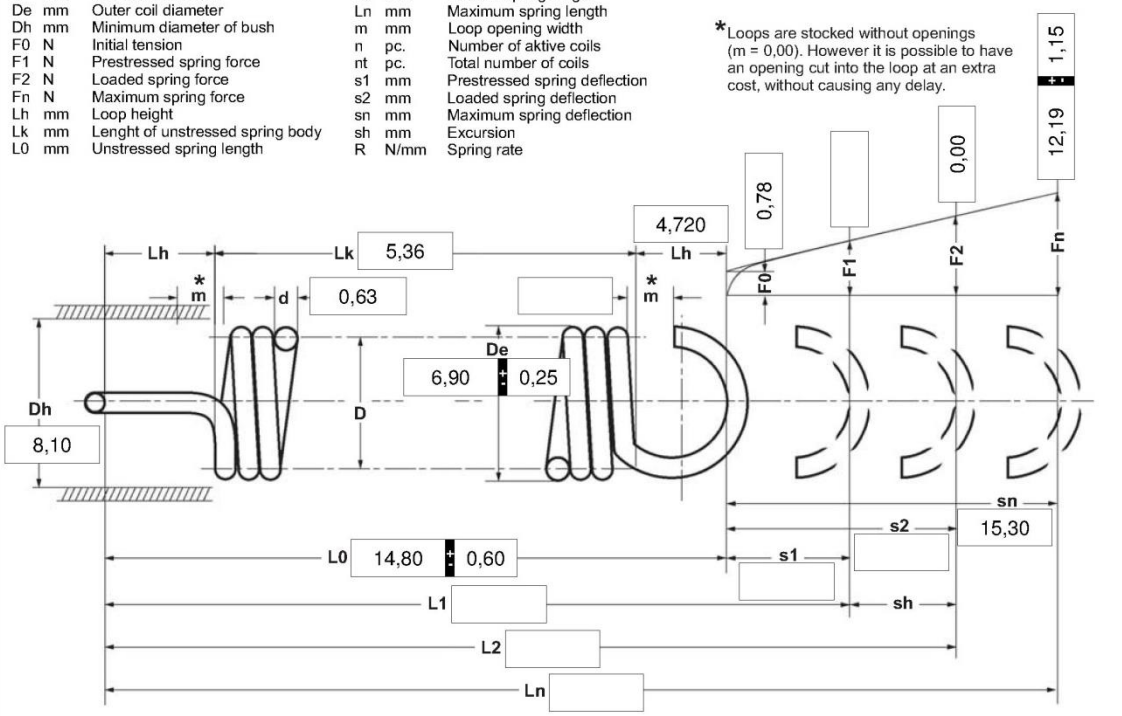

n | nt | R 0,745 | Weight 0,450

Spring test acc. to DIN ISO 2859/1 test level II

1 Coiling direction
☐ left ☒ right

2 Loop shape and loop position
Loop shape: 1/1 German loop
Loops offset to one another by 180,0 ± 19,0 degrees (in the dir. of the right helix)

3 Excursion sh mm

4 Stress cyc. end. N

5 Stress cycle frequ. n /

6 Application temp. °C

7 Material
EN 10270-3-1.4310

8 Wire or rod surface
☒ drawn ☐ rolled ☐ metal-cut

9 Surface treatment

10 Tolerances to DIN 2097

Grade	De,Di,D	L0	F0-Fn	Loops	Wire diameter d to DIN 2076
1	☐	☐	☐	☐	
2	☒	☒	☒	☒	
3	☐	☐	☐	☐	☒

11 Production compensation through

A spring resistance, associated length of tensed spring and L0	F0, D ☒
A spring resistance, associated length of tensed spring and F0	L0, n, d ☐ / L0, D ☐
Two spring resistances and associated length of tensed spring	L0, n, d ☐ / F0,D ☐

Remarks

Prices

Quantity scale	Single price [EUR]
1	2,8300 €
7	1,9200 €
17	0,9600 €
37	0,6200 €
75	0,4900 €
125	0,4518 €
175	0,4355 €
250	0,4246 €
350	0,3975 €
450	0,3888 €

Gutekunst + Co.KG Spring Factories · Carl-Zeiss-Straße 15 · D-72555 Metzingen
Sales +49 7123 960-192 · Customize springs +49 7123 960-193 · Main +49 7123 960-0
Fax +49 7123 960-195 · E-mail: order@gutekunst-co.com

Appendix D

Excel-VBA script: pressure profiles

```
Sub graph()
'delete the previous table'
  Sheets("graphs").Select
  Range("A17:D25").Select
  Selection.Contents

'find the filling pressure value and copy it's time in the tabe'
If Range("C1").Value = 50 Then
a = ActiveWorkbook.Worksheets("transition-times").Range("C2").Value
b = ActiveWorkbook.Worksheets("transition-times").Range("C6").Value
Sheets("graphs").Select
Range("B9").Value = a
Range("B11").Value = b
ElseIf Range("C1").Value = 313 Then
a = ActiveWorkbook.Worksheets("transition-times").Range("C3").Value
b = ActiveWorkbook.Worksheets("transition-times").Range("C7").Value
Sheets("graphs").Select
Range("B9").Value = a
Range("B11").Value = b
ElseIf Range("C1").Value = 607 Then
a = ActiveWorkbook.Worksheets("transition-times").Range("C4").Value
b = ActiveWorkbook.Worksheets("transition-times").Range("C8").Value
Sheets("graphs").Select
Range("B9").Value = a
Range("B11").Value = b
ElseIf Range("C1").Value = 900 Then
a = ActiveWorkbook.Worksheets("transition-times").Range("C5").Value
b = ActiveWorkbook.Worksheets("transition-times").Range("C9").Value
Sheets("graphs").Select
Range("B9").Value = a
Range("B11").Value = b
Else
MsgBox "not filligpressure"
End
End If
Range("D8,D9").Value = Range("C1").Value

'find the wetting pressure value and copy it's time in the tabe'
If Range("C2").Value = 50 Then
c = ActiveWorkbook.Worksheets("transition-times").Range("C10").Value
d = ActiveWorkbook.Worksheets("transition-times").Range("C6").Value
Sheets("graphs").Select
Range("B13").Value = c
Range("B15").Value = d
ElseIf Range("C2").Value = 313 Then
c = ActiveWorkbook.Worksheets("transition-times").Range("C11").Value
d = ActiveWorkbook.Worksheets("transition-times").Range("C7").Value
```

```
Sheets("graphs").Select
Range("B13").Value = c
Range("B15").Value = d
ElseIf Range("C2").Value = 607 Then
c = ActiveWorkbook.Worksheets("transition-times").Range("C12").Value
d = ActiveWorkbook.Worksheets("transition-times").Range("C8").Value
Sheets("graphs").Select
Range("B13").Value = c
Range("B15").Value = d
ElseIf Range("C2").Value = 900 Then
c = ActiveWorkbook.Worksheets("transition-times").Range("C13").Value
d = ActiveWorkbook.Worksheets("transition-times").Range("C9").Value
Sheets("graphs").Select
Range("B13").Value = c
Range("B15").Value = d
Else
MsgBox "not wettingpressure"
End
End If
Range("D12,D13").Value = Range("C2").Value

'copy the still time into the table'
Range("B10,B14").Value = Range("C3").Value

'find the number of cycles and repeat the table as many times as the
number'
If Range("C4").Value = 2 Then
Range("D12:D15").Select
    Selection.Copy
    Range("D16").Select
    ActiveSheet.Paste
    Range("A13:C16").Select
    Selection.Copy
    Range("A17").Select
    ActiveSheet.Paste
    Range("D20").Value = 800
    ActiveSheet.ChartObjects("Diagramm 1").Activate
    ActiveChart.SeriesCollection(1).Select
    ActiveChart.SeriesCollection(1).XValues = "=graphs!$C$8:$C$20"
    ActiveChart.SeriesCollection(1).Values = "=graphs!$D$7:$D$20"
ElseIf Range("C4").Value = 3 Then
Range("D12:D15").Select
    Selection.Copy
    Range("D16,D20").Select
    ActiveSheet.Paste
    Range("A13:C16").Select
    Selection.Copy
    Range("A17,A21").Select
    ActiveSheet.Paste
    Range("D24").Value = 800
    ActiveSheet.ChartObjects("Diagramm 1").Activate
    ActiveChart.SeriesCollection(1).Select
```

```
    ActiveChart.SeriesCollection(1).XValues = "=graphs!$C$8:$C$24"
    ActiveChart.SeriesCollection(1).Values = "=graphs!$D$7:$D$24"
ElseIf Range("C4").Value = 1 Then
ActiveSheet.ChartObjects("Diagramm 1").Activate
    ActiveChart.SeriesCollection(1).Select
    ActiveChart.SeriesCollection(1).XValues = "=graphs!$C$8:$C$16"
    ActiveChart.SeriesCollection(1).Values = "=graphs!$D$7:$D$216"
      Range("D16").Value = 800
Else
MsgBox "too many or not enough cycles"
End
End If
 Range("A1").Select
 Application.CutCopyMode = False
End Sub
```

Appendix E

MATLAB Script:

```
clc
clear
%variable to change
videofile='18-2.mp4'; %to name of the video, where the first number
is the run and the second the repetition
fileplot='G:\master thesis\graphs\' ; %folder to save the graphs
fileimages='G:\master thesis\images\'; %folder to save the images
excelfile= 'dataruns.xlsx' ; %name of excel's file to caopy all data

obj = VideoReader(num2str(videofile)); %Find the properties of the
video and save them
nFrames = obj.NumberOfFrames;
n2Frames=round(nFrames/2);
vidHeight = obj.Height;
vidWidth = obj.Width;
%Create the  structures to storage the movie frames
vidbw(1:nFrames)
=struct('cdata',zeros(vidHeight,vidWidth,1,'uint8'),'colormap',[]);
imtool(read(obj,n2Frames)); %show a frame to select the dimensions
to crop

%% the cropped dimensions are saved
x0=420;
y0=126;
xf=1451;
yf=864;
% two images are tranformed from RGB to gray scale to find the
suitable threshold
imtool(rgb2gray(imcrop(read(obj,n2Frames),[x0,y0,xf-x0,yf-y0])));
imtool(rgb2gray(imcrop(read(obj,nFrames),[x0,y0,xf-x0,yf-y0])));

%% the treshold is selected and three images are shown to reafirm
the choice
threshold=162;
imtool(im2bw(imcrop(read(obj,1),[x0,y0,xf-x0,yf-
y0]),threshold/255));
imtool(im2bw(imcrop(read(obj,n2Frames),[x0,y0,xf-x0,yf-
y0]),threshold/255));
imtool(im2bw(imcrop(read(obj,nFrames),[x0,y0,xf-x0,yf-
y0]),threshold/255));

%% the whole video is converted and cropped frame per frame
imtool close all
for k = 1 : nFrames
    vidbw(k).cdata=im2bw(imcrop(read(obj,k),[x0,y0,xf-x0,yf-
y0]),threshold/255);
end
```

```
%the number of black pixels is counted and stored in a table
for k=1:nFrames
    blacks(k)=nnz(vidbw(k).cdata==0);
end
%the plot is created and saved
filename=[num2str(fileplot) num2str(videofile) '.jpeg'];
plot(blacks);
ylabel('Wet pixels');
xlabel('Video frame');
title(['Threshold ' num2str(threshold)  ' for run '
num2str(videofile)])
hgexport(gcf, filename ,hgexport('factorystyle'), 'Format', 'jpeg');

close all

%show images and video and save images
imshow(rgb2gray(imcrop(read(obj,1),[x0,y0,xf-x0,yf-y0])));
filename=[num2str(fileimages) num2str(videofile) 'gray0.jpeg'];
hgexport(gcf, filename, hgexport('factorystyle'), 'Format', 'jpeg');

imshow(rgb2gray(imcrop(read(obj,n2Frames),[x0,y0,xf-x0,yf-y0])));
filename=[num2str(fileimages) num2str(videofile) 'gray1.jpeg'];
hgexport(gcf, filename, hgexport('factorystyle'), 'Format', 'jpeg');

imshow(rgb2gray(imcrop(read(obj,nFrames),[x0,y0,xf-x0,yf-y0])));
filename=[num2str(fileimages) num2str(videofile) 'gray2.jpeg'];
hgexport(gcf, filename, hgexport('factorystyle'), 'Format', 'jpeg');

imshow(vidbw(1).cdata);
filename=[num2str(fileimages) num2str(videofile) 'bw0.jpeg'];
hgexport(gcf, filename, hgexport('factorystyle'), 'Format', 'jpeg');

imshow(vidbw(n2Frames).cdata);
filename=[num2str(fileimages) num2str(videofile) 'bw1.jpeg'];
hgexport(gcf, filename, hgexport('factorystyle'), 'Format', 'jpeg');

imshow(vidbw(nFrames).cdata);
filename=[num2str(fileimages) num2str(videofile) 'bw2.jpeg'];
hgexport(gcf, filename, hgexport('factorystyle'), 'Format', 'jpeg');

implay(vidbw)

imtool close all;
close all;

%all necessary data is stored in the excel file
xlswrite(num2str(excelfile),transpose(blacks),num2str(videofile))
xlswrite(num2str(excelfile),{'threshold'},num2str(videofile),'C1')
xlswrite(num2str(excelfile),threshold,num2str(videofile),'D1')
xlswrite(num2str(excelfile),{'nFrames'},num2str(videofile),'C2')
xlswrite(num2str(excelfile),nFrames,num2str(videofile),'D2')
```

```
xlswrite(num2str(excelfile),{'total number of pixels in
image'},num2str(videofile),'C3')
[rows columns numberOfColorChannels] = size(vidbw(1).cdata);
numberOfPixels = rows*columns;
xlswrite(num2str(excelfile),numberOfPixels,num2str(videofile),'D3')
xlswrite(num2str(excelfile),{'black pixels
start'},num2str(videofile),'C4')
xlswrite(num2str(excelfile),blacks(1),num2str(videofile),'D4')
xlswrite(num2str(excelfile),{'black pixels
end'},num2str(videofile),'C5')
xlswrite(num2str(excelfile),blacks(nFrames),num2str(videofile),'D5')

fprintf('Done');
```

Appendix F

In Figure 0-1 and Figure 0-2 can be seen how the results are represented and the values elected for a possible response election. The table in columns A and B corresponds to the number of black pixels for every frame. In the table allocated in columns C and D, are noted the information from the MATLAB, explained in section 0, plus some other computations:

- Number of black pixels that corresponds to a introduced percentage of from the last recorded value
- Frame in which the previous quantity of pixels is reached, starting from the end. On the contrary, there might select a mistaken value conditioned to the response's noise
- This last frame value minus the needed frames to reach the filling pressure
- Portion of black pixels at the end in relation with the total number of the image's pixels

Below these values are the pressure values needed to plot.

In the graph can be seen four different data series:

- Vacuum chamber's pressure vs. time in frames
- Number of wet pixels vs. time in frames
- Correspondent percentage intersection
- Total number of image's pixels

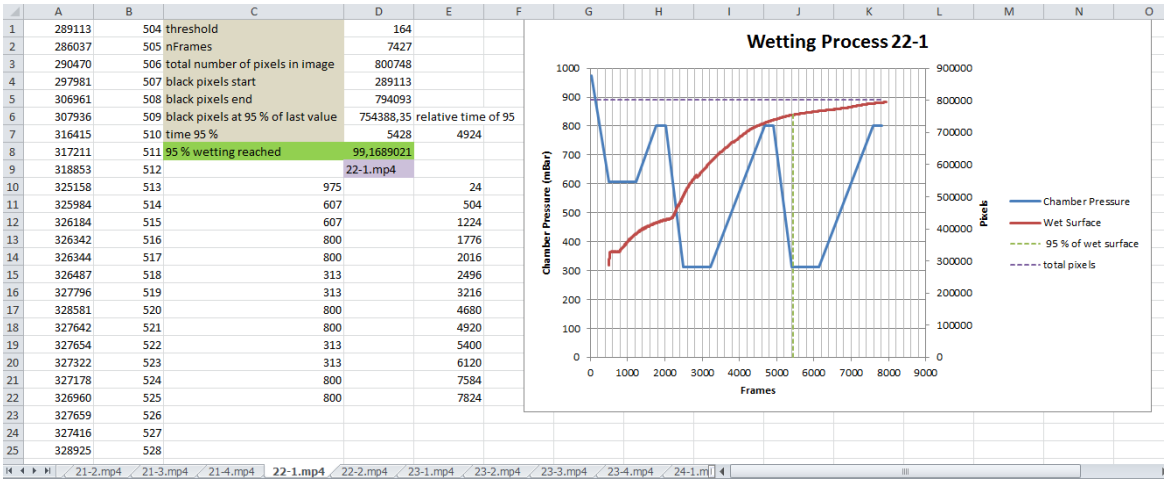

	A	B	C	D	E
1	289113	504	threshold	164	
2	286037	505	nFrames	7427	
3	290470	506	total number of pixels in image	800748	
4	297981	507	black pixels start	289113	
5	306961	508	black pixels end	794093	
6	307936	509	black pixels at 95 % of last value	754388,35	relative time of 95
7	316415	510	time 95 %	5428	4924
8	317211	511	95 % wetting reached	99,1689021	
9	318853	512		22-1.mp4	
10	325158	513	975		24
11	325984	514	607		504
12	326184	515	607		1224
13	326342	516	800		1776
14	326344	517	800		2016
15	326487	518	313		2496
16	327796	519	313		3216
17	328581	520	800		4680
18	327642	521	800		4920
19	327654	522	313		5400
20	327322	523	313		6120
21	327178	524	800		7584
22	326960	525	800		7824
23	327659	526			
24	327416	527			
25	328925	528			

21-2.mp4 | 21-3.mp4 | 21-4.mp4 | **22-1.mp4** | 22-2.mp4 | 23-1.mp4 | 23-2.mp4 | 23-3.mp4 | 23-4.mp4 | 24-1.m

Figure 0-1: Screenshot from the Excel file, page 22-1, which shows all runs information and the multi-plot.

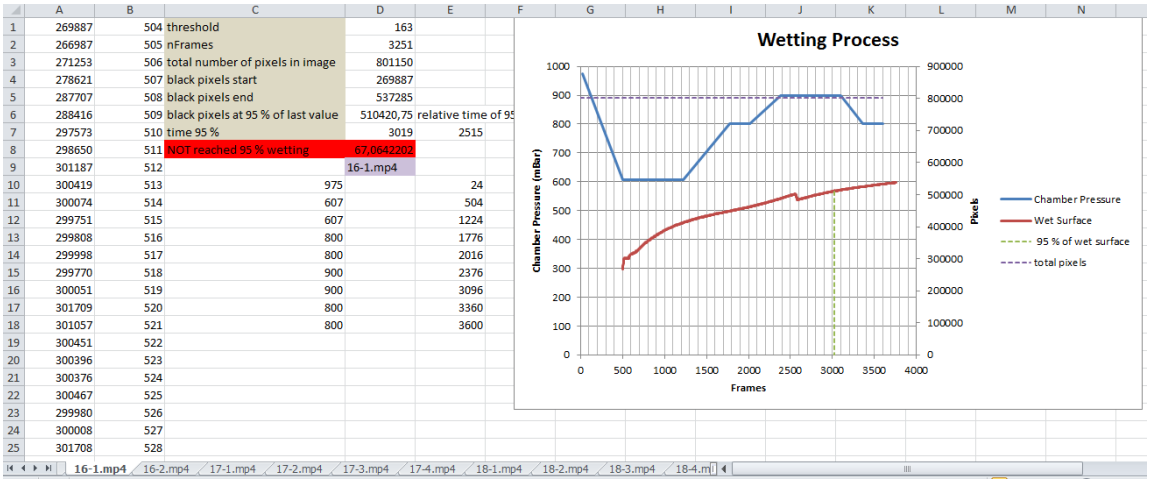

269887	504	threshold	163		
266987	505	nFrames	3251		
271253	506	total number of pixels in image	801150		
278621	507	black pixels start	269887		
287707	508	black pixels end	537285		
288416	509	black pixels at 95 % of last value	510420,75	relative time of 95	
297573	510	time 95 %	3019	2515	
298650	511	NOT reached 95 % wetting	67,0642202		
301187	512		16-1.mp4		
300419	513	975		24	
300074	514	607		504	
299751	515	607		1224	
299808	516	800		1776	
299998	517	800		2016	
299770	518	900		2376	
300051	519	900		3096	
301709	520	800		3360	
301057	521	800		3600	
300451	522				
300396	523				
300376	524				
300467	525				
299980	526				
300008	527				
301708	528				

16-1.mp4 | 16-2.mp4 | 17-1.mp4 | 17-2.mp4 | 17-3.mp4 | 17-4.mp4 | 18-1.mp4 | 18-2.mp4 | 18-3.mp4 | 18-4.m

Figure 0-2: Screenshot from the Excel file, page 16-1, which shows all runs information and the multi-plot.

The scripts associated to this Excel file used to create all representations and evaluate the different requested percentages, are copied below.

The subroutine named as "*all transformations*" draws the plots and calculates all necessary values to get them. The subroutine "*refresh*" change the percentage values for the ones introduced and refresh the plots.

ALL TRANSFORMATIONS

```
Sub alltransformations()
  Dim iPages As Variant
iPages = Application.InputBox(Prompt:="first number's test", Type:=1)
If iPages <> False Then
End If
  Dim nPages As Variant
nPages = Application.InputBox(Prompt:="Final number's test:", Type:=1)
   If nPages <> False Then
   End If
   Dim perctotal As Variant
   perctotal = Application.InputBox(Prompt:="% of total wetting
surface:", Type:=1)
   If perctotal <> False Then
   End If
   Dim perc As Variant
   perc = Application.InputBox(Prompt:=" % of wet form the last wet
value:", Type:=1)
   If perc <> False Then
    End If
   Application.ScreenUpdating = False
   For test = iPages To nPages
   Windows("DoE.xlsm").Activate
       Sheets("tests").Select
```

```
    If Range("H" & test + 1 & "").Value = vbNullString Then
    nReplica = 2
    Else
    nReplica = 4
    End If
    Windows("datarunsauto2.xlsm").Activate
    For replica = 1 To nReplica
    Dim pagina As String
    Let pagina = test & "-" & replica & ".mp4"
    Sheets(pagina).Select
    Dim endrangeA As String
    Dim endrangeB As String
    Dim lastrows As String
    Dim nom As String
    Dim ngraph As String
    lastrow = Range("D2").Value + 1
    Let endrangeA = "A1:A" & lastrow
    Let endrangeB = "B1:B" & lastrow
    Let lastrows = lastrow
    Let nom = Range("D9").Value
        Range("E11").Select
        Application.CutCopyMode = False
        Selection.Copy
        Range("B1").Select
        ActiveSheet.Paste
        Range("B2").Select
        Application.CutCopyMode = False
        ActiveCell.FormulaR1C1 = "=R[-1]C+1"
        Range("B2").Select
       Selection.AutoFill Destination:=Range("B2:B" & lastrows),
Type:=xlFillDefault
        Range("B2:B" & lastrows).Select
        Range("H4").Select
        ActiveSheet.Shapes.AddChart.Select
        ActiveChart.ChartType = xlXYScatterLinesNoMarkers
        ActiveChart.SeriesCollection.NewSeries
        ActiveChart.SeriesCollection(1).Name = "=""Chamber Pressure"""
        ActiveChart.SeriesCollection(1).XValues = "='" & nom &
"'!$E$10:$E$27"
        ActiveChart.SeriesCollection(1).Values = "='" & nom &
"'!$C$10:$C$27"
        ActiveChart.SeriesCollection.NewSeries
        ActiveChart.SeriesCollection(2).Name = "=""Wet Surface"""
        ActiveChart.SeriesCollection(2).XValues = "='" & nom &
"'!$B$1:$B$" & lastrow
        ActiveChart.SeriesCollection(2).Values = "='" & nom &
"'!$A$1:$A$" & lastrow
        ActiveChart.SeriesCollection(2).Select
        ActiveChart.SeriesCollection(2).AxisGroup = 2
    blaksend = Range("D5").Value
    wert = perc / 100 * blaksend
    Range("C7").Value = "time " & perc & " %"
```

```
    Range("C6").Value = "black pixels at " & perc & " % of last value"
    Range("D6").Value = wert
    i = Range("D2").Value
    Do While Range("A" & i).Value > wert
    i = i - 1
    Loop
    Range("D7").Value = i + Range("B1").Value
    Range("D7").Select
        Selection.Copy
         Range("D78:D79").Select
        ActiveSheet.Paste
            Range("D6").Select
             Selection.Copy
             Range("E78").Select
        ActiveSheet.Paste
        Range("E79").Value = 0
    Range("D3").Select
        Selection.Copy
         Range("G78:G79").Select
        ActiveSheet.Paste
        Range("F78").Value = 0
    Range("F79").Value=
Application.WorksheetFunction.Max(Range("E10:E27"))
    Range("D8").Value = Range("D5").Value * 100 / Range("D3").Value
    If Range("D5").Value >= Range("D3").Value * perctotal / 100 Then
    Range("C8").Value = perctotal & " % wetting reached"
    Range("C8:D8").Select
           With Selection.Interior
            .Pattern = xlSolid
            .PatternColorIndex = xlAutomatic
            .Color = 5296274
            .TintAndShade = 0
            .PatternTintAndShade = 0
        End With
    Else
    Range("C8").Value = "NOT reached " & perctotal & " % wetting "
     Range("C8:D8").Select
        With Selection.Interior
            .Pattern = xlSolid
            .PatternColorIndex = xlAutomatic
            .Color = 255
            .TintAndShade = 0
            .PatternTintAndShade = 0
        End With
    End If
         Range("C1:C7").Select
        With Selection.Interior
            .Pattern = xlSolid
            .PatternColorIndex = xlAutomatic
            .ThemeColor = xlThemeColorDark2
            .TintAndShade = -9.99786370433668E-02
            .PatternTintAndShade = 0
```

```
        End With
        Range("D9").Select
          With Selection.Interior
            .Pattern = xlSolid
            .PatternColorIndex = xlAutomatic
            .ThemeColor = xlThemeColorAccent4
            .TintAndShade = 0.599993896298105
            .PatternTintAndShade = 0
        End With
    ActiveSheet.ChartObjects("1 Gráfico").Activate
        ActiveChart.SeriesCollection.NewSeries
        ActiveChart.SeriesCollection(3).Name = "="" " & perc & " % of
wet surface"""
        ActiveChart.SeriesCollection(3).Values = "='" & nom &
"'!$E$78:$E$79"
      ActiveChart.SeriesCollection(3).XValues = "='" & nom &
"'!$D$78:$D$79"
       ActiveChart.SeriesCollection(3).AxisGroup = 2
       ActiveChart.SeriesCollection(3).Select
         With Selection.Format.Line
            .Visible = msoTrue
            .DashStyle = msoLineSysDash
        End With
            With Selection.Format.Line
            .Visible = msoTrue
            .Weight = 1.5
        End With
              ActiveChart.SeriesCollection(1).AxisGroup = 1
            ActiveChart.SeriesCollection(2).AxisGroup = 2
       ActiveChart.SeriesCollection.NewSeries
        ActiveChart.SeriesCollection(4).Name = "=""total pixels"""
        ActiveChart.SeriesCollection(4).XValues = "='" & nom &
"'!$F$78:$F$79"
      ActiveChart.SeriesCollection(4).Values = "='" & nom &
"'!$G$78:$G$79"
       ActiveChart.SeriesCollection(4).AxisGroup = 2
       ActiveChart.SeriesCollection(4).Select
         With Selection.Format.Line
            .Visible = msoTrue
            .DashStyle = msoLineSysDash
        End With
           With Selection.Format.Line
            .Visible = msoTrue
            .Weight = 1.5
        End With
          ActiveChart.SeriesCollection(1).AxisGroup = 1
            ActiveChart.SeriesCollection(2).AxisGroup = 2
        ActiveSheet.ChartObjects("1 Gráfico").Activate
        ActiveSheet.Shapes("1 Gráfico").ScaleWidth 1.49375, msoFalse, _
            msoScaleFromTopLeft
        ActiveSheet.Shapes("1 Gráfico").ScaleHeight 1.5520833333,
msoFalse, _
```

```
            msoScaleFromBottomRight
    ' titles '
        ActiveSheet.ChartObjects("1 Gráfico").Activate
        ActiveChart.SetElement
(msoElementPrimaryCategoryAxisTitleAdjacentToAxis)
        Selection.Format.TextFrame2.TextRange.Characters.Text = "Frames"
        With Selection.Format.TextFrame2.TextRange.Characters(1,
6).ParagraphFormat
            .TextDirection = msoTextDirectionLeftToRight
            .Alignment = msoAlignCenter
        End With
        With Selection.Format.TextFrame2.TextRange.Characters(1, 6).Font
            .BaselineOffset = 0
            .Bold = msoTrue
            .NameComplexScript = "+mn-cs"
            .NameFarEast = "+mn-ea"
            .Fill.Visible = msoTrue
            .Fill.ForeColor.RGB = RGB(0, 0, 0)
            .Fill.Transparency = 0
            .Fill.Solid
            .Size = 10
            .Italic = msoFalse
            .Kerning = 12
            .Name = "+mn-lt"
            .UnderlineStyle = msoNoUnderline
            .Strike = msoNoStrike
        End With
        Range("E5").Select
        ActiveSheet.ChartObjects("1 Gráfico").Activate
        ActiveChart.PlotArea.Select
        ActiveChart.ChartArea.Select
        ActiveChart.SetElement (msoElementPrimaryValueAxisTitleRotated)
        ActiveChart.Axes(xlValue, xlPrimary).AxisTitle.Text = "Chamber
Pressure (mBar)"
        Selection.Format.TextFrame2.TextRange.Characters.Text = _
            "Chamber Pressure (mBar)"
        With Selection.Format.TextFrame2.TextRange.Characters(1,
23).ParagraphFormat
            .TextDirection = msoTextDirectionLeftToRight
            .Alignment = msoAlignCenter
        End With
        With Selection.Format.TextFrame2.TextRange.Characters(1, 7).Font
            .BaselineOffset = 0
            .Bold = msoTrue
            .NameComplexScript = "+mn-cs"
            .NameFarEast = "+mn-ea"
            .Fill.Visible = msoTrue
            .Fill.ForeColor.RGB = RGB(0, 0, 0)
            .Fill.Transparency = 0
            .Fill.Solid
            .Size = 10
            .Italic = msoFalse
```

```
            .Kerning = 12
            .Name = "+mn-lt"
            .UnderlineStyle = msoNoUnderline
            .Strike = msoNoStrike
        End With
        With Selection.Format.TextFrame2.TextRange.Characters(8,
16).Font
            .BaselineOffset = 0
            .Bold = msoTrue
            .NameComplexScript = "+mn-cs"
            .NameFarEast = "+mn-ea"
            .Fill.Visible = msoTrue
            .Fill.ForeColor.RGB = RGB(0, 0, 0)
            .Fill.Transparency = 0
            .Fill.Solid
            .Size = 10
            .Italic = msoFalse
            .Kerning = 12
            .Name = "+mn-lt"
            .UnderlineStyle = msoNoUnderline
            .Strike = msoNoStrike
        End With
        ActiveChart.ChartArea.Select
        ActiveChart.SetElement
(msoElementSecondaryValueAxisTitleRotated)
        ActiveChart.Axes(xlValue, xlSecondary).AxisTitle.Text = "Pixels"
        Selection.Format.TextFrame2.TextRange.Characters.Text = "Pixels"
        With Selection.Format.TextFrame2.TextRange.Characters(1,
6).ParagraphFormat
            .TextDirection = msoTextDirectionLeftToRight
            .Alignment = msoAlignCenter
        End With
        With Selection.Format.TextFrame2.TextRange.Characters(1, 6).Font
            .BaselineOffset = 0
            .Bold = msoTrue
            .NameComplexScript = "+mn-cs"
            .NameFarEast = "+mn-ea"
            .Fill.Visible = msoTrue
            .Fill.ForeColor.RGB = RGB(0, 0, 0)
            .Fill.Transparency = 0
            .Fill.Solid
            .Size = 10
            .Italic = msoFalse
            .Kerning = 12
            .Name = "+mn-lt"
            .UnderlineStyle = msoNoUnderline
            .Strike = msoNoStrike
        End With
        ActiveSheet.ChartObjects("1 Gráfico").Activate
         ActiveChart.SetElement (msoElementChartTitleAboveChart)
        ActiveChart.ChartTitle.Text = "Wetting Process for " & test & "-
" & replica
```

```
        Selection.Format.TextFrame2.TextRange.Characters.Text = "Wetting
Process"
        With Selection.Format.TextFrame2.TextRange.Characters(1,
15).ParagraphFormat
            .TextDirection = msoTextDirectionLeftToRight
            .Alignment = msoAlignCenter
        End With
        With Selection.Format.TextFrame2.TextRange.Characters(1,5).Font
            .BaselineOffset = 0
            .Bold = msoTrue
            .NameComplexScript = "+mn-cs"
            .NameFarEast = "+mn-ea"
            .Fill.Visible = msoTrue
            .Fill.ForeColor.RGB = RGB(0, 0, 0)
            .Fill.Transparency = 0
            .Fill.Solid
            .Size = 18
            .Italic = msoFalse
            .Kerning = 12
            .Name = "+mn-lt"
            .UnderlineStyle = msoNoUnderline
            .Strike = msoNoStrike
        End With
    Columns("C:C").EntireColumn.AutoFit
    Range("J10").Select
    Next replica
    Next test
    MsgBox "done"
    End Sub
```

REFRESH

```
    Sub refresh()
     Dim iPages As Variant
    iPages = Application.InputBox(Prompt:="first number's test",
Type:=1)
    If iPages <> False Then
    End If
    Dim nPages As Variant
    nPages = Application.InputBox(Prompt:="Final number's test:",
Type:=1)
    If nPages <> False Then
    End If
    Dim perctotal As Variant
    perctotal = Application.InputBox(Prompt:="% of total wetting
surface:", Type:=1)
    If perctotal <> False Then
    End If
    Dim perc As Variant
    perc = Application.InputBox(Prompt:=" % of wet form the last wet
value:", Type:=1)
    If perc <> False Then
     End If
```

```
Application.ScreenUpdating = False
For test = iPages To nPages
Windows("DoE.xlsm").Activate
Sheets("tests").Select
If Range("H" & test + 1 & "").Value = vbNullString Then
nReplica = 2
Else
nReplica = 4
End If
Windows("datarunsauto2.xlsm").Activate
For replica = 1 To nReplica
Dim pagina As String
Let pagina = test & "-" & replica & ".mp4"
Sheets(pagina).Select
blaksend = Range("D5").Value
wert = perc / 100 * blaksend
Range("C7").Value = "time " & perc & " %"
Range("C6").Value = "black pixels at " & perc & " % of last value"
Range("D6").Value = wert
i = Range("D2").Value
Do While Range("A" & i).Value > wert
i = i - 1
Loop
Range("D7").Value = i + Range("B1").Value
Range("E7").Value = i
Range("E6").Value = "relative time of " & perc & ""
Range("D7").Select
    Selection.Copy
     Range("D78:D79").Select
    ActiveSheet.Paste
        Range("D6").Select
         Selection.Copy
         Range("E78").Select
    ActiveSheet.Paste
If Range("D5").Value >= Range("D3").Value * perctotal / 100 Then
Range("C8").Value = perctotal & " % wetting reached"
Range("C8:D8").Select
       With Selection.Interior
        .Pattern = xlSolid
        .PatternColorIndex = xlAutomatic
        .Color = 5296274
        .TintAndShade = 0
        .PatternTintAndShade = 0
    End With
Else
Range("C8").Value = "NOT reached " & perctotal & " % wetting "
 Range("C8:D8").Select
    With Selection.Interior
        .Pattern = xlSolid
        .PatternColorIndex = xlAutomatic
        .Color = 255
        .TintAndShade = 0
```

```
        .PatternTintAndShade = 0
    End With
End If
 Columns("C:C").EntireColumn.AutoFit
Next replica
Next test
MsgBox "Refresh Done"
End Sub
```

Appendix G

Table of the times to reach 95 % of the final value of pixels

Table 20: Times to reach 95 % of the final value of pixels

Run	Replicas	Mean time to 95 % [s]	StDev time to 95 % [s]	Run	Replicas	Mean time to 95 % [s]	StDev time to 95 % [s]
1	2	119.1	53.92	**22**	2	190.3	50.71
2	4	250.5	82.79	**23**	4	77.1	7.34
3	2	176.3	9.87	**24**	2	236.6	40.51
4	2	287.5	3.33	**25**	4	258.1	97.68
5	2	177.6	28.23	**26**	2	216.6	99.79
6	2	130.6	16.00	**27**	4	202.8	39.79
7	4	169.4	25.59	**28**	2	168.4	23.31
8	4	241.4	38.15	**29**	4	231.2	102.17
9	2	167.5	82.32	**30**	4	308.3	76.82
10	4	135.4	6.49	**31**	2	252.7	45.28
11	4	134.1	19.44	**32**	2	199.3	12.61
12	4	169.9	22.57	**33**	2	220.2	7.07
13	4	181.1	47.41	**34**	2	216.8	9.02
14	4	244.0	59.98	**35**	2	166.2	10.37
15	2	207.9	6.66	**36**	2	100.3	2.80
16	2	132.4	9.34	**37**	2	180.7	6.51
17	4	151.9	14.80	**38**	2	352.0	85.18
18	4	124.1	3.25	**39**	2	120.8	3.56
19	4	217.3	15.10	**40**	4	229.2	72.72
20	2	163.4	1.62	**41**	2	133.2	3.18
21	4	204.7	22.11	**42**	2	158.5	5.27

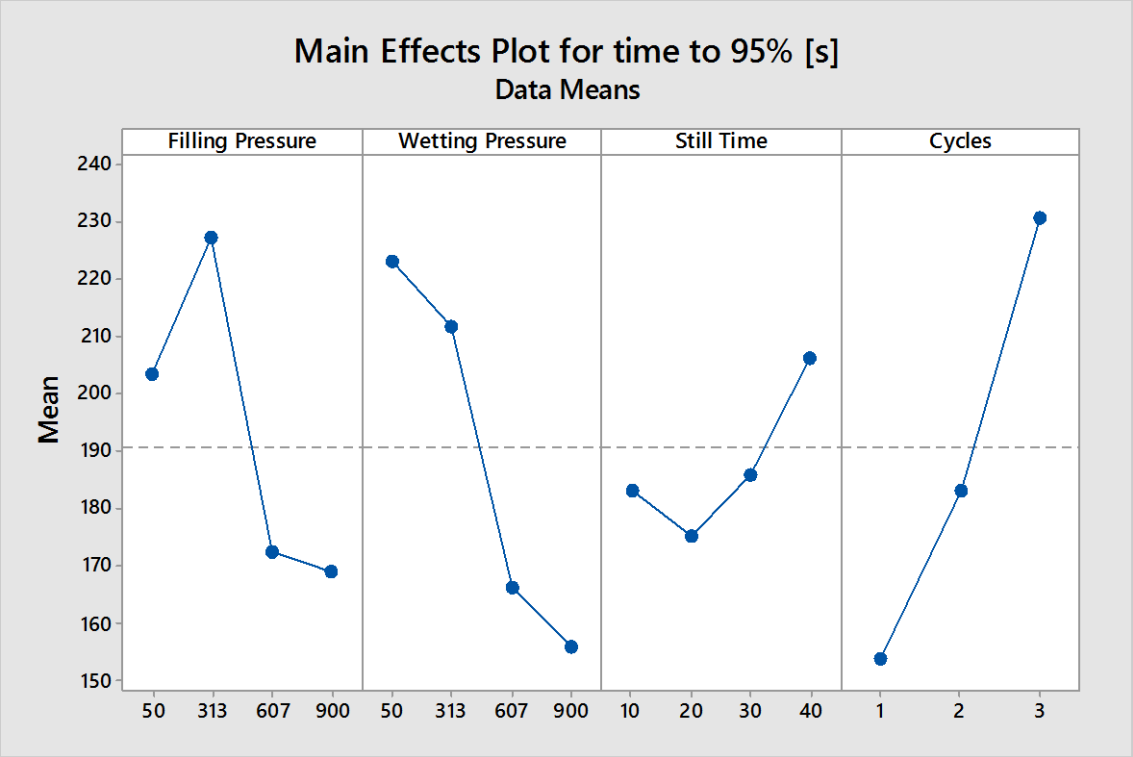

Figure 0-3: Main effects plot for time 95 %

Appendix H

Table 21: Wet pixels for al tests

Test	Wet pixels [%]	Test	Wet pixels [%]	Test	Wet pixels [%]	Test	Wet pixels [%]
1-1	71.74	11-3	87.02	20-1	100.00	30-1	99.95
1-2	88.02	11-4	95.16	20-2	100.00	30-2	99.99
2-1	100.00	12-1	93.93	21-1	67.26	30-3	97.90
2-2	82.84	12-2	90.44	21-2	91.03	30-4	95.91
2-3	96.67	12-3	97.45	21-3	98.13	31-1	99.91
2-4	99.98	12-4	96.65	21-4	91.77	31-2	95.88
3-1	90.36	13-1	67.98	22-1	99.17	32-1	97.07
3-2	99.88	13-2	98.34	22-2	100.00	32-2	97.55
4-1	95.45	13-3	64.11	23-1	72.09	33-1	87.65
4-2	88.43	13-4	83.55	23-2	61.23	33-2	98.23
5-1	99.99	14-1	100.00	23-3	78.00	34-1	98.99
5-2	99.78	14-2	94.34	23-4	73.40	34-2	96.56
6-1	84.72	14-3	66.67	24-1	100.00	35-1	92.52
6-2	98.42	14-4	91.18	24-2	99.88	35-2	99.34
7-1	95.48	15-1	96.65	25-1	99.87	36-1	75.07
7-2	100.00	15-2	96.51	25-2	91.64	36-2	72.40
7-3	94.10	16-1	67.06	25-3	76.35	37-1	99.61
7-4	99.95	16-2	77.44	25-4	89.51	37-2	97.68
8-1	81.91	17-1	82.13	26-1	98.80	38-1	99.54
8-2	87.97	17-2	99.58	26-2	100.00	38-2	93.25
8-3	100.00	17-3	93.74	27-1	73.69	39-1	81.34
8-4	95.59	17-4	80.72	27-2	100.00	39-2	94.66
9-1	99.99	18-1	93.87	27-3	95.65	40-1	97.21
9-2	97.75	18-2	72.29	27-4	96.40	40-2	100.00
10-1	94.38	18-3	81.31	28-1	98.83	40-3	100.00
10-2	96.73	18-4	89.52	28-2	98.45	40-4	90.20
10-3	82.68	19-1	89.39	29-1	99.99	41-1	70.99
10-4	85.31	19-2	97.63	29-2	100.00	41-2	89.48
11-1	100.00	19-3	93.92	29-3	98.78	42-1	97.23
11-2	100.00	19-4	93.36	29-4	99.98	42-2	98.01

Eidesstattliche Erklärung

Ich erkläre hiermit eidesstattlich, dass ich die vorliegende Arbeit selbständig angefertigt habe. Die aus fremden Quellen direkt oder indirekt übernommenen Gedanken sind als solche kenntlich gemacht.

Die Arbeit wurde bisher keiner anderen Prüfungsbehörde vorgelegt.

Garching, den 15.04.2015

Sergi Rexach